PONTIFICIA UNIVERSIDAD CATOLICA DE CHILE

ESCUELA DE INGENIERIA

ANALYSIS OF SPECTRAL WAVE ENERGY TRANSFER METHODOLOGIES FROM DEEP TO SHALLOW WATER

JUAN C. DOMINGUEZ

Thesis submitted to the Office of Research and Graduate Studies in partial fulfillment of the requirements for the Degree of Master of Science in Engineering

Advisor:

RODRIGO CIENFUEGOS

Santiago de Chile, August, 2011

PONTIFICIA UNIVERSIDAD CATOLICA DE CHILE
ESCUELA DE INGENIERIA

ANALYSIS OF SPECTRAL WAVE ENERGY TRANSFER METHODOLOGIES FROM DEEP TO SHALLOW WATER

JUAN C. DOMINGUEZ

Members of the Committee:

RODRIGO CIENFUEGOS

JORGE GIRONÁS

PATRICIO CATALÁN

PABLO IRARRAZAVAL

Thesis submitted to the Office of Research and Graduate Studies in partial fulfillment of the requirements for the Degree of Master of Science in Engineering

Santiago de Chile, August, 2011

A todas aquellas personas que me apoyaron en el camino, en especial a mis padres, familiares y amigos.

ACKNOWLEDGEMENTS

Although Spanish is my native language, I will try my best to sincerely express my feelings of gratitude in English, without losing their true meaning.

The first person I would like to thank in this bounded space is my advisor, Rodrigo Cienfuegos, who actually became my guide long before my investigation started. Thanks to him I managed to understand for the first time what was behind those complexes –but awesome- natural phenomena that occurred day by day in the sea and that were a complete mystery to me. The dedication and motivation in his way of teaching triggered my willingness to accept his thesis proposal, and eventually lead me to embark in this investigation.

In second place, and without wanting to establish an order of importance, I thank the company PRDW Aldunate Vásquez –and especially Andrés Puelma and Benjamín Carrión- not only for supporting this research and providing me with essential data, but also for the constant good will they showed to help me. Their contributions gave me the first lights to develop this thesis. Likewise I also thank the collaboration of HydroChile S.A., for putting critical data at my disposal in the framework of this investigation.

Finally, I sincerely thank Patricio Catalán, whom with a wise comment, lighted the way for this research and transformed it into what it ultimately is.

CONTENTS

Page

TABLES INDEX

Page

FIGURES INDEX

Page

RESUMEN

Antes de diseñar cualquier obra marítima es necesario conocer primero las condiciones de oleaje reinante a la cual estará sometida a fin de lograr un diseño adecuado. Como las boyas de medición son escasas considerando el tamaño del océano, los ingenieros generalmente recurren a modelos numéricos de generación de oleaje para determinar estas condiciones. El problema: el número de simulaciones que se requiere hacer en el modelo para generar una estadística completa es elevado, y el tiempo computacional que requiere cada simulación también lo es.

En este trabajo se aborda el problema de la propagación espectral de oleaje desde aguas profundas a aguas someras, formalizando un método robusto de transferencia de climas de oleaje que permite ahorrar tiempos significativos de cálculo. Otros métodos de propagación son también descritos y comparados. El método propuesto consiste en propagar un número limitado de espectros sintéticos en el modelo y con esa información transformar un número cualquiera de espectros reales, mediante superposición lineal. El resultando de esa transformación es equivalente a haber propagado todos los espectros reales en el modelo numérico.

El método logra reducir significativamente el número de simulaciones requeridas y al mismo tiempo representar adecuadamente la forma y los parámetros resumen del espectro de salida, con diferencias en estos menores al 1% en comparación con la propagación espectral completa. La desventaja del método es que sólo es válido en casos donde los efectos no-lineales son poco importantes.

La información espectral de un estado de mar además presenta varias ventajas contra la información resumida en parámetros estadísticos de resumen. Entre ellas: (1) entrega mejores resultados al propagar estados de mar en un modelo numérico y (2) entrega una mejor estimación de la potencia media de oleaje. Los parámetros de resumen tienden a sobreestimar esta última; y la forma en que estos se extraen del espectro puede tener un gran impacto en los resultados.

Palabras Claves: propagación espectral, transferencia de energía de oleaje, reconstrucción espectral, métodos de propagación, transformación de espectros.

ABSTRACT

Before designing any maritime structure, it is first necessary to know the prevailing wave conditions to which the structure will be subjected in order to achieve a suitable design. As measurement buoys are scarce considering the size of the ocean, engineers generally rely on numerical spectral wave models to determine these conditions. The problem: the number of simulations that needs to be done in the model to generate a complete wave statistics is high, and so is the computational time required for each simulation.

In this paper, the spectral propagation of waves from deep to shallow water is studied and a robust method of wave climate transference that significantly reduces calculation time is formalized. Other methods of propagation are also described and compared. The proposed method's idea is to propagate a limited number of synthetic spectrums in the model and with that information transform any number of real spectrums, using linear superposition. The result of this transformation is equivalent perform a full spectral propagation.

The proposed method is able to significantly reduce the required number of simulations while adequately representing the shape and the wave parameters of the output spectrum, with differences in these smaller than 1% compared to the full spectral propagation. The downside of this method is that it only applies in cases where non-linear effects are unimportant.

The representation of a sea state through spectral information has several advantages over the representation through summarized statistical wave parameters. Among them: (1) Better results when propagating sea states in a numerical model are obtained, and (2) a better approximation of the mean wave power is achieved. Statistical wave parameters tend to overestimate the latter; and the way they are extracted from the spectrums can have an important impact in the results.

Keywords: spectral propagation, wave energy transference, wave spectrum, spectrum reconstruction, wave propagation methods, spectrum transformation.

1. INTRODUCTION

In the design and operation of any kind of structure, natural conditions play a fundamental role. For the engineers, knowing these conditions allows them to properly determine the design parameters to which the structure will be subjected. In the case of ocean engineers, who focus in the design of offshore platforms, ports, dykes, beaches and ships, among others, the marine environment takes most of their attention, for being the natural surroundings to their designs. To them, waves play a very important role, and thus properly determining, understanding and predicting wave conditions is the key to their success.

Unlike other natural parameters such as wind, temperature or pressure, waves are not being extensively measured, because of the complexity of the process, the cost of deploying and operating instruments, and the size of the ocean. Instead, waves are mostly hindcasted through numerical models that consider these measured variables (wind, pressure and temperature, among others) and are calibrated and validated using wave observations (e.g. WAMDI Group, 1988; Komen et al., 1994). The information delivered by these models is finally recorded in so called virtual buoys, which are simply pre defined locations in the ocean for which the numerical model produces the output. This all happens in deep oceanic waters, where the bottom bathymetry has a negligible influence over wave propagation.

Near the coast, a different type of model is used, which better accounts for the effect that the ocean's bottom has over the waves (Booij, Ris, & Holthuijsen, 1999). This type of model generally takes the information recorded in the virtual buoys and propagates it from that location towards the coast. They are fairly accurate (Booij et al., 1999), but have the downside of requiring too much computational effort for the propagations. When a wave study is required in coastal waters, the use of these models is almost compulsory.

In the case of Chile for example, the Hydrological and Oceanographic Service of the Navy (SHOA) requires the propagation of a database of at least 20 years long using a coastal spectral model for the approval of any study of oceanographic nature (SHOA, 2005). Because virtual buoys integrate wave data every 3 hours, propagating 20 years of

data results in 58400 numerical simulations, which is inconveniently costly. For this reason, an alternative approach is proposed and validated in this thesis, which should allow obtaining the same results, but with a considerably reduced number of simulations in the model.

In the following chapters, first, a general overview of some important concepts regarding sea wave's theory as well as a description of wave modeling is presented (Chapter 2); then, four existing propagation methods are described and the proposed propagation method is explained in depth (Chapter 3); afterwards, a validation of the proposed method is carried out using experimental data and a comparison is made between the different propagation methods (Chapter 4); later, a real application of the proposed method is done (Chapter 5); and finally, some conclusions of this work are presented (Chapter 6).

2. WAVE THEORY AND PROPAGATION MODELS

In this chapter, the most useful concepts related to this work are summarized. The chapter is divided in 3 sections: first, a brief introduction on the sea wave's statistics and the spectrum concept is made; then, the linear wave theory is briefly explained along with the most important processes of propagation and transformation of waves; finally, wave modeling based on spectral propagation is presented. This final section also includes a description of the SWAN wave model, which is used in the development of this work.

2.1 Waves statistics and sea waves spectra

A picture of the sea in a breezy day taken from above may look like a random representation of the sea-surface elevation (Figure 2-1). Distinguishing single waves visually can be rather difficult. The reason, is that the sea at that moment is composed of a large number of superposed waves, each with a different amplitude, period, direction and phase.

To measure waves, different techniques are available, which can be divided into *in situ* techniques (e.g. wave buoys and wave poles) and remote-sensing techniques (e.g. ground radars, airplanes and satellites). The most common result of a wave measurement is a time record of the sea-surface elevation at a fixed location, like the one in Figure 2-2 (Holthuijsen, 2007).

From these time records, representative wave parameters can be found. This is done by identifying individual waves in the record and assigning to each wave a corresponding wave height and period. The standard technique for doing this is utilizing the zero-upcrossing or the zero-downcrossing method (Goda, 2000).

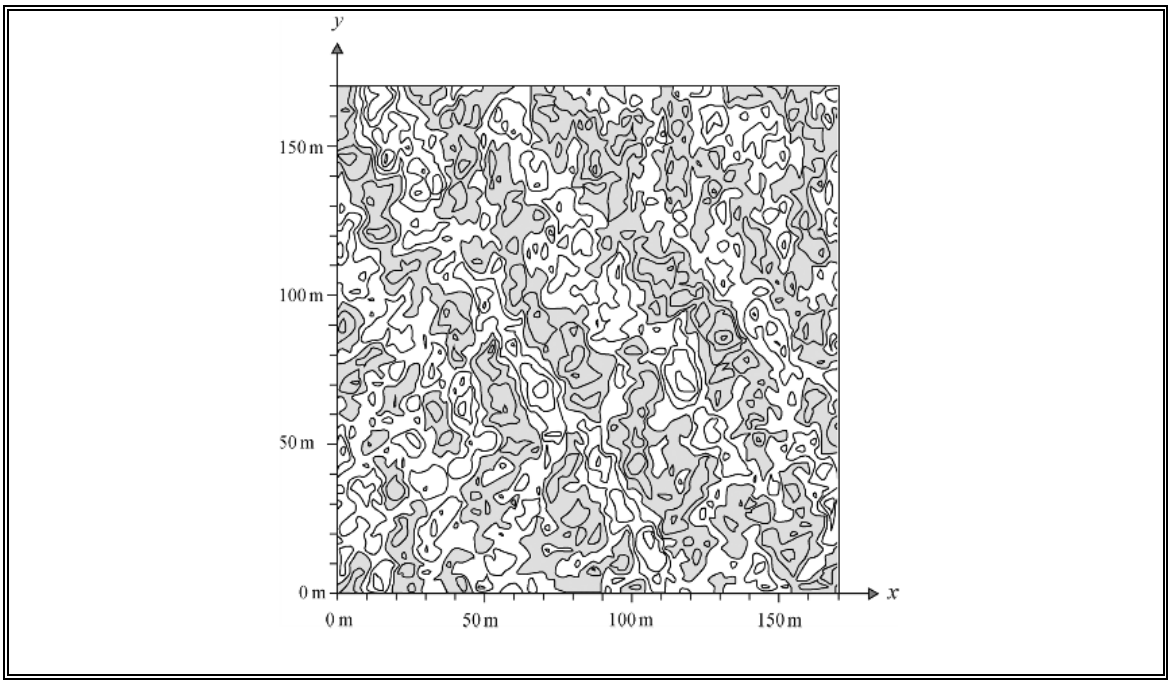

Figure 2-1: Bird's eye view of sea-surface elevation at one moment. Contour lines represent 0.2 m; shaded areas are below mean sea level. (Holthuijsen, 2007).

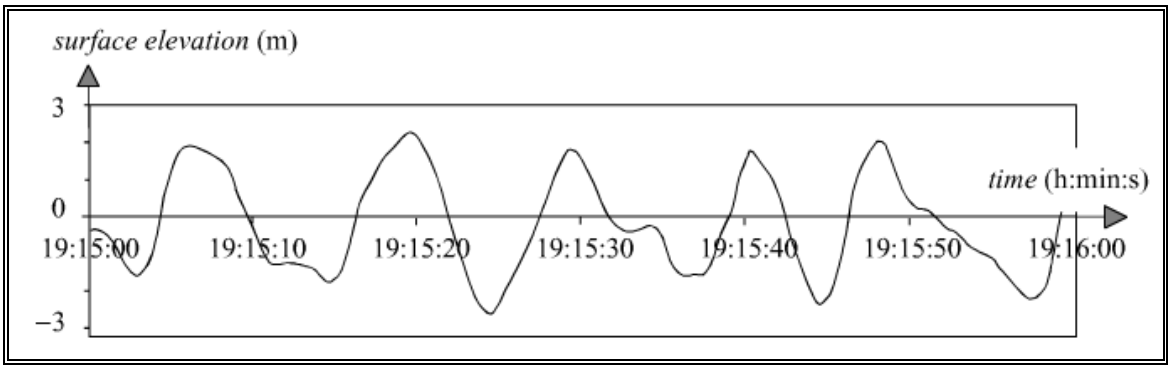

Figure 2-2: Example of a wave measurement result; the sea-surface elevation at one location as a function of time (Holthuijsen, 2007).

With this information, representative waves can be found: highest wave, highest one-tenth wave, highest one-third wave and mean wave. Among them, the most frequently used is the highest one-third wave (Goda, 2000), commonly called "significant wave". The significant wave is obtained by ordering the individual waves of the record in descending order of wave height until one-third of the total

number of waves is reached. Then, the mean height and period of this group of waves is calculated, and denoted $H_{1/3}$ and $T_{1/3}$ respectively. These parameters are called the significant wave height and the significant wave period respectively.

From the time record, it is also possible to decompose the sea-surface elevation $\eta(t)$ (where t is time) into its different harmonic wave components by means of Fourier analysis (Stewart, 2002; Percival & Walden, 1993).

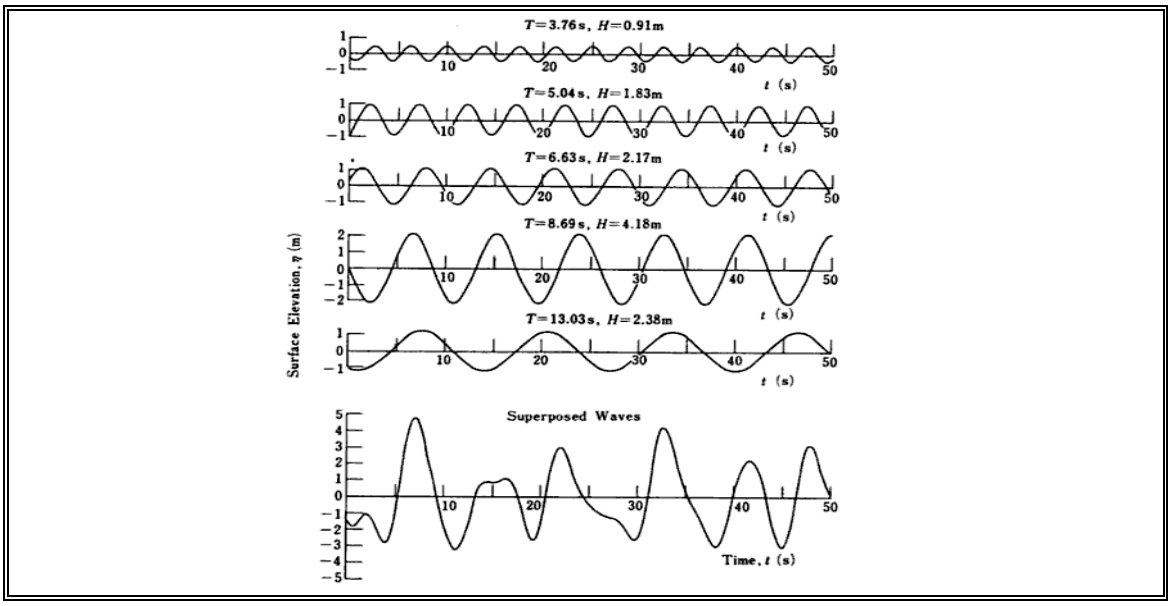

Figure 2-3: Example of the wave profile $\eta(t)$ as a superposition of 5 different sinusoidal waves; each with different height, period and phase. (Goda, 2000).

The example in Figure 2-3 shows how 5 different sinusoidal waves with different height (H), period (T) and phase (horizontal position in the time axis), can be superposed to form the wave profile at the bottom. This indicates that the time record can actually be reproduced with a Fourier series, as shown on equation (2.1), where, a_i and α_i are the amplitude and phase respectively, of each frequency f_i (which corresponds to the inverse of the period; i.e., $f = 1/T$).

$$\eta(t) = \sum_{i=1}^{N} a_i \cos(2\pi f_i t + \alpha_i) \qquad (2.1)$$

When a Fourier analysis is applied to the wave record, it is possible to determine the phase and amplitude of each frequency, and therefore obtain the record's spectrum in amplitude and phase (Holthuijsen, 2007) (Figure 2-4). The phase can be distributed uniformly between 0 and 2π depending on the situation (e.g. distance to the generation point) and will be ignored for now, but must be taken into account if equation (2.1) is used to create a synthetic record (in that case, a random phase is created independent of the amplitude spectrum). The amplitude spectrum on the other hand provides important information of the sea state.

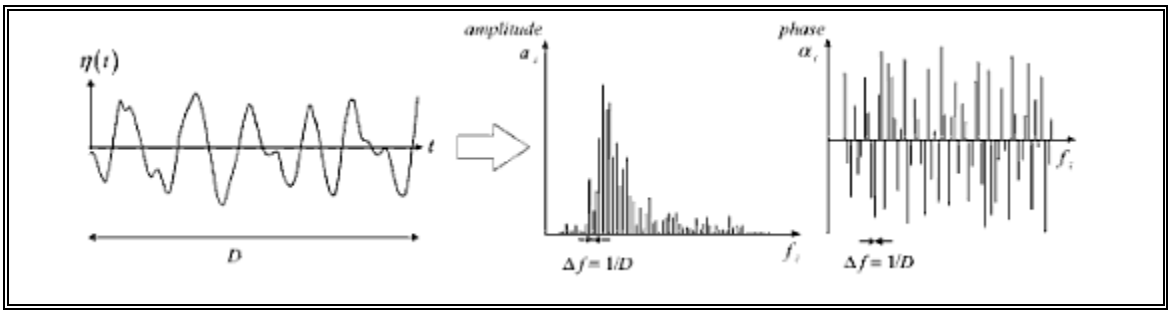

Figure 2-4: The result of transforming the time record via Fourier analysis into its corresponding amplitude and phase spectrum. (Holthuijsen, 2007).

In practice, the time record is cut into segments and the Fourier analysis is repeated for each segment in order to obtain an average amplitude spectrum because the value of $\bar{a}_i$ converges when the number of segments increases (Stewart, 2002). Also, the variance of each wave component $\frac{1}{2}\overline{a_i^2}$ instead of the average amplitude $\bar{a}_i$ is used to represent the spectrum. The reasons are that: (1) the variance is more statistically relevant than the average amplitude, and (2) the variance is proportional to the energy of the waves, making it more convenient to use (Holthuijsen, 2007). Finally, because all frequencies are present in nature (not only the chosen f_i's), the variance spectrum is transformed into the variance density spectrum $E(f_i)$:

$$E(f_i) = \frac{1}{\Delta f_i} E\left\{\frac{1}{2}\underline{a}_i^2\right\} \tag{2.2}$$

Where $E\{.\}$ represents expected value and E(.) is the symbol for variance density. Underscore of $\underline{a}$ indicates amplitude treated as a random variable.

A continuous variance density spectrum can also be constructed by making:

$$E(f) = \lim_{\Delta f \to 0} \frac{1}{\Delta f} E\left\{\frac{1}{2}\underline{a}^2\right\} \tag{2.3}$$

The whole transformation process can be seen in Figure 2-5. The final variance density spectrum, from now on called simply "frequency spectrum", has units of $m^2 \cdot s$.

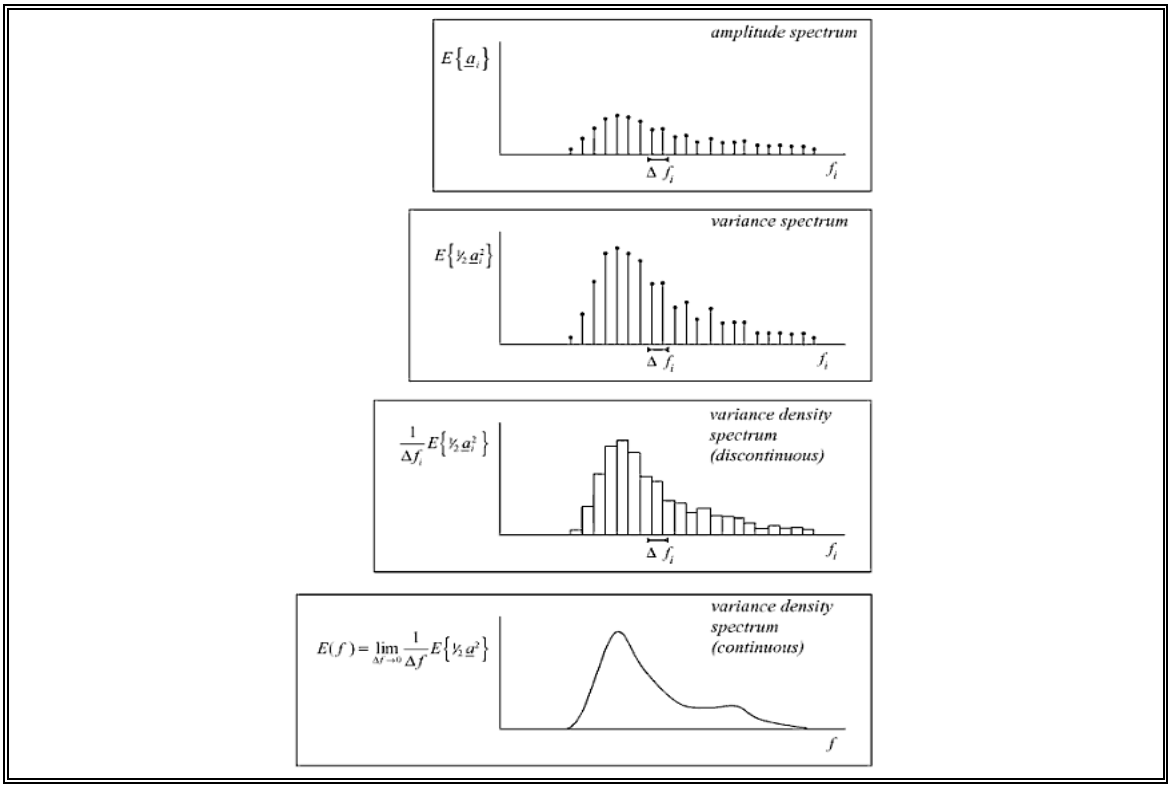

Figure 2-5: Transformation process from the amplitude spectrum obtained through Fourier analysis to the continuous variance density spectrum. (Holthuijsen, 2007).

Standard frequency spectrum shapes and parameterizations have been proposed based on observations in the deepwater zone (zone where the waves are not influenced by the sea bottom). The most important contribution in this context

comes from the Joint North Sea Wave Project, or JONSWAP (Hasselmann et al, 1973). As a result, Hasselmann et al.(1973) proposed the JONSWAP spectrum (Figure 2-6), which can be rewritten in approximate form in terms of the parameters of significant wave height $H_{1/3}$, peak period T_p and a "peakedness" factor γ that controls the sharpness of the spectral peak (Goda, 1988):

$$E(f) = \beta_J H_{1/3}^2 T_{\mathrm{p}}^{-4} f^{-5} \exp\left[-1.25\left(T_p f\right)^{-4}\right] \gamma^{\exp\left[-\left(T_p f-1\right)^2/2\sigma^2\right]} \qquad (2.4)$$

Where,

$$\beta_J = \frac{0.0624}{0.230+0.0336\gamma-0.185(1.9+\gamma)^{-1}}\left[1.094 - 0.01915\ln\gamma\right] \qquad (2.5)$$

$$T_p \cong T_{1/3}/[1 - 0.132(\gamma + 0.2)^{-0.559}] \qquad (2.6)$$

$$\sigma = \begin{cases}\sigma_a : f \le f_p \\ \sigma_b : f \ge f_p\end{cases} \qquad (2.7)$$

$\gamma = 1\sim7$ (mean of 3.3), $\sigma_a \cong 0.07, \sigma_b \cong 0.09$

The peak period refers to the period associated with the frequency that has the maximum energy in the variance density spectrum (i.e., $T_p = \frac{1}{f_p}$, with f_p being the frequency of the spectrum's peak, like shown in Figure 2-6).

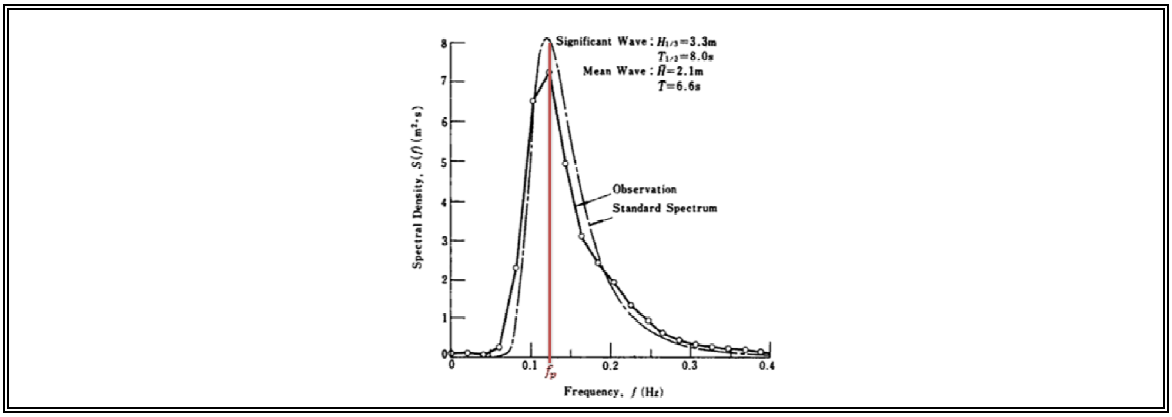

Figure 2-6: Example of a JONSWAP spectrum with $\gamma = 1$ (Goda, 2000).

Now, if the direction of waves is taken into consideration, the frequency spectrum $E(f)$ is replaced with the directional spectrum $E(f,\theta)$. This concept is introduced because sea waves cannot be adequately described by the frequency spectrum alone; there are many component waves propagating in various directions. The directional spectrum therefore represents the distribution of energy not only in the frequency domain but also in direction, as it can be seen in Figure 2-7.

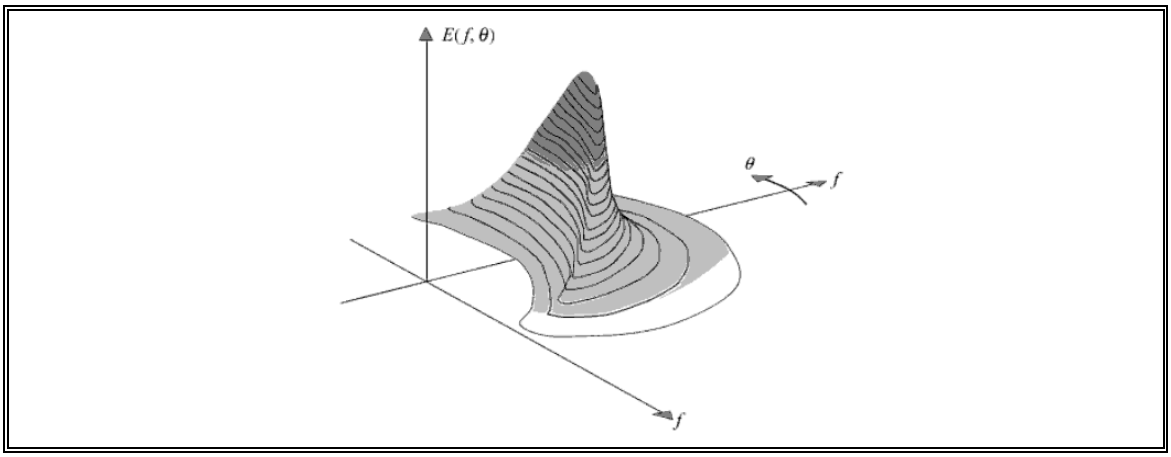

Figure 2-7: The directional spectrum is a two-dimensional representation of the energy distribution in the frequency and direction domain. In the figure, it is shown in polar co-ordinates. (Holthuijsen, 2007).

The directional spectrum can be expressed as follows:

$$E(f,\theta) = E(f)G(\theta|f) \tag{2.8}$$

Where $G(\theta|f)$ is the directional spreading function, which has been found to vary with frequency (Mitsuyasu et al., 1975). This function is normalized such that:

$$\int_{-\pi}^{\pi} G(\theta|f)\, d\theta = 1 \tag{2.9}$$

As with the frequency spectrum, a number of shapes have been proposed for the directional spreading function. However, the establishment of a standard functional form for the directional wave spectrum has not been achieved yet, in

contrast to the case of the frequency spectrum (Goda, 2000). Mitsuyasu et al. (1975) proposed the following function based on field measurement:

$$G(\theta|f) = G_0 \cos^{2s}\left(\frac{\theta}{2}\right) \tag{2.10}$$

$$G_0 = \left[\int_{\theta_{\min}}^{\theta_{\max}} \cos^{2s}\left(\frac{\theta}{2}\right)\right]^{-1} \tag{2.11}$$

Where θ is the azimuth measured from the principal wave direction, θ_{min} and θ_{max} is such that it satisfies the condition in equation (2.9) and parameter s, that was redefined by Goda & Susuki (1975), is a spreading parameter related to the frequency in the following way:

$$s = \begin{cases} (f/f_p)^5 s_{\max} & : f \le f_p \\ (f/f_p)^{-2.5} s_{\max} & : f \ge f_p \end{cases} \tag{2.12}$$

Parameter $s_{\max}$ was introduced by Goda & Susuki (1975) as the principal parameter for the purpose of engineering applications, and corresponds to the peak value of s.

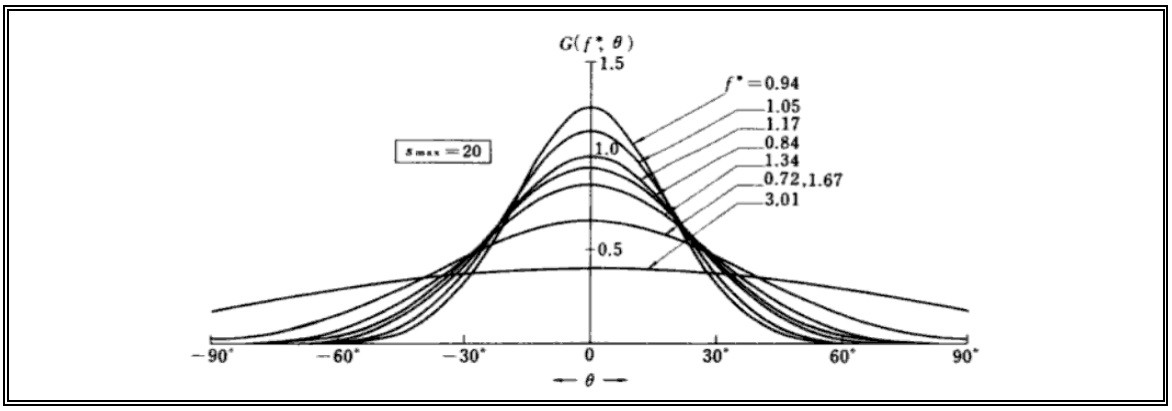

Figure 2-8: Example of Mitsuyasu-type spreading function for $s_{\max}$= 20, where $f^* = f/f_p$ (Goda, 2000).

Upon integration over all directions in the two-dimensional spectrum, the one dimensional spectrum (i.e., the frequency spectrum) is obtained. The variance

density spectrum, when multiplied by $\boldsymbol{\rho g}$ ($\boldsymbol{\rho}$ being the density of water and $\boldsymbol{g}$ the gravitational acceleration), gives the energy density spectrum (Holthuijsen, 2007).

From the wave spectra, characteristic wave dimensions such as height and periods of representative waves can be obtained. For example, to obtain the root-mean square value of the surface elevation η_{rms}, first, the spectrum is integrated over all directions and frequencies to obtain parameter m_0 (equation (2.13)). This integral, that has units of m^2 or similar dimensions, is by definition equal to the variance of the surface elevation, so then, η_{rms} can be obtained with equation (2.14).

$$m_0 = \int_0^{\infty} \int_0^{2\pi} E(f,\theta) df d\theta \tag{2.13}$$

$$\eta_{rms} = \sqrt{\overline{\eta^2}} = \sqrt{m_0} \tag{2.14}$$

With the value of η_{rms}, the significant wave height $H_{1/3}$can be obtained through a proportion supported by many wave observation data obtained through the world (Goda, 2000), this is:

$$H_{1/3} = 4.004\eta_{rms} = 4.004\sqrt{m_0} \tag{2.15}$$

When the significant wave height is obtained through this method, it is often called H_{m_0} to differentiate it from $H_{1/3}$ derived from the zero-upcrossing or zero-downcrossing method. Other common notation for the significant wave height is H_{sig} or simply H_s. Note that η_{rms} and $H_{1/3}$ are different conceptually, so the expression in equation (2.15) is just a rule of thumb. The expression is only applicable when wave heights are Rayleigh distributed.

In the case of wave periods, parameter $T_{1/3}$ cannot be derived through the spectrum theoretically. Instead, the main period parameter obtainable from the spectrum is the peak period T_p , and then, a relation with $T_{1/3}$ can be found based on field measurements or numerical simulation.

Finally, the mean wave direction (i.e. the direction normal to the wave crests) can be obtained from the spectrum with the following equation:

$$MWD = \arctan\left[\frac{\int \sin(\theta)E(f,\theta)dfd\theta}{\int \cos(\theta)E(f,\theta)dfd\theta}\right] \quad (2.16)$$

2.2 Linear wave theory and physical processes of transformation and deformation of waves in coastal waters

If the above definitions show that random ocean waves are actually formed by the sum of a large number of independent harmonic waves, then, the linear wave theory explains how each of these harmonic waves behave. The linear wave theory, also known as the Airy wave theory, is based on the assumption that harmonic waves don't affect one another while traveling. In other words, each component wave (waves with different frequency and direction) travels independently. The main requirement for this to apply is that the wave's amplitude must be small compared with the wave length and small compared to the water depth (Dean & Dalrymple, 1991). From the linear wave theory, an important relationship is obtained: the dispersion relationship.

$$c = \frac{L}{T} = \sqrt{g/k \tanh(kh)} \quad (2.17)$$

The dispersion relationship, shown in equation (2.17) in terms of the propagation speed c (i.e. the phase speed), relates the wave's length L with its period T. In the equation, k is referred to as the wave number and it's equal to $2\pi/L$; h corresponds to the water depth, and g is the gravitational acceleration. The dispersion relationship shows that for deep water ($\tanh(kh) \to 1$ for $kh \to \infty$), the propagation speed depends only on the wave period (equation (2.18)), while for shallow water ($\tanh(kh) \to kh$ for $kh \to 0$), it depends only on the water depth (equation (2.19)). Subscript 0 in (2.18) indicates deepwater condition.

$$c_0 = \frac{g}{2\pi}T \quad (2.18)$$

$$c = \sqrt{gh} \quad (2.19)$$

Thus, in areas where the water depth is greater than about one-half of the wavelength ($h > L/2$; called the deepwater zone), waves propagate without being

influenced by the ocean's bottom. However, once the waves get to the intermediate and shallow water areas, the bottom starts playing an important role on the waves propagation, and a series of physical processes occur which produce changes in the wave's height, direction and energy; therefore, transforming the spectrum (note that the spectrum also suffers transformations in deepwater due to other phenomena such as dispersion, wind growth, whitecapping and wave-wave interactions, which will be explained later).

In this section, the most important processes involved in the coastal region (intermediate to shallow waters) will be briefly summarized. These are: shoaling (change in the wave's height), refraction (change in the wave's direction) and generation - dissipation (change in the wave's energy). Other processes that are important for understanding the wave's behavior will be addressed briefly.

2.2.1 Shoaling

To understand the shoaling effect, first, the energy balance equation must be introduced.

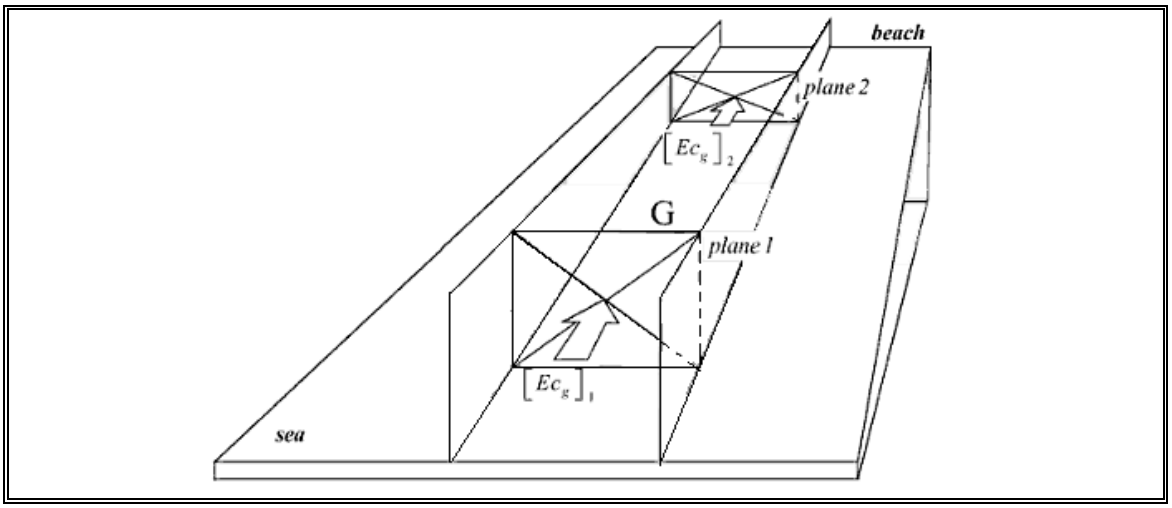

Figure 2-9: Wave approaching a straight coastline. In the absence of generation or dissipation all energy that enters plane 1 leaves through plane 2. (Holthuijsen, 2007)

$$[Ec_g]_2 = [Ec_g]_1 \rightarrow \frac{1}{2}\rho g a_2^2 c_{g,2} = \frac{1}{2}\rho g a_1^2 c_{g,1} \quad (2.20)$$

$$c_g = \frac{1}{2} * \left(1 + \frac{2kh}{\sinh(2kh)}\right) c \quad (2.21)$$

Equation (2.20) represents the conservation of energy flux between 2 vertical planes normal to the wave's direction (Figure 2-9). In the absence of generation and dissipation of wave energy, all energy that enters plane 1 must leave through plane 2 (without energy entering or leaving through the lateral sides). In other words, the rate at which energy enters and leaves is the same. In equation (2.20) c_g represents the group velocity (the speed of waves traveling in group rather than alone, equation (2.21)) and a represents the wave amplitude (or one half of the wave height H). From equation (2.20), the following relation can be easily obtained:

$$a_2 = \sqrt{\frac{c_{g,1}}{c_{g,2}}} a_1 \quad (2.22)$$

According to equation (2.17) and (2.21), as a group of waves approaches the coast over a uniform, gently sloping bottom, the group velocity initially increases slightly, but then decreases and approaches zero at the waterline. This effect, called Shoaling, causes the amplitude to initially decrease and then grows unbounded (equation (2.22); Figure 2-10). Of course, before that happens, the theory breaks (the basic assumptions for the linear theory are violated) and other processes such as depth-induced breaking (explained later) take place. This effect may also be referred to as "energy bunching" (the horizontal compacting of energy) (Holthuijsen, 2007) (Figure 2-11).

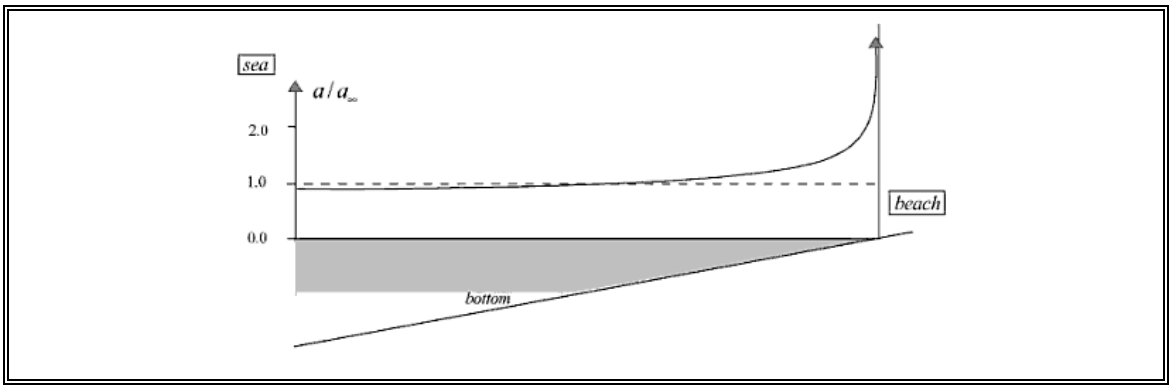

Figure 2-10: Evolution of amplitude due to shoaling, where a is the amplitude and a_∞ is the amplitude in deepwater. $a/a_\infty = 1$ in deepwater (far left of the picture). (Holthuijsen, 2007).

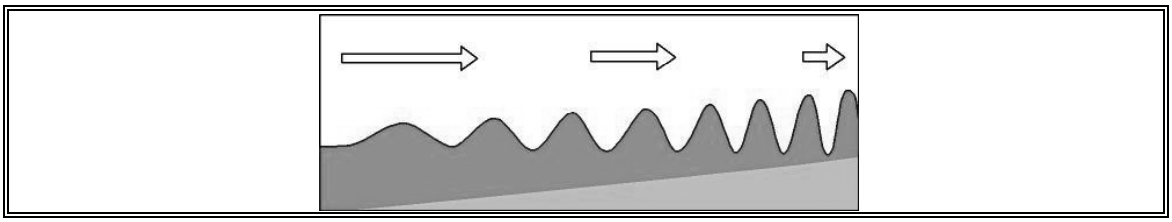

Figure 2-11: Waves approaching the coast showing the shoaling effect. Arrow length represents group velocity. (Butt, 2008).

2.2.2 Refraction

Another consequence of waves slowing down as they approach the coast (equation (2.17)) is the refraction process. Refraction typically occurs when harmonic waves approach the coast at an angle rather than straight, but also happens when waves encounter bottom variations. The crest in the shallower water portion will propagate slower than the one in the deeper portion, making the wave to turn toward the coast (Figure 2-12). The process is similar to a car applying more brake on one side, in which case, the car will turn to that side.

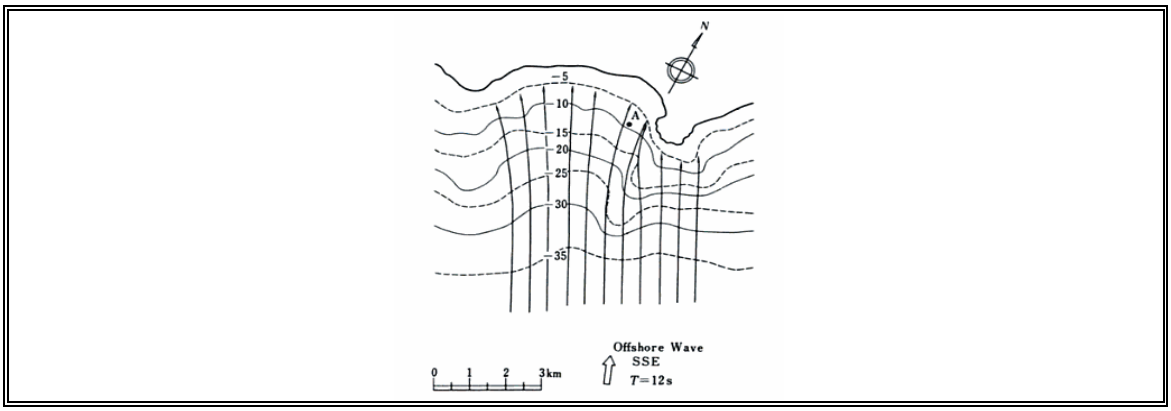

Figure 2-12: Example of refracting waves propagating towards the coast in an irregular bathymetry. (Goda, 2000)

2.2.3 Generation and dissipation

Generation and dissipation processes are responsible for adding and subtracting energy from the waves. The main generation process is wind generation, in which the atmosphere interacts with the sea surface, transferring energy from the wind to the ocean. This causes the waves to form and grow. The main dissipation processes are white-capping (Komen et al., 1984; Janssen, 1991a; Komen et al., 1994), bottom friction (Hasselmann et al., 1973; Collins, 1972; Madsen et al., 1988) and depth-induced breaking (Battjes & Janssen, 1978).

White-capping is the breaking of the waves in deep water. Although it's a very complicated phenomenon, it is reasonable to assume that it is controlled by the steepness of the waves (i.e., the relation between the wave height and length), being $H/L \approx 0.14$ an upper limit (Holthuijsen, 2007). This process limits the wave growth by wind generation.

Bottom friction is essentially the energy loss due to the transfer of energy and momentum from the orbital motion of the water particles to the turbulent layer just above the bottom of the sea. The bottom friction therefore depends on the wave field and the characteristics of the bottom.

Depth-induced breaking (or surf-breaking) as the name implies, is the breaking of the waves caused by the bottom. The process takes place when the waves cannot

longer grow because of shoaling and they finally collapse. This is found to happen throughout experiments (for a 10 s period wave and a beach slope of 1/30) when $\gamma = H/h \approx 0.75$; being H the wave height and h the water depth. This value can vary depending on the bottom slope and the relative water depth h/L_0 (where L_0 is the wave length in shallow water; $1.56T^2$ approx. in units of m and s) (Goda, 1970).

2.2.4 Other processes

Other important processes involved in the transformation and deformation of waves includes diffraction, reflection and non-linear wave-wave interactions.

Diffraction is the process in which waves pivot around and obstacle (e.g.: breakwater, island, head-land) during propagation in order to cover the shadow zone of the obstacle. In other words, it is the spreading of energy in directions other than that of wave propagation, and occurs whenever an obstacle imposes an energy flux discontinuity. In the absence of refraction, waves will travel into the shadow zone in an almost circular pattern of rapidly diminishing amplitudes. In cases where the bottom is not horizontal, both refraction and diffraction can occur.

Reflection occurs when the energy of the wave is not 100% absorbed by the coast and a portion of the energy is reflected. As a consequence, a wave will propagate backwards (or at an angle). Reflection in fact will probably always happen to some degree, being more dramatic in some cases (e.g. a vertical cliff in contrast to a gentle beach). This process finally results in the superposition of the incident and the reflected wave, and it's important to account for in some cases (e.g. inside a harbor) (Goda, 2000).

The non-linear wave-wave interaction is a mechanism that affects the wave growth. It consists on energy transfer among different component waves (i.e. frequencies), through resonance. There are 2 types: (1) triad wave-wave interaction, when 2 superposed waves interact with a third propagating wave that has the same wave speed, length and direction of the 2 superposed waves; and (2), quadruplet wave-wave interaction, when 2 superposed waves interact with another

2 superposed waves (with the same resonance conditions). Because of the dispersion relationship (equation (2.17)), triads cannot exist in deepwater (the conditions cannot be met), thus they are only important in shallow water. The interaction between waves causes an energy exchange among them (Nwogu, 1994) and therefore, a change in the spectral distribution of energy.

2.3 Wave modeling

In most coastal engineering problems, statistical characteristics of the wave's parameters are needed in order to make proper designs. The problem is that wave observations are rarely available. As an alternative, models are used to simulate wave conditions. The type of model and complexity depends on each case, but generally, they can be divided into 2 types: phase-resolving models and phase-averaged models (Battjes, 1994).

Phase-resolving models reconstruct the sea surface elevation in space and time, while accounting for such effects as refraction and diffraction (and sometimes triads and quadruplets). They are usually based on Hamiltonian (e.g. Miles, 1981; Radder, 1992), Boussinesq (e.g. Peregrine, 1966; Freilich & Guza, 1984; Madsen & Sørensen, 1992) or on the mild-slope equations (e.g. Berkhoff, 1972; Radder, 1979; Kirby, 1986) (for more information see Dingemans (1997)). The problem is that wave generation by wind is absent in these models, making them inconvenient in many coastal applications where storms conditions are of particular interest. Moreover, the space and time resolution required for these models are of the order of a small fraction of the wave length and period, limiting the use of these models to small regions (say, 1 km x 1 km) (Booij et al., 1999). For these reasons, phase-resolving models are not suitable for this investigation.

Phase-averaged models on the other hand are based on the energy or action balance equations (explained later) and are better suited for applications at larger scales. They follow the random-phase/amplitude model (equation (2.1)), which states that the sea surface elevation is the summation of large number of independent wave components. These models "follow" each wave component

across the ocean and account for all the physical processes encountered. In deepwater; generation, wave-wave interaction and dissipation are the more important processes, while in shallow water; shoaling, refraction, diffraction and triads must also be considered. Although the model description may sound like a Lagrangian approach, in the present, an Eulerian approach is used for computational reasons (WAMDI Group, 1988). For this study an Eulerian phase-averaged model, which will be explained later in detail, is used.

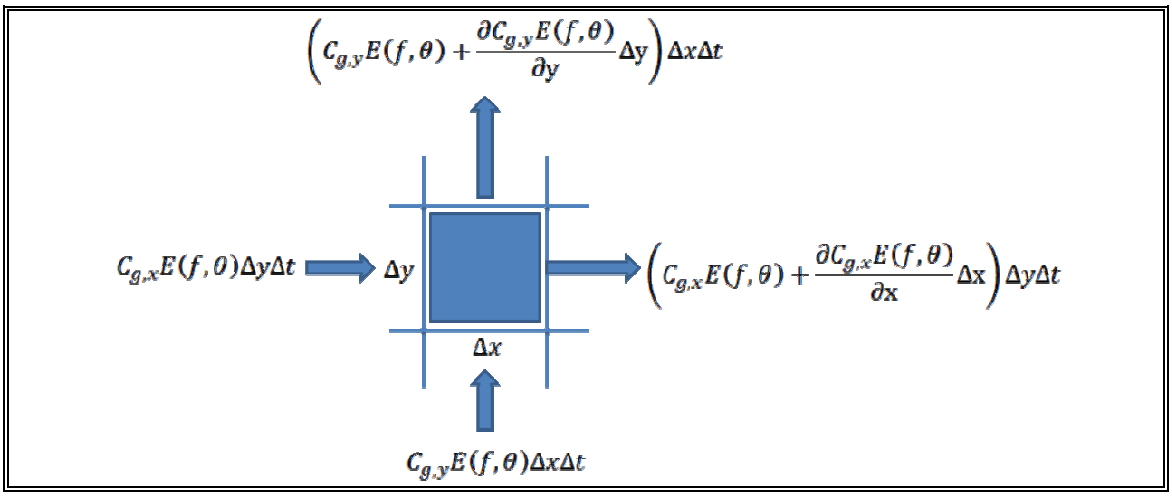

Figure 2-13: Representation of energy propagation through one cell of the domain, in the x-y plane (adapted from Holthuijsen, 2007).

For modeling waves, an energy balance is defined in each cell of the domain (Figure 2-13). In the case of deepwater propagation, where waves maintain their direction (i.e., no refraction-diffraction), the energy balance takes the following form (Holthuijsen, 2007):

$$\frac{\partial E(f,\theta;x,y,t)}{\partial t}+\frac{\partial c_{g,x}E(f,\theta;x,y,t)}{\partial x}+\frac{\partial c_{g,y}E(f,\theta;x,y,t)}{\partial y}=S(f,\theta;x,y,t) \qquad (2.23)$$

This is the spectral energy balance equation, where the first term represents the change of energy in the cell, the second and third terms represent the net import of energy in x and y respectively, and the term on the right represents the local

generation (or dissipation) of energy. Term $E(f,\theta;x,y,t)$ corresponds to the energy of the wave component with frequency f and direction θ, in the (x,y) spatial position at time t. Terms $c_{g,x}$ and $c_{g,y}$ correspond to the group velocity in the x and y directions respectively (i.e., $c_{g,x} = c_g cos(\theta)$; $c_{g,y} = c_g \sin(\theta)$). Term $S(f,\theta;x,y,t)$ represents the source terms and will be explained with detail later.

In the case of coastal waters (i.e., shallow waters), the energy balance equation is formulated the same way as in deepwater, but it now needs to account for shoaling, refraction and diffraction. Also, the number and complexity of source terms is now greater.

Shoaling is readily accounted for by using the depth-dependant group velocity in the equation (see equation (2.21)). In the case of refraction and diffraction, a new term is required to account for energy propagation, not only in the x-y space, but also through the θ-space. This new term propagates the energy through the directional bins of the spectrum (Figure 2-14).

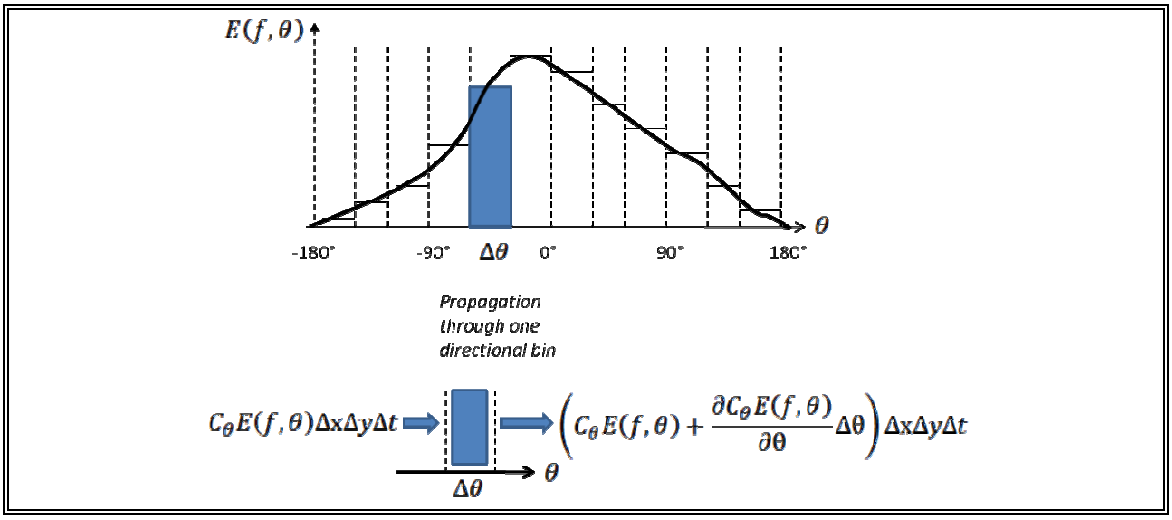

Figure 2-14: Representation of energy propagation between directional bins in a spectrum (adapted from Holthuijsen, 2007).

The energy balance equation for coastal waters therefore takes the following form (Holthuijsen, 2007):

$$\frac{\partial E(f,\theta;x,y,t)}{\partial t} + \frac{\partial c_{g,x} E(f,\theta;x,y,t)}{\partial x} + \frac{\partial c_{g,y} E(f,\theta;x,y,t)}{\partial y} + \frac{\partial c_\theta E(f,\theta;x,y,t)}{\partial \theta} = S(f,\theta;x,y,t) \quad (2.24)$$

Where c_θ is the refraction (or diffraction) turning rate of the individual wave components.

Finally, when ambient currents are present, the energy balance equation needs to be modified to include the effects of energy transfer between waves and currents. One of the consequences of this interaction is the frequency-shifting of waves (Whitham, 1974). This can be accounted by adding an extra term to the equation, similar to the refraction term but now on the frequency space. Because of the complexity of representing the energy transfer between waves and current, a simpler approach is considered. This is to replace the energy balance equation with the action balance equation. The action balance equation is identical to the energy balance equation, but the energy density $E(\sigma,\theta)$ is replaced with the action density $N(\sigma,\theta) = E(\sigma,\theta)/\sigma$. Here, σ represents the relative radian frequency (the radian frequency in a system moving with the current). The reason is that wave action is conserved in the presence of currents, in contrast to wave energy (Whitham, 1974). The action balance equation with frequency shifting included therefore takes the following form (Holthuijsen, 2007):

$$\frac{\partial N(\sigma,\theta;x,y,t)}{\partial t} + \frac{\partial c_{g,x} N(\sigma,\theta;x,y,t)}{\partial x} + \frac{\partial c_{g,y} N(\sigma,\theta;x,y,t)}{\partial y} + \frac{\partial c_\theta N(\sigma,\theta;x,y,t)}{\partial \theta} + \frac{\partial c_\sigma N(\sigma,\theta;x,y,t)}{\partial \sigma} = \frac{S(\sigma,\theta;x,y,t)}{\sigma} \quad (2.25)$$

The source term $S(f,\theta)$ can be divided into terms representing wind generation $S_{in}(f,\theta)$, non-linear wave-wave interactions $S_{nl}(f,\theta)$ and dissipation $S_{diss}(f,\theta)$.

$$S(f,\theta) = S_{in}(f,\theta) + S_{nl}(f,\theta) + S_{diss}(f,\theta) \quad (2.26)$$

Non-linear wave-wave interactions can be divided into triads $S_{nl3}(f,\theta)$ and quadruplets $S_{nl4}(f,\theta)$. Dissipation can be divided into white-capping $S_{wc}(f,\theta)$,

bottom friction $S_{bfr}(f,\theta)$ and depth-induced breaking $S_{surf}(f,\theta)$. Other processes of wave dissipation may also be added.

For each source term, different formulations (usually empirical) by different authors have been proposed, but will not be treated here.

2.3.1 The SWAN wave model

The SWAN wave model is a freely available, open source, computer model developed by the Delft University of Technology (the Netherlands), and widely used by scientist and engineers for research and consultancy practice (Holthuijsen, 2007), which is why it is the choice for this study.

SWAN (Simulating WAves Nearshore) is a third-generation, phase-averaged wave model based on the action balance equation (equation (2.25)) that includes all the processes described in section 2.2. Being a third generation model means that the spectrum is free to develop without any shape imposed a priori, as opposed to the second and first generation models used in the past (Holthuijsen, 2007).

SWAN solves the action balance equation using finite differences. In contrast to other third-generation wave models, the numerical propagation scheme in SWAN is implicit, which implies that the computations are more economic in shallow water. Being implicit indicates that all derivates of the action density equation (in time *t*, and horizontal coordinates *x* and *y*) are formulated at the same computational level, except the derivative in the integration dimension, in which also the previous (or up-wave) level is used. The discretization of the action balance equation takes the following form (Holthuijsen, 2007):

$$\left[\frac{N^{i_t}-N^{i_t-1}}{\Delta t}\right]^{n}_{i_x,i_y,i_\sigma,i_\theta}+\left[\frac{(c_{g,x}N)_{i_x}-(c_{g,x}N)_{i_x-1}}{\Delta x}\right]^{i_t,n}_{i_y,i_\sigma,i_\theta}+$$

$$\left[\frac{(c_{g,y}N)_{i_y}-(c_{g,y}N)_{i_y-1}}{\Delta y}\right]^{i_t,n}_{i_x,i_\sigma,i_\theta}+$$

$$\left[\frac{(1-\nu)(c_\sigma N)_{i_\sigma+1}+2\nu(c_\sigma N)_{i_\sigma}-(1+\nu)(c_\sigma N)_{i_\sigma-1}}{2\Delta\sigma}\right]_{i_x,i_y,i_\theta}^{i_t,n} +$$
$$\left[\frac{(1-\eta)(c_\theta N)_{i_\theta+1}+2\eta(c_\theta N)_{i_\theta}-(1+\eta)(c_\theta N)_{i_\theta-1}}{2\Delta\theta}\right]_{i_x,i_y,i_\sigma}^{i_t,n} = \left[\frac{S}{\sigma}\right]_{i_x,i_y,i_\sigma,i_\theta}^{i_t,n} \quad (2.27)$$

Where i_t is the time-level index (for non-stationary computations) i_x, i_y, i_σ and i_θ are grid counters and Δt, Δx, Δy, $\Delta\sigma$ and $\Delta\theta$ are the increments in time, geographic space and spectral space respectively (defined by the user). The index n indicates the iteration number and coefficients ν and η indicates the degree to which the scheme in the spectral space is up-wind or central (used to control the numerical diffusion).

For the source terms, SWAN gives the user the option to choose from different formulations (e.g., bottom friction can be represented by Hasselmann et al. (1973) Collins (1972) or Madsen et al. (1988)). The different alternatives are reviewed in Ris et al. (1999).

The SWAN model results agree well with analytical solutions, laboratory observations, and (generalized) field observations (Booij et al., 1999).

3. SPECTRAL ENERGY TRANSFER METHODS

Wave observations are rarely available, which is why wave simulations have to be carried out by numerical models to estimate wave conditions.

To determine the wave conditions at large scales, global information of wind, sea surface temperature, ice concentrations (among others) is collected from different sources such as satellites, buoys, ships and meteorological stations. This information is then used as an input in a global wave prediction model like the NWW3 (NOAA Wave Watch III) (Tolman, 2002b) or the WAM wave model (WAMDI Group, 1988) and a wave hindcast is made.

Global models simulate the generation and propagation of waves, mainly in the deepwater zone, and record the wave data in virtual buoys in the points of interest. This data can be registered in means of wave parameters (height, period and direction) or spectrally (energy of each component wave). Notice that wave parameters can be obtained from spectral data by integration.

To determine the wave conditions in a coastal area (shallow water zone), input information, most importantly bathymetry and incoming wave conditions (i.e., boundary conditions), is needed. Other input information can include wind and ambient currents. Incoming wave conditions are usually obtained from a global model output. With this information, the coastal model accounts for processes such us refraction and shoaling, and propagates the waves from the deepwater zone to the points of interest, obtaining spectral (or wave parameters) information in that area. The whole process can be summarized in Figure 3-1.

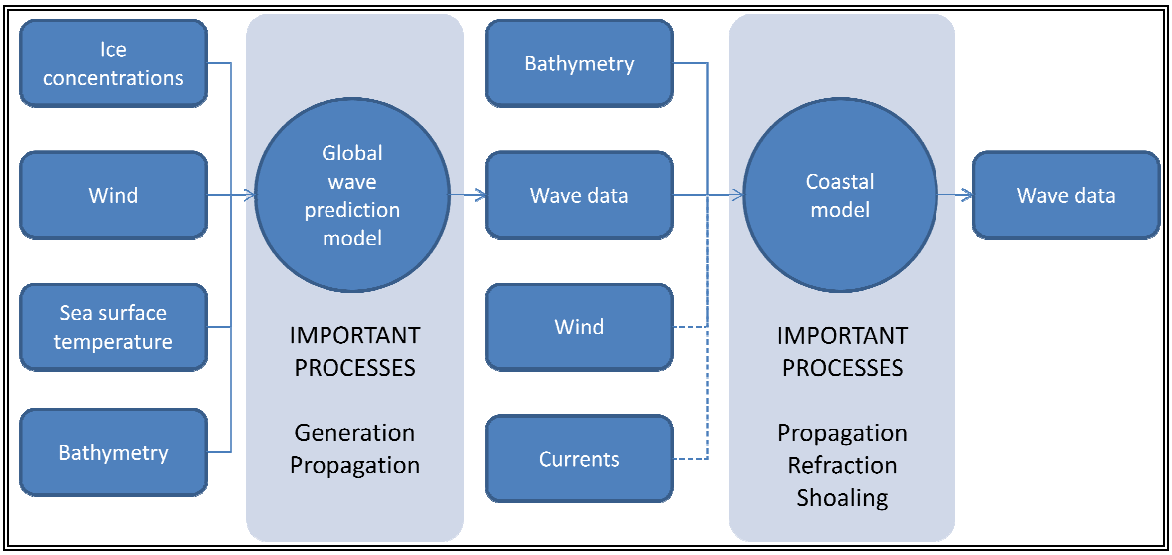

Figure 3-1: Example of a process to obtain wave data in a coastal region.

Often, a long set of wave data is required in the coastal area to make an engineering study. In the case of Chile, the Hydrological and Oceanographic Service of the Navy (SHOA) requieres the use of a database of at least 20 year long for the approval of any study of oceanographic nature (SHOA, 2005). The deepwater data provided by global models is frequently commercialized and provides good covering in time and space, but propagating each 3 hour sea state in the coastal model can be inconveniently time consuming. For this reason, an alternative is often used in engineering practice. The method consists basically in running a few model simulations to generate a transference functions, and then applying this function to the whole deepwater data. In this way, the equivalent spectrums in the site of interest are obtained without propagating all the spectral data in the model.

This work focuses in the propagation of the waves in the coastal region, i.e., in the transformation of the spectrum from deepwater (obtained through a global model) to a site of interest located in shallow waters, through the transference function technique. First, a state of the art involving different transference methods is presented and then a new method based on these ideas is proposed.

3.1 State of the art

Deepwater wave information can be available in spectral form (information of the energy distribution among the different frequencies that compose the sea state) or through statistic wave parameters (the complete sea state summarized in 3 parameters: significant wave height, peak period and mean direction of the waves). For instance, energy transfer methods can be classified into 2 different categories accordingly: (1) spectrum propagation, when complete spectrum information in deepwater is available; and (2) wave parameter propagation, when this information is only available through statistic wave parameters (significant wave height, peak period and mean direction), with no information on the shape of the spectrum.

On the other hand, when the amount of data that needs to be propagated is prohibitively large (so long that a traditional numerical simulation approach would require excessive computational time), a different kind of energy transfer method is required to solve the problem. Then, another division can be made depending on the quantity of data: (1) full propagation, when the amount of data is short enough to conduct a full numerical simulation of each sea state and/or non-linear effects are important (explained later); and (2) unitary propagation, when the amount of data is so long that cannot be transferred through regular methods and non-linear effects are not important.

Although there's not much scientific information regarding unitary energy transfer techniques (Nicolau del Roure, 2004; Fassardi, 2008), the concept was in a way introduced by Goda (2000), who defined a refraction coefficient for random sea waves based on the basis that "the variation in the heights of sea waves is determined by the contributions of all components, each component wave undergoing the process of refraction individually" (Goda, 2000).

In this section, a general view of 4 existing propagation methods is presented: full spectrum propagation, unitary spectrum propagation, full wave parameters propagation and unitary wave parameters propagation. A summary of the transference methods and their classification is presented in Figure 3-2. The method selection is based on the type and amount of data available.

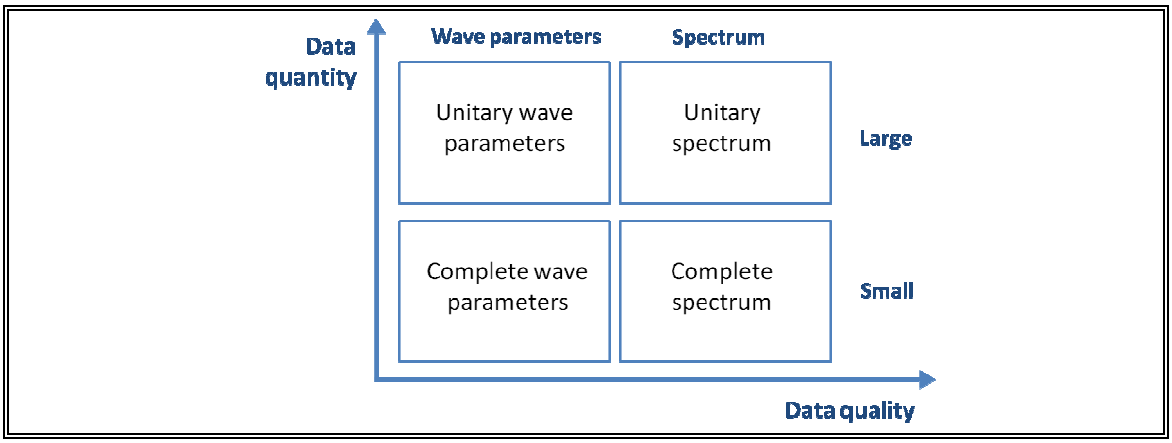

Figure 3-2: Propagation method selection depending on the type and quantity of data.

3.1.1 Full spectrum propagation method

The full spectrum propagation method consists in propagating into the site of interest the complete spectral information measured or hindcasted in deepwater, obtaining in this way the transformed spectrum in shallow waters. This is done through a spectral model such as SWAN. The advantage of this method is that the real spectral information is used; allowing to account in the simulation for non-linear processes such as wave-wave interactions, generation and dissipation, if necessary (in contrast to the unitary methods described later which doesn't work with such non-linear processes). This method is used as a benchmark when analyzing the performance of the other methods considered in this work.

When the deepwater spectral information is discretized too coarsely in the direction domain (e.g. bins every 15° or more) and a finer discretization is needed (for better representing wave directions for example), an alternative can be used that allows increasing the resolution without increasing too much the number of bins (so the computational effort doesn't increase much). This consists in truncating the spectrum to keep only the portion of directions heading towards the coast (typically a 180° sector) and then interpolating that portion to increase the resolution. This can be done because all energy contained in the discarded portion of the spectrum propagates away from the domain (i.e. it never reaches the site of

interest). It is important to notice though that the discarded portion can be important though if, for example, wave-wave interactions are considered. As an example of the benefits of this alternative, if the spectrum data covered 360 degrees every 15º, it can truncated to 180º every 5º. This produces an increase from 24 to 36 directional bins, but that is far compensated with the resolution gained.

3.1.2 Unitary spectrum propagation method

The unitary spectrum propagation method consists in creating a transference function with a few model simulations and then applying it to the complete spectral database.

The process is done in the following way: First, different synthetic 2D spectrums of significant wave height 1 meter (hence the name "unitary") but with different peak directions and peak frequencies are created. Then, these spectrums are propagated in the model one by one and output spectrums are obtained, with which the transference function is created. Finally, the transference function is applied to the each real spectrum of the time series, and the equivalent transformed spectrums in the site of interest are created. Hence the transformation process through the transference function doesn't require much computational effort and time.

The real advantage of this method is that once the transference function is obtained, the transformation process from the real deepwater spectrums to the site of interest is much faster. As an example, if 20 years of data measured every 3 hours were to be propagated from deep to shallow waters, it would take 58400 simulations using a full spectral propagation. If the same problem is addressed using the unitary method, it would take, around 70 simulations (assuming 10 different peak periods from 7 different directions). The 58400 cases can then be propagated to shallow waters using the principle of linear superposition.

This method, although very practical, has some limitations and problems.

The main limitation of this method is that it is valid only in cases where non-linear processes (like wave-wave interactions, generation and dissipation) are not important. This is because in order for the superposition principle to apply, the synthetic spectrums propagations must be carried out in a linear way (i.e., the simulation must not include non-linear processes). In that way the additivity condition is met ($f(x+y) = f(x) + f(y)$).

Nicolau del Roure (2004) proposed a method in which 3 types of transference functions are created, using 1, 4 and 7 meter waves. In this way he creates energy dependent functions which were presumably obtained including non-linear processes in the simulation (if not, the functions would be equal). The difference between applying this method and the regular (1 meter waves only) unitary spectrum propagation method was insignificant in all the test cases. This might be because non-linear processes were not relevant in these cases (i.e., small Ursell number).

The main problem of the unitary spectrum method is that there is no documentation about how to obtain and apply the transference function to transform the real spectrums. Most consultancies, like Baird & Associates for example, have their own spectral transformation methods and they use it like a black box, as it is seen in Nicolau del Roure (2004). Unfortunately, there is also no way of telling how precise their results are.

3.1.3 Full wave parameters propagation method

When the deepwater data is limited only to wave parameters (significant wave height, peak period and mean direction), without any information about the spectral shape or energy distribution, the propagation has to be made through a wave parameter propagation method.

In order to use a spectral model for the propagation of wave parameters, first, an spectral energy distribution in deepwater should be assumed. This has to be done in both, the frequency and the directional domain. Here, the most important parameters are: (1) the peakedness factor gamma, if a JONSWAP spectrum is used

for the frequency domain, and (2) the directional spreading parameter $s_{\max}$ if the Goda & Susuki (1975) directional distribution is used (see Chapter 2.1; equations (2.4) and (2.10)). Once an energy distribution is assumed, the propagation is made through a spectral model for each event in the time series. A summary of the process is show in Figure 3-3.

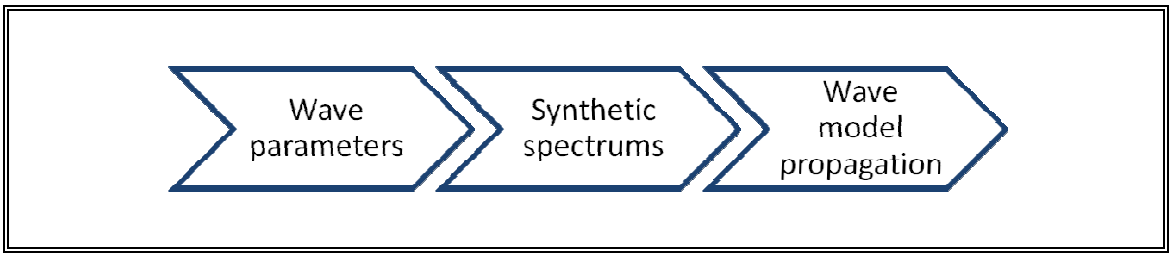

Figure 3-3: The full wave parameters propagation method. With the wave parameters, an energy distribution is assumed to build synthetic spectrums that are finally propagated one-by-one in the wave model.

Wave parameters data can also be available with wind-sea and swell separation. This separation consists in dividing the original spectrum around the 8 seconds period (in the frequency space) and then calculating the wave parameters H_{sig} (significant wave height), T_p (peak period) and mean wave direction for each portion of the spectrum. This brings more detail in the data of wave parameters but does not identify different peaks, so a peak located around the 8 seconds period could be split in half (and therefore, the real spectrum would be poorly recreated).

3.1.4 Unitary wave parameters propagation method

In the case of wave parameters, it is also useful to apply the unitary method in cases where the deepwater database is too large. This is done in a similar, but simpler way than the unitary spectrum propagation method, in the following way:

1.- Synthetic spectrums with the same energy distribution but different mean direction and peak periods are propagated one by one through a spectral model. Each spectrum with a significant wave height of 1 meter.

2.- In the site of study (a single point in the domain), values of H_{sig} and mean direction are recorded in each propagation. A matrix with wave height transformation coefficients (taken directly from the recorded H_{sig} value) is then formed by assigning each value to its corresponding period – direction pair in deepwater. A second matrix is constructed the same way, using the mean direction values for each deepwater period – direction pair.

3.- For each data of the real time series in deepwater, the significant wave height is transformed by multiplying the deepwater height by the corresponding coefficient for that period – direction pair. The mean direction is taken directly from the second matrix so it doesn't need transformation. The peak period is maintained (this is an assumption that the peak period doesn't change in the propagation). When the direction and period of the deepwater data doesn't match exactly with a direction – period pair in the matrix, the coefficients can be linearly interpolated.

A scheme summarizing the process is presented in Figure 3-4.

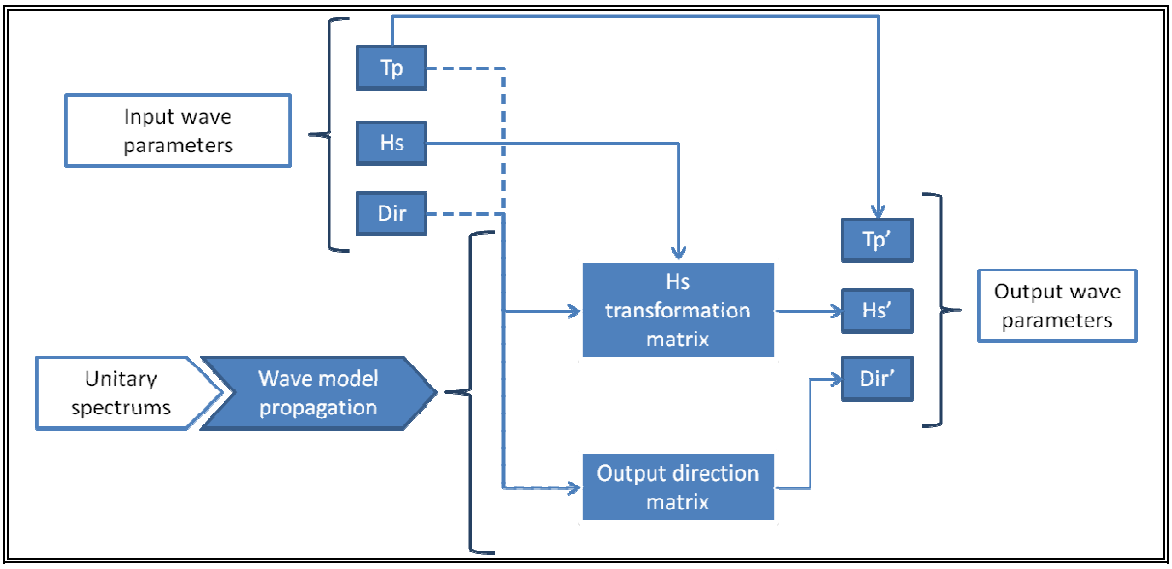

Figure 3-4: Unitary wave parameters propagation method. First, unitary spectrums are propagated in the model to obtain transformation matrixes; then, using the input wave parameters and the matrixes, output wave parameters are found.

The unitary wave parameter propagation method was formalized by Claudio Fassardi (2008) who defined a "wave transformation coefficient" obtained by propagating unitary ($H_{sig} = 1$ m) waves as:

$$C_t = f(T, WD_{\text{deep water}}, WL) \tag{3.1}$$

Where *T* is the wave period, *WD* is the wave direction and *WL* is the water level. (Notice the inclusion of different water levels in the unitary propagations).
The transformations are done in the following way:

$$H_{\text{shallow water}} = H_{\text{deep water}} \times C_t \tag{3.2}$$

$$WD_{shallow\ water} = f(T, WD_{deep\ water}, WL) \tag{3.3}$$

$$T_{shallow\ water} = T_{deep\ water} \tag{3.4}$$

Fassardi (2008) compares the waves parameters obtained through numerical modeling applying his method and measurements. He reports good results for his method when modeling small, short period waves (<16 s), but no consistency in the case of high long period waves (>16 s). This inconsistency may be derived from measuring problems (Fassardi, 2008). He also limits his methodology to areas where wave breaking is not important.

3.2 Proposed energy transfer method

An energy transfer method is proposed based on the unitary spectrum propagation method. The main idea of the proposed transformation function is reconstructing an energy spectrum in shallow waters by superposing different unitary spectrums propagated from deepwater. This is achieved by: (1) constructing the deepwater unitary spectrums U_i, (2) transferring the deepwater unitary spectrums U_i with a spectral model to obtain the transformed spectrums U'_i in the site of interest, (3) finding the coefficients α_i that allow reconstructing the real deepwater spectrums R using the unitary spectrums U_i, and (4) using these coefficients α_i and the model

results U'_i to construct the equivalent shallow water spectrums R'. The process, summarized in Figure 3-5, will now be described step by step.

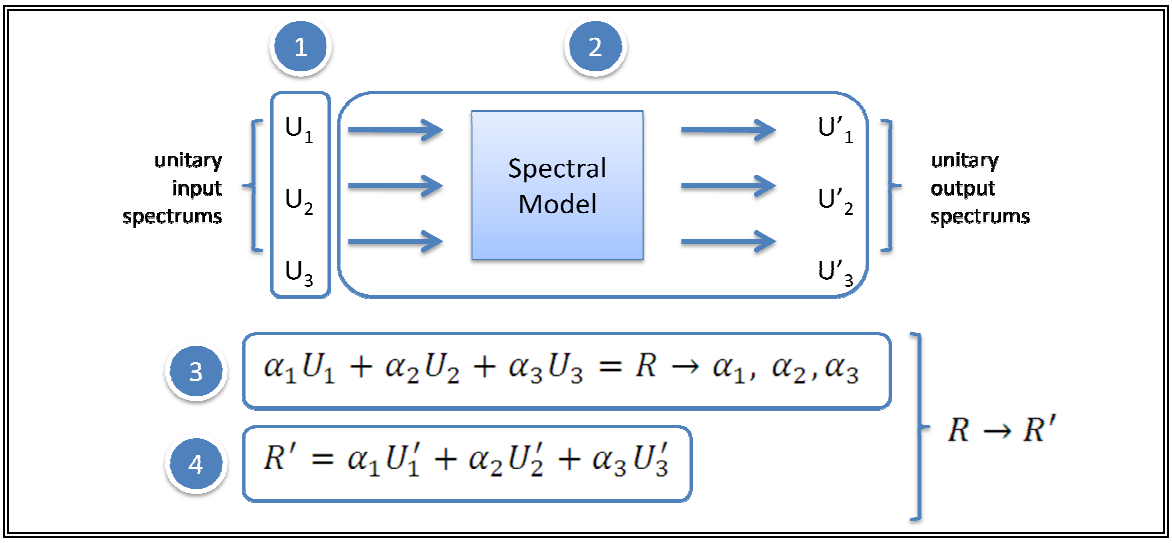

Figure 3-5: Example of the proposed method with its four steps to transform the deepwater spectrum R into the shallow water spectrum R'. Steps 1-2 have to be done once while steps 3-4 are repeated for each deepwater spectrum.

3.2.1 Unitary spectrums construction

The first step of this propagation method is to create synthetic unitary spectrums. The reason is that spectral models work with an energy distribution rather than single isolated wave components; besides, making one simulation for each component, in frequency and direction, would result in too much computational time, thus losing efficiency in the method.

Things that need to be considered for the construction of these spectrums are:

- Resolution of the spectrum in frequency and direction
- Energy distribution in frequency and directions
- Peak periods and directions for each spectrum
- Total energy of the spectrums

a) Spectral resolution

The frequency resolution of the spectrum is usually defined by a minimum and a maximum frequency, with the resolution being proportional to the frequency itself (i.e. logarithmic, e.g., $\Delta f = 0.1\ f$). The upper and lower limits should be determined by the spectral model limitations. Typical frequencies in the sea go between 0.03 Hz and 1 Hz (Munk, 1950).

In the case of the directional resolution there is a tradeoff between accuracy and computational time. In general, it should be high enough to fulfill the study needs but without generating too much computational effort. Another important thing to keep in mind is that the resolution should be high enough to represent the directional spreading of the spectrum; if not, spectrums with low directional spreading will not be represented properly. A way to increase the spectral resolution without increasing too much the number of directional bins is to consider only the portion of the energy that travels toward the coast (i.e. a 180º sector) and have a good discretization in that portion (e.g. bins every 5º).

b) Energy distribution

The energy distribution in the frequency space should be a unimodal (single energy peak) parametrical distribution like a JONSWAP spectrum for example. In that case, the "peakness" factor $\gamma = 3.3$ can be used.

The energy distribution in the directional space (i.e. the directional distribution) can follow a cosine power distribution like the one proposed by Goda & Susuki (1975). The most important consideration here is that the directional spreading (expressed as $s_{\max}$ in the equation (2.12)) should be small, in order to concentrate the energy in a narrow band of directions and in that way make each case more representative. If the Goda & Susuki (1975) distribution is used (equation (2.10)), a recommended value for $s_{\max}$ is 60.

The proposed method is actually independent of the chosen energy distribution. The reason a parametrical distribution is recommended is that wave models include parametrical distributions, so the user only has to choose one and define

the required parameters. On the other hand, most spectral wave models work with energy distributions, and concentrating all energy in one bin would therefore be unrealistic.

c) Peak periods and directions

The number of unitary spectrums, and therefore the peak periods and directions of each one, should be chosen to cover most of the direction – frequency space but without over-generating spectrums, in order to optimize the process (too many spectrums will result in too many simulations, which could be unnecessary). A solution that works well for this method is to choose one peak period for each frequency bin, with a defined max and min depending on the problem, and one peak direction every 15 degrees, for a 180º sector. The reason for choosing a 15º separation is that the directional distribution is symmetrical and covers a 15º gap between spectrums, even with a low directional spreading.

d) Total energy

The total energy of the spectrums should represent a significant wave height of 1 meter. That is to say that the total energy m_0 should be approximately 0.0625 m^2 according to equation (2.15). The reason is rather arbitrary, but it is a good choice because (1) a larger wave could grow too much and exceed the breaking criteria in some locations (assuming that breaking is off in the model), and (2) because a smaller wave would carry less energy, which could bring approximation problems in the energy bins (e.g. energy too close to 0 in some bins) and complicate the mathematical process.

3.2.2 Spectral model propagation

The spectral model propagation is the most important part of the proposed method because it provides the base results for the transference function construction. It is assumed in the next steps that the model's output is trustworthy; therefore, the simulation has to be carried out with special concern.

There are many aspects in the simulation that can affect the results; e.g. the type of grid, the spatial resolution, the bathymetric data and the spectral model itself. Although all of these aspects are extremely important, in the case of the proposed method special consideration is needed regarding the spectral resolution and the physical processes active in the simulation.

The spectral resolution of the model is important for the same reason than in the construction of the spectrums; the resolution in the directional space should be high enough to properly represent a spectrum with a narrow directional spreading. The ideal case is to use the same discretization employed in the construction of the unitary spectrums (in both, frequency and directional space) so that the input and the output spectrums share the same bins.

The selection of the physical processes active in the model is essential because the simulation has to meet the assumptions made for the proper application of the method: non-linear processes like wind growth, depth induced breaking, whitecapping, bottom friction, triads and quadruplet wave-wave interactions have to be disabled. For this reason, this method should not be applied in problems were these physical processes are important.

Once all considerations have been made, the propagation of each single unitary spectrum U can be simulated in the model to get the resultant output spectrums U' in the site of interest. These output and input spectrums should have the same discretization.

3.2.3 Determination of coefficients

In this phase, the coefficients that allow building the final output spectrums (i.e. the equivalent output spectrum for each real deepwater spectrum) are found. This is done by determining the coefficients that form the real deepwater spectrums as a linear combination of the unitary input spectrums.

The first step for determining the coefficients is to interpolate either the unitary input spectrums or the real deepwater spectrums so that they are discretized equally. Typically, the real deepwater spectrum needs interpolation to match the

discretization of the constructed unitary spectrums, because of its lower resolution. If the constructed unitary spectrums consider only a sector of directions, the real deepwater spectrums should be truncated. The energy left out is not considered because it is assumed that because of its direction, it never reaches the point of interest.

Once the bins from the real and the unitary spectrums match, the second step is to form a linear system to find the coefficients that construct the real deepwater spectrums R as a combination of the unitary spectrums U. For this, one equation for each energy bin (i.e., for each frequency – direction pair) of the real spectrum has to be formed (equation (3.5)). This brings one multiplier for each unitary spectrum and one equation for each energy bin, thus making the system overdetermined (assuming of course that the number of bins is greater than the number of spectrums).

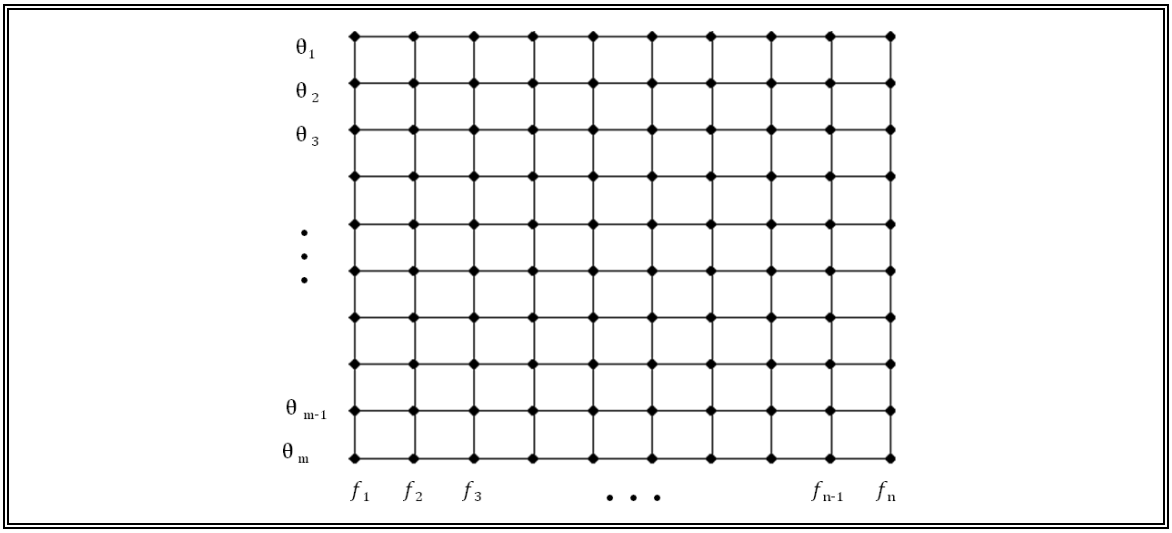

Figure 3-6: Representation of a discretized spectrum, each dot corresponding to an energy bin.

$$r_{f_i,\theta_i} \cong \sum_{k=1}^{p} \alpha_k \times u_{f_i,\theta_j}^{k} \tag{3.5}$$

Equation (3.5) shows that every bin of the real spectrum r_{f_i,θ_i}can be written as the weighted sum of the energy contained in that same bin $u^k_{f_i,\theta_j}$ in each unitary spectrum U^k.

To form the system, the energy bins of each unitary spectrum k have to be arranged in a single column, as shown in Figure 3-7. The same has to be done with the energy bins of the real spectrum. Then, matrix A can be formed arranging the p unitary spectrums U^k into columns (Figure 3-9). This, along with equation (3.5), results in the system shown in Figure 3-10. Because the system is overdetermined, it has to be solved by minimum squares.

$$U^k = \begin{bmatrix} u^k_{f_1,\theta_1} \\ u^k_{f_2,\theta_1} \\ \vdots \\ u^k_{f_n,\theta_1} \\ u^k_{f_1,\theta_2} \\ u^k_{f_2,\theta_2} \\ \vdots \\ u^k_{f_i,\theta_j} \\ \vdots \\ u^k_{f_n,\theta_m} \end{bmatrix}$$

Figure 3-7: Energy bins of the unitary spectrum k arranged in a single column.

$$R = \begin{bmatrix} r_{f_1,\theta_1} \\ \vdots \\ r_{f_n,\theta_m} \end{bmatrix}$$

Figure 3-8: Components of the real deepwater spectrum arranged in a single column.

$$A = \begin{bmatrix} & & & & \\ U^1 & \dots & U^k & \dots & U^p \\ & & & & \end{bmatrix}$$

Figure 3-9: The arrange of each unitary spectrum in columns forms matrix A.

$$\begin{bmatrix} u^1_{f_1,\theta_1} & \cdots & u^p_{f_1,\theta_1} \\ \vdots & \ddots & \vdots \\ u^1_{f_n,\theta_m} & \cdots & u^p_{f_n,\theta_m} \end{bmatrix} \times \begin{bmatrix} \propto_1 \\ \vdots \\ \propto_p \end{bmatrix} = \begin{bmatrix} r_{f_1,\theta_1} \\ \vdots \\ r_{f_n,\theta_m} \end{bmatrix}$$

Figure 3-10: The final linear system. Notice that $p < n \times m$ so the system is overdetermined.

To verify the solution, equation (3.6) can be used. The synthetic deepwater spectrum S constructed by the sum of the unitary spectrums U should be almost identical to the real deepwater spectrum R.

$$S = \sum_{k=1}^{p} \alpha_k \times U^k \tag{3.6}$$

$$S \approx \mathrm{R} \tag{3.7}$$

3.2.4 Construction of the synthetic output spectrum

Solution of the system in Figure 3-10 delivers the necessary multipliers to construct the synthetic output spectrum R' in the site of interest. This is done by linearly combining the unitary output spectrums U' (the ones obtained after propagating the unitary spectrums in the model) and the coefficients α, as show on equation (3.8).

$$R' = \sum_{k=1}^{p} \alpha_k \times U'^k \tag{3.8}$$

This solution applies only for one real deepwater spectrum R. In consequence, the linear system of Figure 3-10 has to be solved and equation (3.8) has to be applied each time.

Notice that the solved system didn't have any sign restriction, so the coefficients α can be either positive or negative. Adding the non-negativity restriction to the α coefficients brings worst results and restricting the summation in equation (3.5) to be always positive doesn't ensure that the summation in equation (3.8) will be, so this can bring the problem of having negative energy values in some bins of the synthetic output spectrum. To solve the problem, the negative energy bins are simply approached to 0. This can be done because the negative values should be significantly small (i.e. close to zero). Moreover, the sum of energy contained solely in the positive bins is closer to the real total energy than the sum of energy in the positive and negative bins. Despite this, before approaching to 0 it's important to check every case for negative values under a certain threshold that could show signs of error in the method.

4. METHOD VALIDATION AND COMPARISON

In this section, the validation of the proposed method is carried out by measuring the errors incurred in the application of the method in comparison to a full spectrum propagation. The error is expected to be relatively small and far compensated by savings in computational time. Once the method is validated, a comparison between the 4 propagation methods earlier described is made. Furthermore, an overview of the SWAN wave model is presented.

The test case description, the simulation details and the results analysis are shown below.

4.1 Test case description

The proposed method validation was made using field data provided by PRDW-AV, an international coastal engineer consultancy. The site of study is located in Ancon, a district located 30 km. north of Lima, Peru. The information provided included bathymetric data, hindcasted deepwater spectral information and wave parameters measured with an ADCP at a 15 meter depth area, every 2 hours, for a 2 month period. This gives a total of 245 measurements, with one deepwater spectrum for each measurement. The bathymetry includes several geographical accidents (e.g. islands of different sizes and bays). This, along with the location of the deepwater node and the ADCP location, can be seen in Figure 4-1.

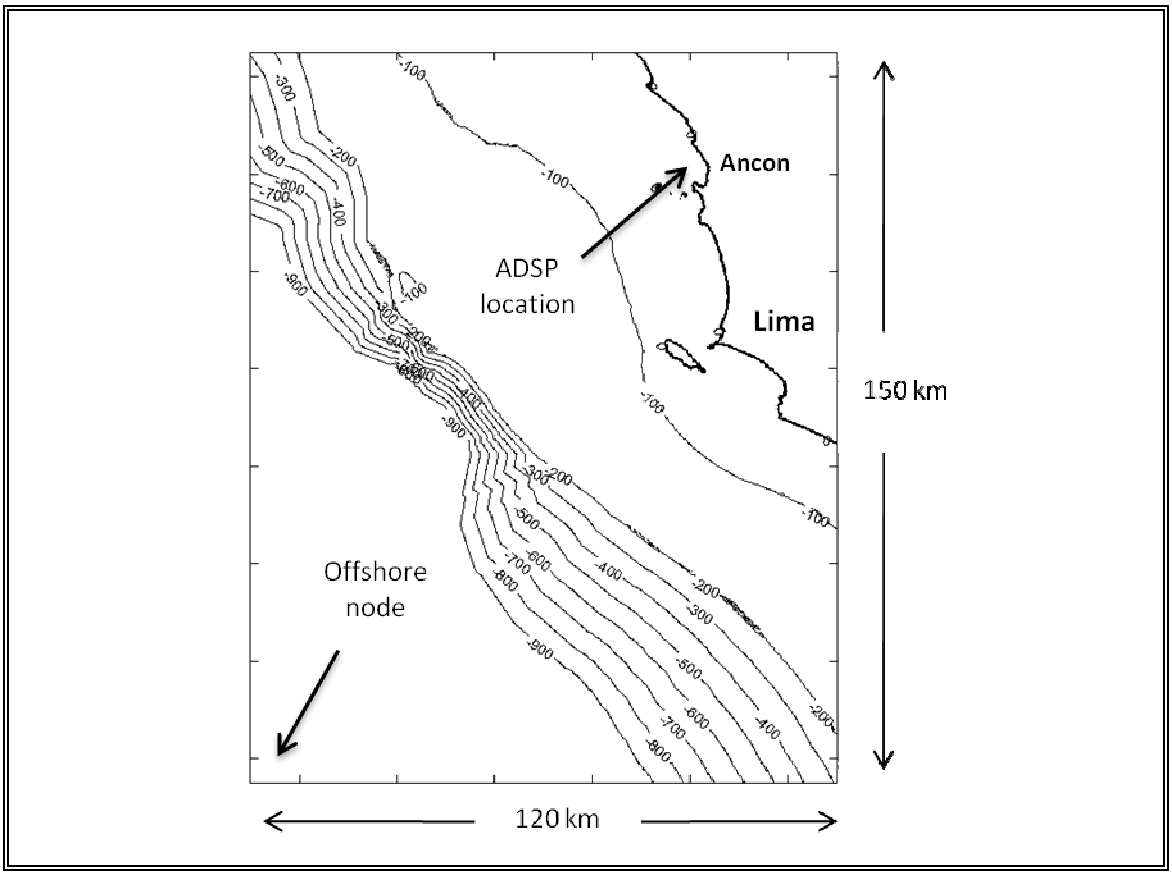

Figure 4-1: Ancon bathymetry and location of the ADSP and deepwater node.

Notice that for validating the proposed method, field measured data was not really required. The validation of the proposed method is carried out by comparing the output spectrums obtained from (1) a full spectrum propagation of every deepwater spectrum and (2) the unitary spectrum propagation method, so the simulations for this purpose could've been done using synthetic data (computer-created deepwater spectrums and bathymetry). The reason real data was used for the validation of the method is that (1) it allows testing the model under real and complex bathymetric conditions, and (2) a parallel verification of the SWAN spectral model can be made using the wave measurement data.

The deepwater data show a mean significant wave height of 2 meters during the measuring period, with only 5 events going over the 3 meter threshold. The maximum significant wave height was 3.4 meters in the entire record (Figure 4-2).

The mean peak period in the data was 11.5 seconds, with a maximum and minimum of 18.4 and 7.2 seconds respectively; the peak directions were comprised in the range between 170º and 240º, with a mean of 200º; both records can be seen in the appendices section.

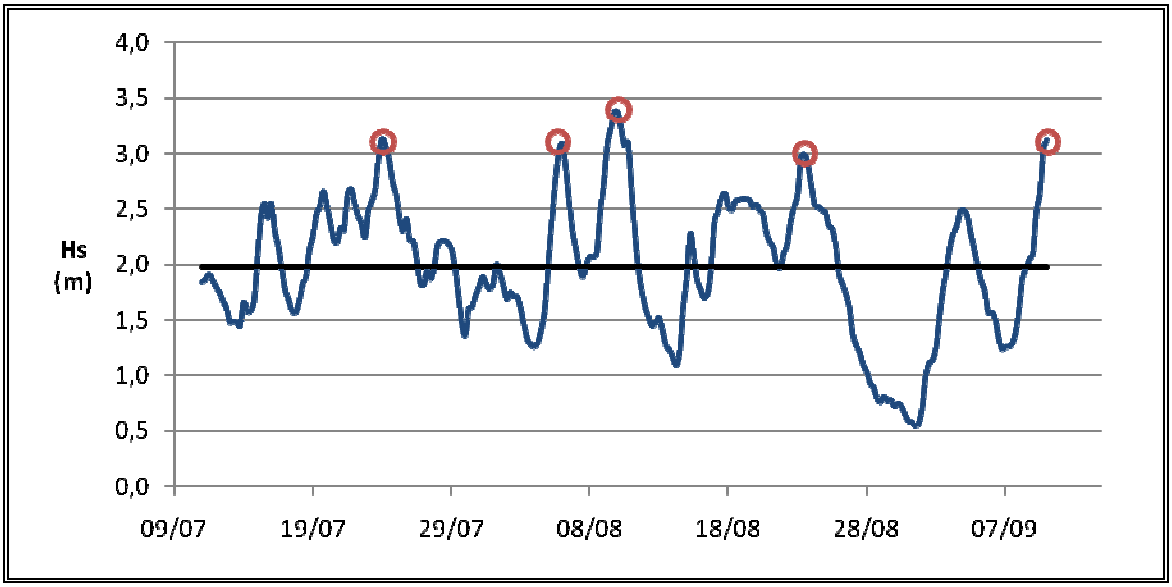

Figure 4-2: Incident significant wave height record taken from the deepwater spectrums during the 2 month period. The record shows a mean value of 2 meters and 5 peaks over the 3 meter threshold.

The wave record shows that no major events (i.e. storms) occurred during the measuring time. Peak periods were contained in a normal range and the peak direction was mainly SSW, which in the case of Ancon is almost parallel to the coast.

The deepwater spectrums are bimodal in almost all the record. The first peak is located around the 8 seconds, with a 190º direction, while the second peak is located near the 14 seconds, with a 220º direction. This evidences the fact that a swell and a sea wind component are present. In Figure 4-3, an average of the 245 spectrums is shown.

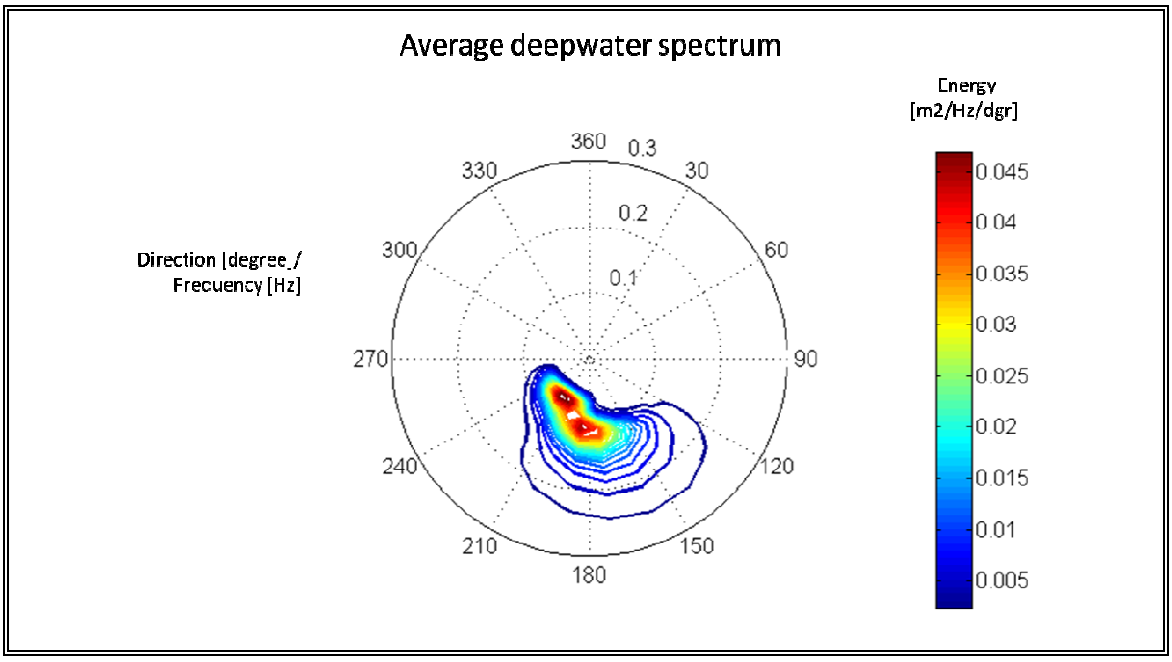

Figure 4-3: An average of the 245 deepwater spectrums shows that a bimodal behavior is almost always present.

4.2 Simulation

Every simulation, regardless of the method, was carried out using the same setup in the wave model; that is to say, the grid, the spatial, and the spectral resolution, were exactly the same in every case. The summary of this information is shown in Table 4-1. The calculation grid used was a regular grid with 3 open boundaries where the spectral condition was imposed, and one closed boundary corresponding to land.

Table 4-1: Spatial and spectral resolution used in the simulation.

Spatial resolution			
X length [m]	Y length [m]	Delta X [m]	Delta Y [m]
120,000	150,000	300	300

Spectral resolution				
Min frequency [Hz]	Max frequency [Hz]	Delta frequency	Direction range [degree]	Delta θ [degrees]
0.035	0.55	0.1 * f	180 – 360	5

Because of the restrictions of the proposed method, non-linear processes (wave-wave interactions, generation and dissipation) were turned off in the model for the propagation of unitary spectrums. However, a simulation including these processes (in particular: triads, bottom friction, breaking and whitecapping) was made, to (1) test the model accuracy, (2) use the results as a benchmark for the other methods, and most importantly (3) measure the relevance of non-linear processes in this case.

The unitary spectrums for this simulation were created using the same resolution shown in Table 4-1. After the analysis of the real deepwater spectrums, which showed a small range of peak periods, it was decided that 15 different peak periods would be created, ranging between 22 and 5 seconds and coinciding with each frequency bin (which are logarithmically distributed).

In the directional space, 12 peak directions were considered. These directions correspond to one peak every 15º for a 180º sector.

In total, 180 unitary spectrums were created for this problem (15 frequencies × 12 directions), which covered most of the frequency-direction domain (Figure 4-4). In Figure 4-4, each unitary spectrum has the same amount of energy, the reason they look different is that the chosen directional distribution has more spreading in the higher frequencies (equation (2.12)).

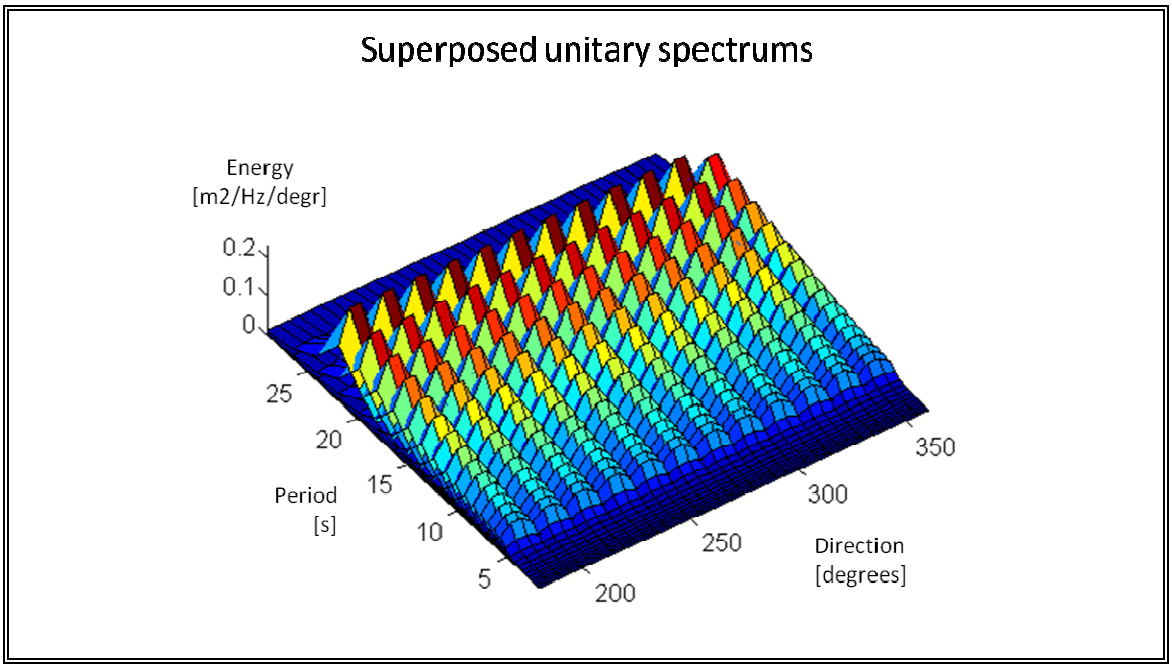

Figure 4-4: The 180 unitary spectrums superposed cover most of the frequency-direction domain.

Each unitary spectrum was constructed using a JONSWAP distribution with $\gamma = 3.3$ for the frequencies and a Goda & Susuki (1975) distribution with a s_{max} parameter equal to 60 for the directions. The significant wave height of each unitary spectrum was equal to 1 meter.

It is important to recall at this point that the energy distribution for the unitary spectrums (in frequency and direction) was chosen only for convenience, because the method works independent of this selection. Nevertheless, there are 3 reasons to support this selection: (1) Most wave models include these distributions, so the user only has to enter the required parameters to form the spectrums, (2) wave models work with a distribution of energy, so if any distribution is to be assumed, it's better to choose a realistic one, and (3) as it will be seen, this selection provides excellent results (although no comparison was made with another selection).

Regarding the total number of peak frequencies and directions considered (i.e. the total number of unitary spectrums); it was found that lowering the total number of unitary spectrums significantly worsened the results (shown later).

These unitary spectrums were used to obtain results based on the unitary spectrum (proposed method) and the unitary wave parameters propagation method.

For the full wave parameter propagation, synthetic spectrums with the same frequency and energy distribution of the unitary spectrums were used. The significant wave height, peak period and peak direction of each of these spectrums was obtained from the wave parameters of the real deepwater spectrums. Because in this case, the deepwater information came only in means of spectral information, the wave parameters had to be manually obtained, and this was done in two ways: (1) for the full spectrum, and (2) for the 180° sector of wave directions inbound to the coast. A comparison between these two options was then made. A summary of the simulation process is shown in Figure 4-5.

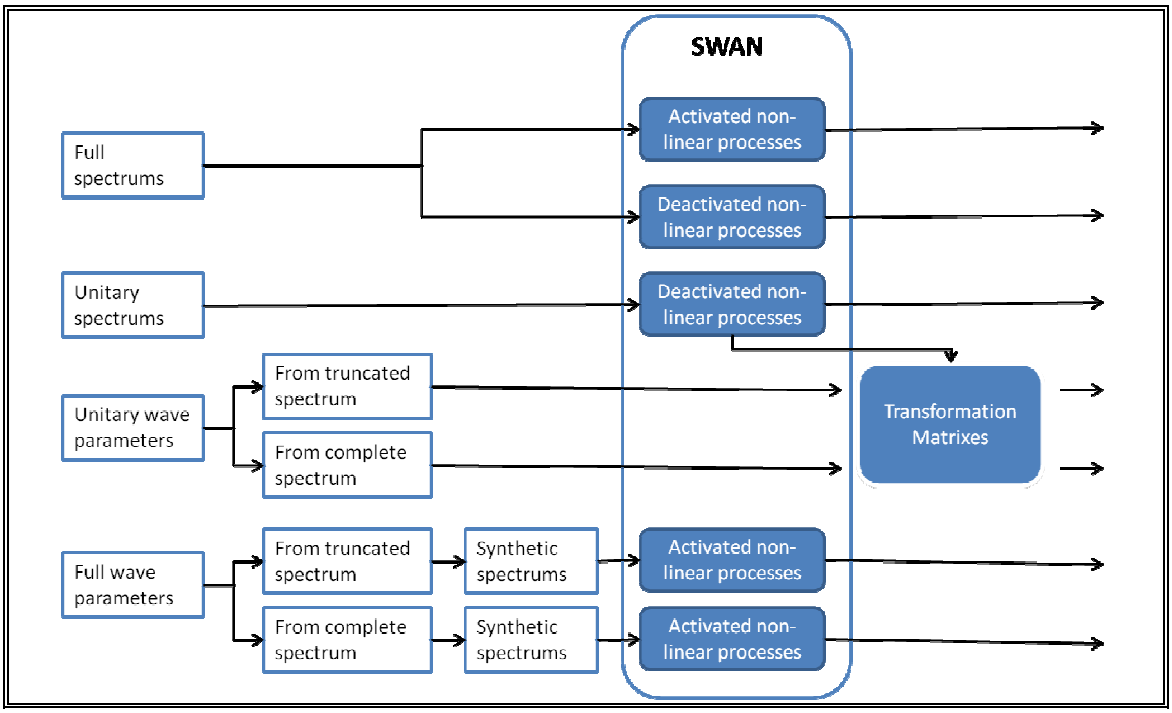

Figure 4-5: Diagram showing a summary of all the simulations.

4.3 Results analysis

After the simulations and the application of the different propagation methods, several comparisons where made: (1) between the full spectrum propagation and the measurements, to test the wave model; (2) between spectral propagation without non-linear processes and the unitary spectrum propagation, to test the proposed method; (3) between wave parameters method (full and unitary) and measurements; and finally (4) between the 4 propagation methods.

4.3.1 SWAN wave model results

For the full spectral propagation, the 245 deepwater spectrums were propagated from the open boundaries of the model to the shallow water node where the measurements were made (Figure 4-1). This was done using (a) activated non-linear processes, (b) deactivated non-linear processes, and (c) deactivated non-linear processes but with depth induced breaking on. Table 4-2 compares the mean relative error between the simulations and the measurements, which is calculated in the following way:

$$\text{Error} = \frac{1}{N}\sum_N \left(\frac{|Y_n - X_n|}{X_n} * 100\right) \quad (4.1)$$

Where X_n are the observations, Y_n are the model's results, and N is the total number of simulations (and observations).

As Table 4-2 shows, the best results are obtained when all non-linear processes are considered; nevertheless, the difference between activating and deactivating these processes in the simulation is not significant, which suggests that non-linear processes are relatively unimportant in this particular case. This is a relevant conclusion because it indicates that, in this case, the proposed method can be applied without distorting the results.

Table 4-2: Mean relative error of simulations compared to the observations for the main wave parameters. Differences between active and inactive non-linear processes are small.

	Significant wave height	Peak period	Peak direction
Non-linear processes activated	10.62%	7.70%	3.59%
Non-linear processes deactivated	11.39%	7.94%	3.58%
Non-linear processes deactivated with breaking	11.34%	7.94%	3.56%

About the results, the mean relative error in the case of significant wave height, peak period and peak direction is relatively small in magnitude, showing that the SWAN wave model is reliable and accurate. Another conclusion from Table 4-2 is that the increased error due to not including depth-induced breaking is minimal, which suggest that this process in particular is not very important in this case. Note that because the water depth is 15 m at the measuring point the breaking is not necessarily happening there, but it can happen in the islands and land projections between the offshore and onshore points (Figure 4-1).

To have an idea of the magnitude of the error, Table 4-3 shows the root mean square (RMS) error and the bias, for the case of deactivated non-linear processes, which are defined in the following way:

$$\text{Error}_{rms} = \sqrt{\frac{1}{N}(Y_n - X_n)^2} \tag{4.2}$$

$$\text{Bias} = \overline{Y_n - X_n} \tag{4.3}$$

It can be seen in Table 4-3 that the RMS error for the main wave parameters is relatively small, even with non-linear processes deactivated. The bias, which is simply the mean error, shows that the model has a tendency to slightly overestimate the wave height and the peak period.

Table 4-3: RMS error and bias of the simulation with deactivated non-linear processes.

	Significant wave height [m]	Peak period [s]	Peak direction [degrees]
RMS error	0.07	1.59	8.01
Bias	+0.02	+0.18	(+3.44)

Figure 4-6 through Figure 4-8 show the difference in wave parameters between the simulation with non-linear processes deactivated and the measurements, for the entire measuring period. In Figure 4-6 and Figure 4-7 (significant wave height and peak period respectively) it is observed that errors occur during short intervals. The erratic behavior of the model in these intervals could be explained by the presence of strong winds. Unfortunately, no wind information was collected during the measuring campaign.

In the case of the peak direction (Figure 4-8), the model results fit with the tendency of the measured directions, but because of the spectral discretization in the directional space (5º in this case), it is not accurate enough. A better comparison could have been done with the mean direction instead of the peak direction, but this information was not available in the measurements.

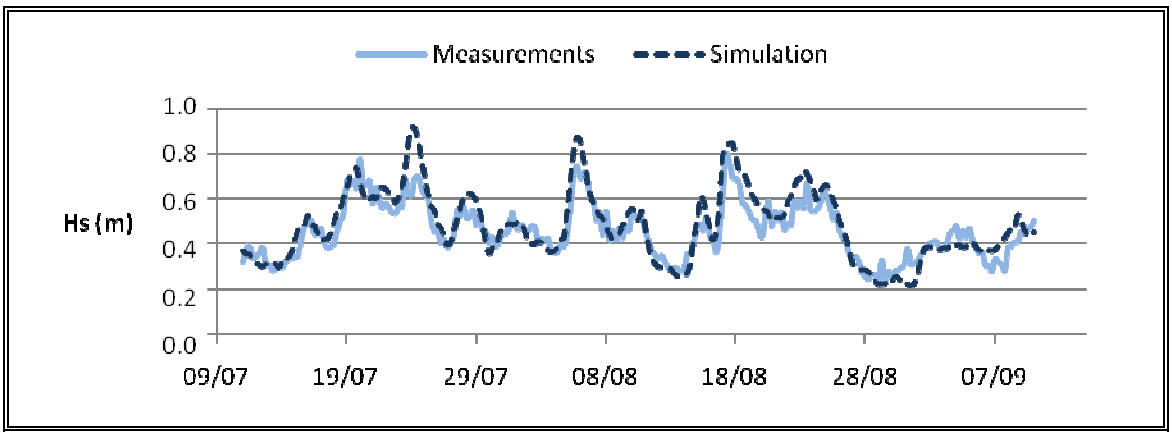

Figure 4-6: Differences in significant wave height between measurements and simulation without non-linear processes for the entire measuring period.

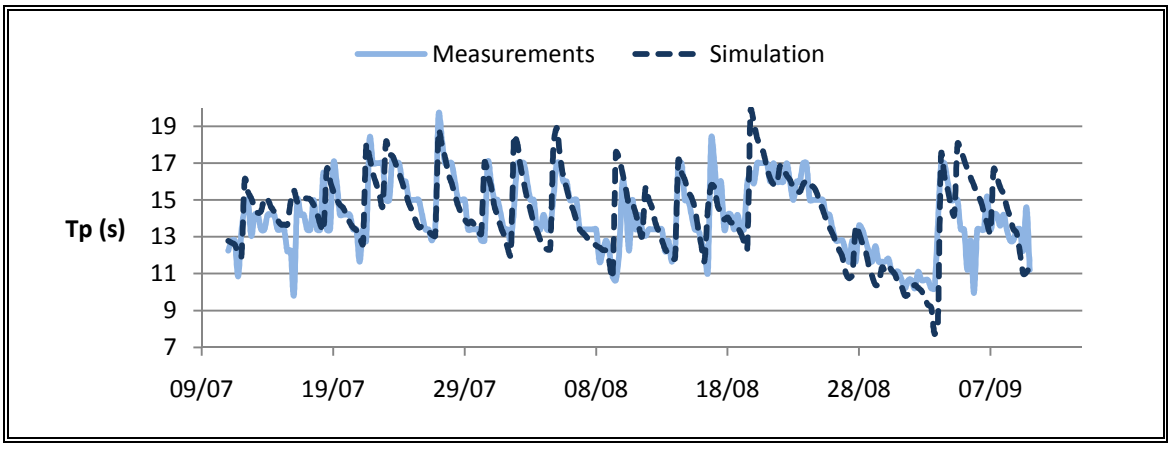

Figure 4-7: Differences in peak period between measurements and simulation without non-linear processes for the entire measuring period.

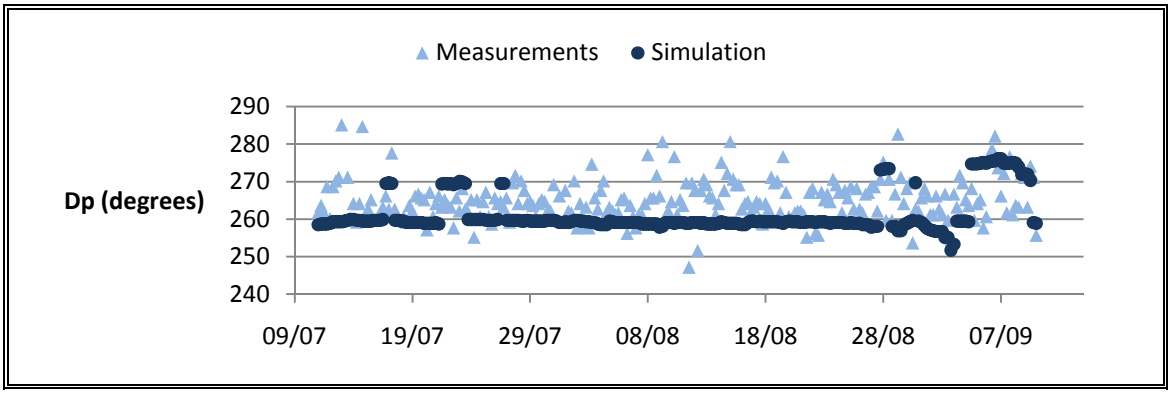

Figure 4-8: Differences in peak direction between measurements and simulation without non-linear processes for the entire measuring period.

4.3.2 Proposed method validation

To test the effectiveness of the proposed method, a comparison was made between the proposed method and the full spectral simulation with non-linear effects off. The reason for this comparison is that, as said before, the unitary simulation is made without non-linear effects; therefore the best possible result for this method is to get the same results than the full spectrum propagation method with non-linear processes deactivated (hence the importance of testing first the relevance of non-linear processes in the problem). The full spectral propagation with non-linear

processes deactivated therefore was used as a benchmark for calculating the errors in the proposed method. The results of this comparison can be seen in Table 4-4. The table shows that the mean relative error incurred when applying the proposed method is smaller than 1% for each wave parameter, which is a very good result.

Table 4-4: Error incurred when applying the proposed method instead of the full spectral propagation with non-linear effects deactivated. Error is smaller than 1% in each wave parameter.

	Significant wave height [m]	Peak period [s]	Peak direction [degrees]	Mean direction [degrees]
Mean relative error	0.80%	0.19%	0.19%	0.51%
RMS error	0.00	0.04	1.16	0.98
Bias	0.00	-0.02	(0.31)	(0.91)

Figure 4-9 through Figure 4-11 show the difference in significant wave height, peak period and peak direction respectively between doing a unitary and a full spectral propagation. Besides an outlier in the peak direction, the differences between both results are barely noticeable.

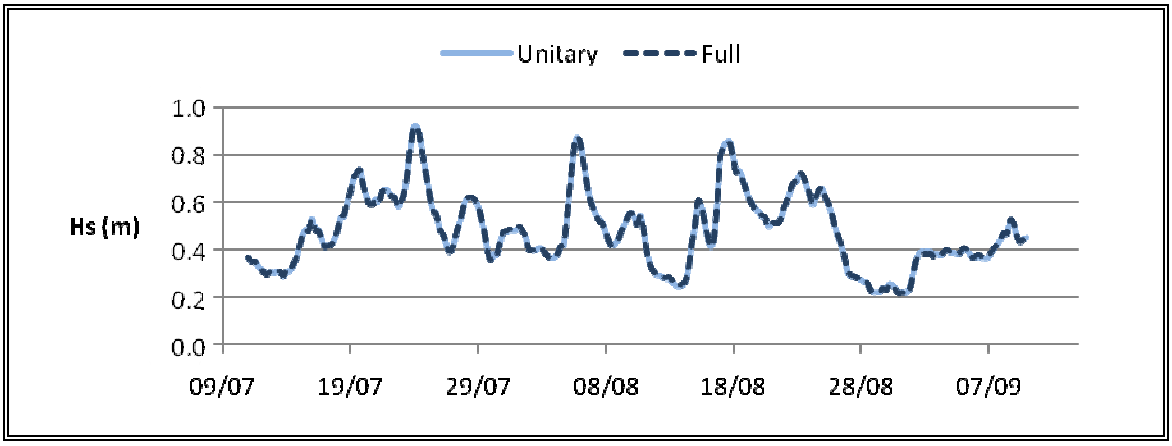

Figure 4-9: Differences in significant wave height between unitary and full spectral propagation.

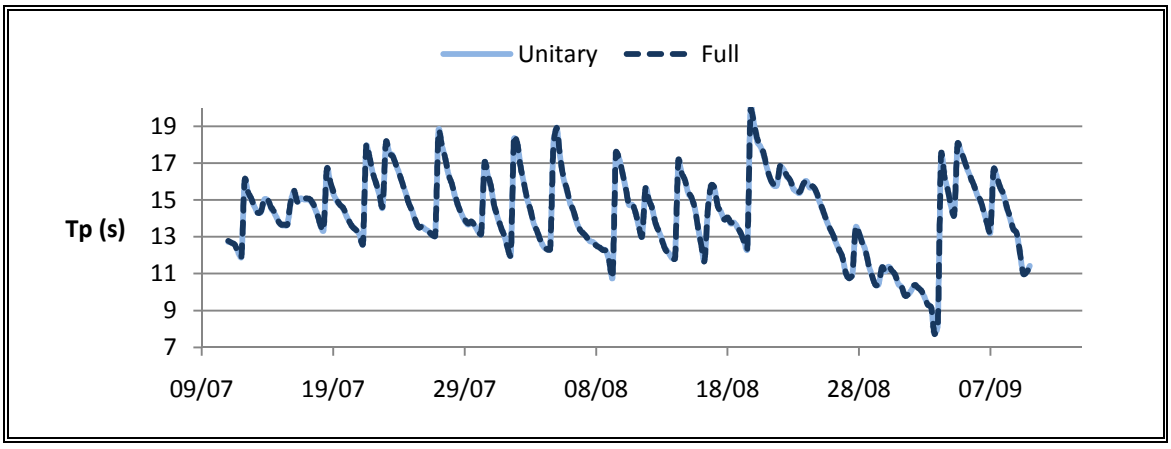

Figure 4-10: Differences in peak period between unitary and full spectral propagation.

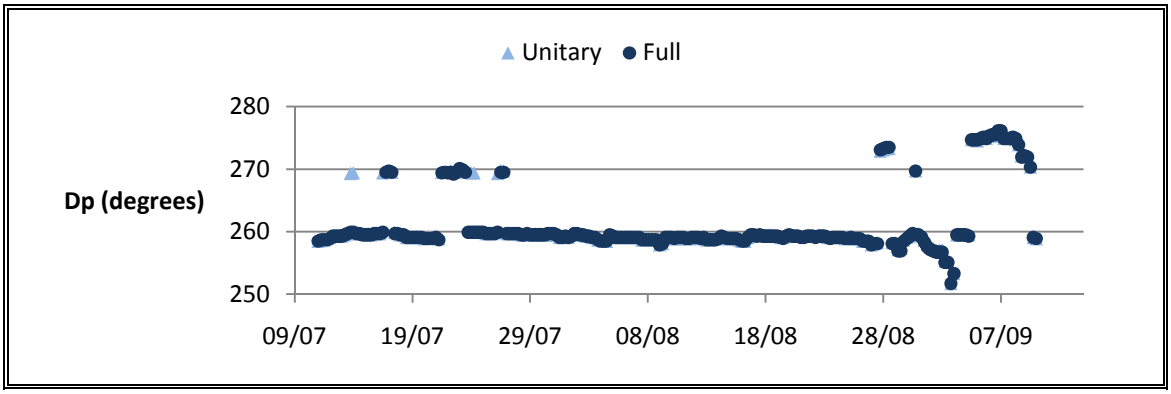

Figure 4-11: Differences in peak direction between unitary and full spectral propagation.

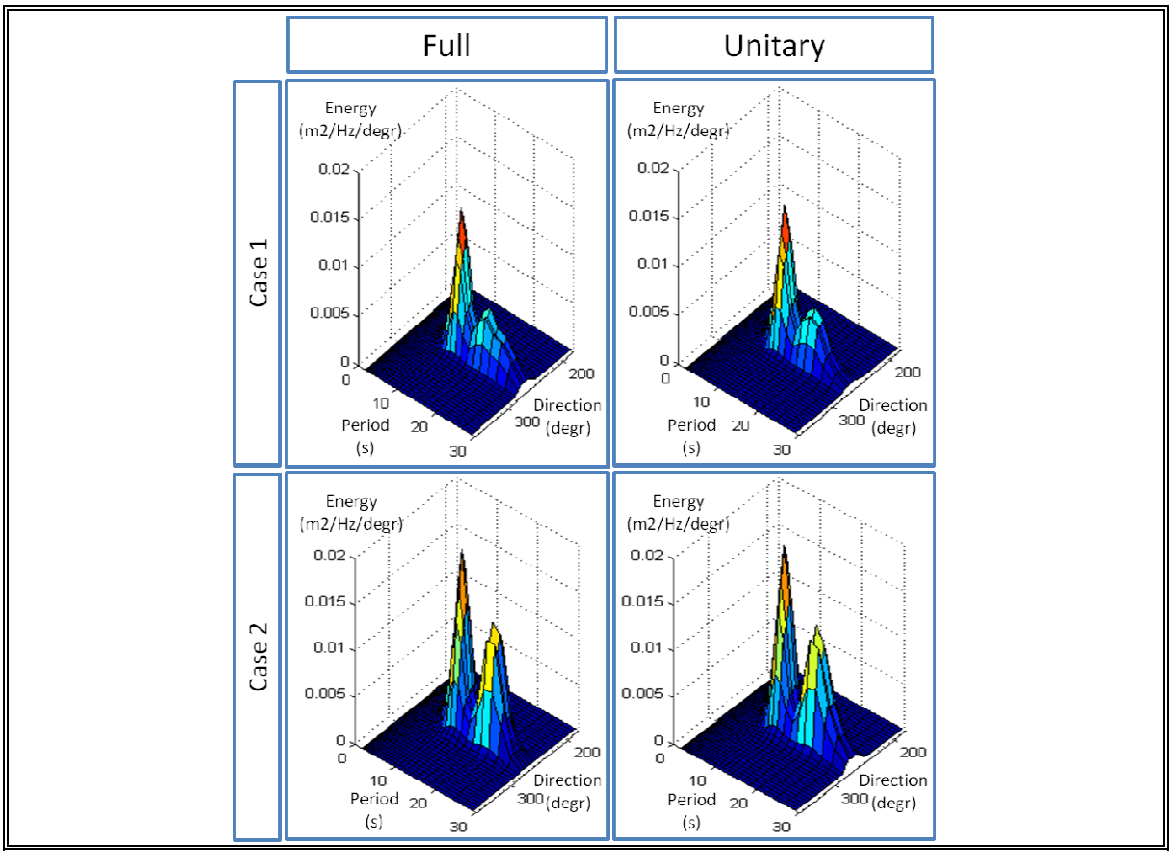

Figure 4-12: Two random cases selected to demonstrate the visual differences in spectral shape between the full and the unitary method propagation. The similarities are visible.

In Figure 4-12, two cases were randomly chosen to inspect the visual differences in the spectrum's shape between the full and the unitary propagation. The figure shows that even in multi-modal cases, the method was able to accurately represent the spectrum's shape. This visual comparison was actually made for every spectrum of the time series (245 in total) throughout a video, but here, only 2 examples are shown. In each of the 245 cases, the visual match was almost perfect. Regarding the advantages of the method, for the unitary method, the total number of propagations was 180; in opposition to the 245 simulations required for the full spectrum propagation method. In this case, the difference is not too big, and it's probably better to propagate the full 245 spectrums and account for non-linear effects; nevertheless, with those 180 unitary propagations, any number of

deepwater spectrums can be transferred, so if a larger spectral database is acquired, the difference grows significantly. As an example, propagating the 20 years data every 3 hours required to make a study in Chile would take 58400 simulations, which is approximately 324 times longer than doing it with the 180 simulations of the unitary method.

Note that when less unitary propagations are used, the results worsen significantly. A simulation was made using the same number of unitary spectrums in the direction (12, coming from a 180º sector every 15º) but half the number of peak period (one peak period every other frequency, i.e. 8 in total), and the mean error of the wave parameters grew above 100%. Visually, the spectrums didn't match. This happened because when these 96 spectrums were superposed, some areas of the direction-frequency domain were barely covered.

4.3.3 Wave parameters results

The goal of making wave parameters simulations is to compare the results of each method. As said before, the deepwater information came in the form of spectrums, therefore, wave parameter (significant wave height, peak period and peak direction) had to be manually extracted from the spectrums. This was done for (1) the complete spectrums, and (2) for the truncated spectrums (where wave parameters were extracted only from the portion of directions traveling to the coast).

For the unitary wave parameters propagation, the same unitary spectrums from the unitary spectrum propagation method were used. Once each unitary spectrum was propagated, a matrix containing the resultant wave heights and another containing the resultant directions for each propagation were constructed. With these matrices, a record containing the wave parameters in shallow water was created for both types of wave parameters (from complete and from truncated spectrum). The transformation matrices, when plot, are shown in Figure 4-13.

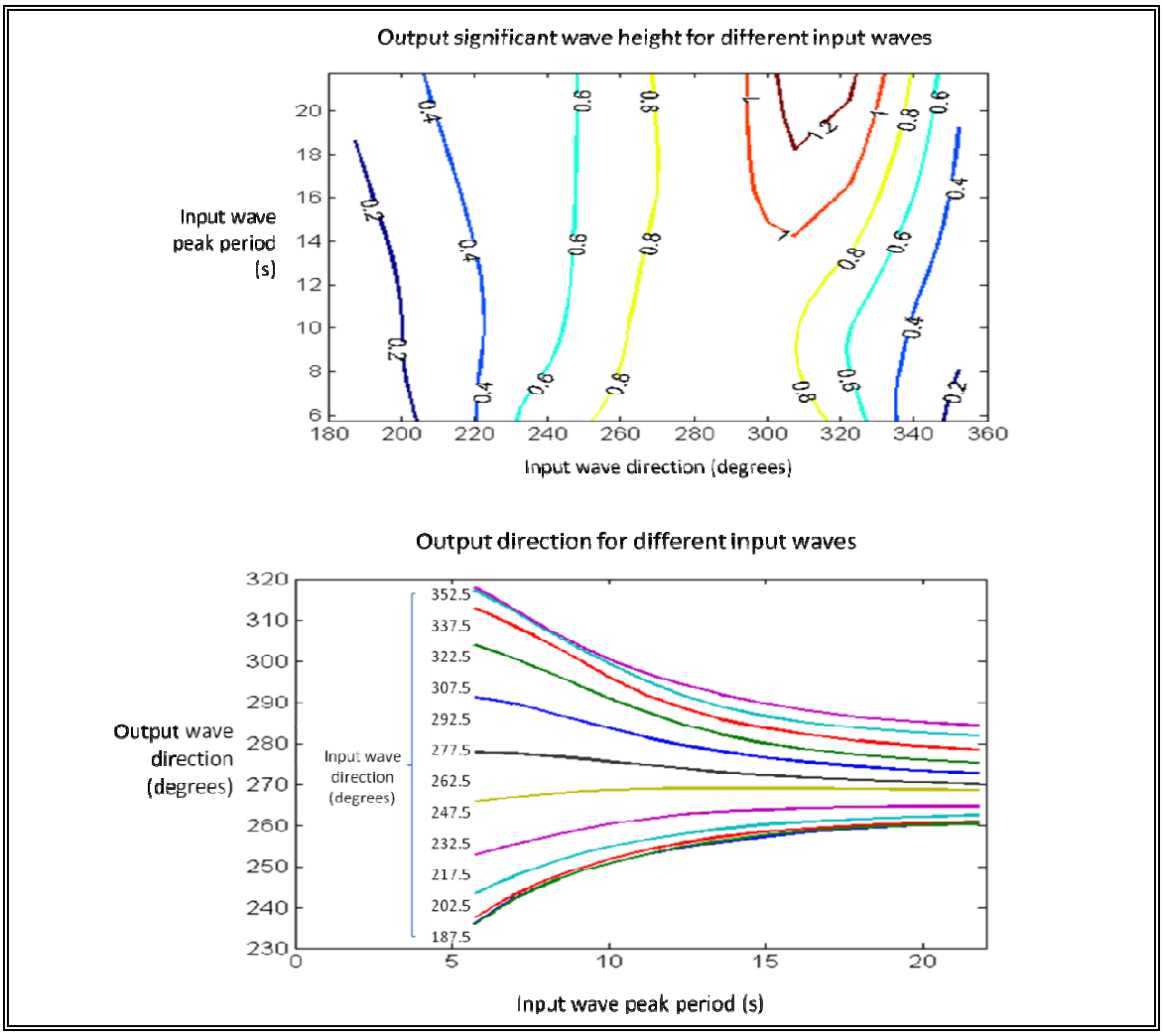

Figure 4-13: Plot of the transformation matrices for the significant wave height and the mean wave direction. The peak period is not transformed but maintained.

In the case of the full wave parameters propagation, 245 synthetic spectrums, constructed with wave parameters taken from the complete and the truncated deepwater spectrums, were propagated, using activated non-linear processes.

The mean relative error between the wave parameters propagations and the measurements can be seen in Table 4-5.

Table 4-5: Comparison of the wave parameters propagation methods in means of average relative error. The way wave parameters are extracted have a deep impact in the results.

Type of propagation	Wave parameters	Significant wave height	Peak period	Peak direction
Unitary	Taken from a truncated spectrum	15.55%	11.88%	5.86%
	Taken from the complete spectrum	28.99%	10.11%	5.62%
Full	Taken from a truncated spectrum	40.44%	12.01%	4.19%
	Taken from the complete spectrum	46.42%	18.81%	4.62%

The first thing to notice from Table 4-5 is the relevance in the way wave parameters are extracted. In this particular case, taking the wave parameters directly from the complete spectrum brings significantly worse results than taking them from the truncated spectrum. This happens for the unitary and the full wave parameters method. The reason of this difference, in the case of Ancon, is that a considerable amount of energy in the spectrums doesn't reach the coast, and instead, propagates offshore (Figure 4-3).

If the complete spectrum is considered for calculating wave parameters, the wave parameters are averaged in the whole spectrum, and this can lead to assume that all the energy contained in the spectrum will travel towards the coast. On the other hand, by truncating the spectrums, only the portion of energy that travels toward the coast is being considered, which represents a much better approximation of the incident waves the coast will get. If most of the energy in the spectrum is traveling onshore, the difference between the wave parameters obtained through the complete spectrums and through the truncated spectrums shouldn't differ much.

In the case of the unitary wave parameters propagation, when the complete spectrum was used for obtaining wave parameters, only 56% of the deepwater data

could be propagated; in the other 44%, the resultant mean direction extracted from the spectrum pointed offshore, and therefore, the method couldn't be applied (the significant wave height would've been 0). As a result, the information in Table 4-5 only considers this 56% of the cases.

The second thing to notice from Table 4-5 is the difference between the full and the unitary methods. Contrary to the belief, the unitary wave parameters method delivered better results than the full wave parameters method. This outcome is further discussed in section 4.3.4.

To have an idea of the magnitude of the error, the RMS error and bias are also presented. Again, for the unitary method with full spectrum extraction, only 56% of the data is used. The bias indicates that the 2 methods underestimate in this case the significant wave height and peak period.

Table 4-6: RMS error of the wave parameters propagation.

Type of propagation	Wave parameters	Significant wave height [m]	Peak period [s]	Peak direction [degrees]
Unitary	Taken from a truncated spectrum	0.08	2.59	12.39
	Taken from the complete spectrum	0.15	2.51	11.43
Full	Taken from a truncated spectrum	0.22	2.63	9.27
	Taken from the complete spectrum	0.27	3.77	9.87

Table 4-7: Bias of the wave parameters propagation.

Type of propagation	Wave parameters	Significant wave height [m]	Peak period [s]	Peak direction [degrees]
Unitary	Taken from a truncated spectrum	-0.03	-1.49	(-10.38)
	Taken from the complete spectrum	-0.13	-1.32	(-9.96)
Full	Taken from a truncated spectrum	-0.02	-1.49	(-6.90)
	Taken from the complete spectrum	-0.03	-2.58	(-7.93)

4.3.4 Comparison between the 4 propagation methods

The comparison between the 4 propagation methods is made by using the mean relative error of the resulting wave parameters as an indicator. In this way, the error of the different wave parameters can be compared in the same scale (Figure 4-14).

For the full spectrum propagation, the case with activated non-linear processes was chosen for being the most favorable case. In the case of the wave parameters propagation (both, full and unitary), the wave parameters from the complete spectrums were considered for the comparison, for being the standard form of extraction. It is important to notice though, that in the case of Ancon, this is particularly unfavorable (as seen before (Figure 4-3), a lot of the energy in the spectrum doesn't get to the coast).

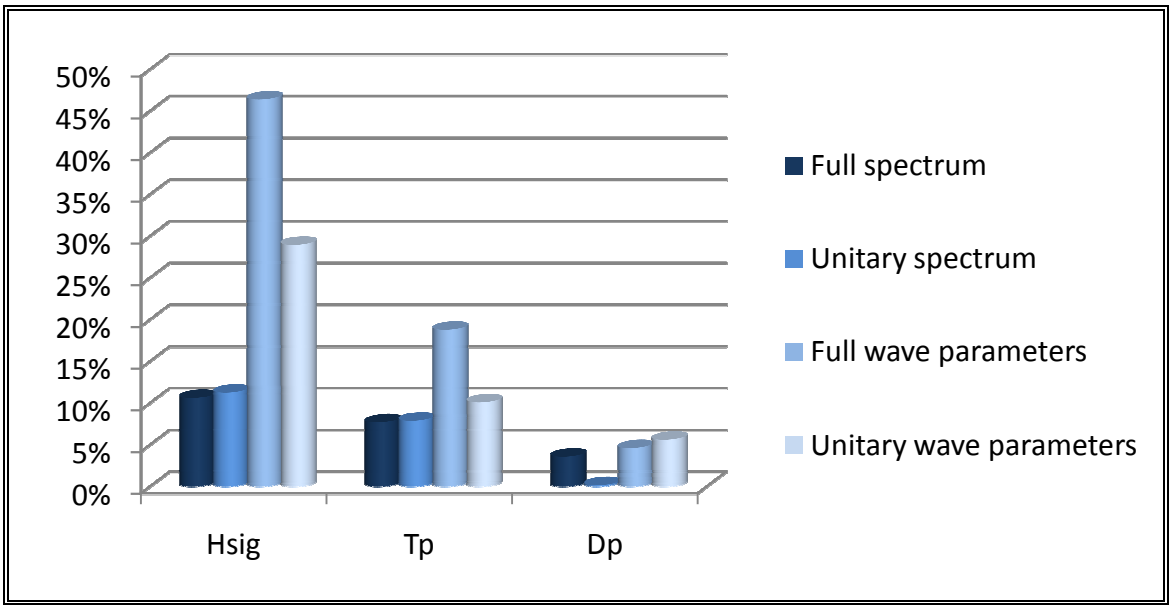

Figure 4-14: The 4 propagation methods compared by means of average relative error in the wave parameters.

One of the conclusions from the comparison, beside the fact that the spectral propagations are better, is that the unitary wave parameters propagation gives better results than the full wave parameters propagation, which wasn't expected. The full wave parameters propagation includes non-linear effects and calculates the peak period, while the unitary wave parameters method doesn't include these effects and assumes that the period doesn't change from deep to shallow water; thereby, the full wave parameters method should deliver the best results. This unexpected behavior may have occurred due to a bad selection of the energy distribution for building the synthetic spectrums from the wave parameters; but what's more important, it exemplifies that full wave parameters propagation is not always better than unitary wave parameters propagation.

Another conclusion derived from this comparison is that the error incurred when using the proposed method is explained mostly for not including non-linear effects. The error added for using this method instead of the full propagation with non-linear processes deactivated is negligible. Besides, the increase of error for not

including non-linear effects is far compensated in this case by the reduced calculation time, which is the method's purpose.

Finally, it is important to recall that both spectral propagation methods not only give results in means of wave parameters but they also deliver the resulting spectrum, which is a much better and complete type of information.

5. PROPOSED METHOD APPLICATION

To exemplify the use of the proposed method and to further verify its validity, an application of the method is made in another site of study. This application also intends to further compare the different propagation methods described in this paper.

5.1 Test case description

In 2009, the University of Valparaiso (Chile) carried out a study for HydroChile S.A. to determine the energy potential of the wave resources along the Chilean coast (Universidad de Valparaiso, 2009). One of the modeled sites was Curaumilla, a cliff-like point located south of the city of Valparaiso. The site had good bathymetric information as well as deepwater spectral information, which is why it was chosen to be modeled in this study.

The bathymetry for the modeling was extracted from navigational charts which due to the proximity of a port presented high-quality information. The spectrums where obtained from a 6 years database hindcasted by Fugro-Oceanor, with information every 3 hours.

Because, in this case, the propagation of the full spectrums for the 6 years period is very long, the unitary spectral propagation method was chosen. Prior to the application of the method, the relevance of non-linear processes for this case is estimated.

5.2 Simulation

For the simulation of this test case, the spatial and spectral discretization shown in Table 5-1 was used. The problem domain, along with the bathymetry provided by HydroChile S.A., is shown in Figure 5-1. The spectral information for the grid boundaries was taken from a previous run in a coarser grid (1000 x 1000 m cells). Spectral information was then extracted in 3 points located at 50, 20 and 10 meters of water depth, also shown in Figure 5-1.

Table 5-1: Spatial and spectral resolution used in the simulation.

Spatial resolution			
X length [m]	Y length [m]	Delta X [m]	Delta Y [m]
20,000	20,000	50	50

Spectral resolution				
Min frequency [Hz]	Max frequency [Hz]	Delta frequency	Direction range [degree]	Delta θ [degrees]
0.035	0.55	0.1 * f_i	180 – 360	5

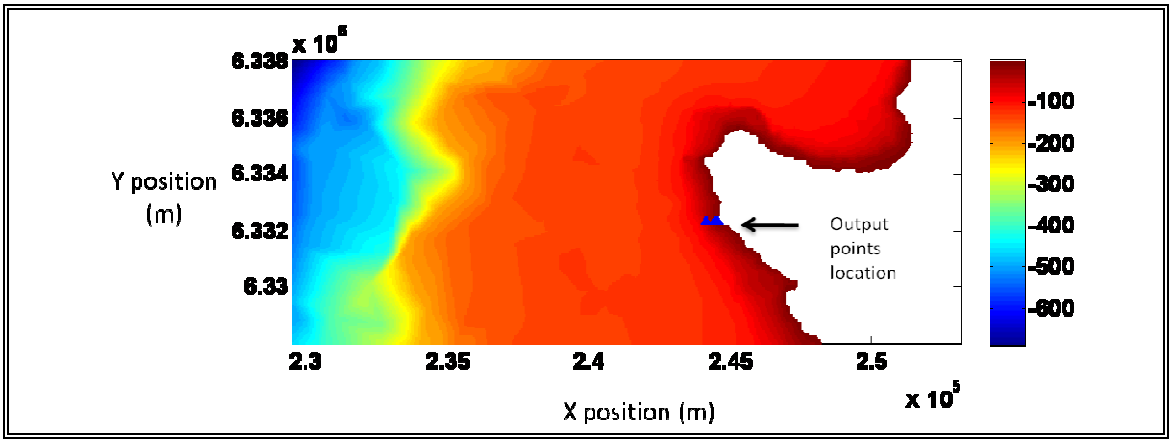

Figure 5-1: Curaumilla's bathymetry and location of output points.

For the construction of the unitary spectrums, an analysis of the deepwater spectrums was previously carried out to determine the range of the peak periods (i.e. maximum and minimum) in the entire registry. It was found that in this case, the peak periods ranged between the 23.9 and the 4.7 seconds, resulting in 18 different peak periods for the unitary spectrums (considering one peak period for each frequency bin of the spectrum). This gave a total of 216 unitary spectrums (18 peak periods x 12 directions; with one direction every 15° for a 180° sector). The energy for the unitary spectrums was distributed using a JONSWAP with $\gamma = 3.3$ and a Goda & Susuki with $s_{\max} = 60$ distribution in the frequency and direction domain respectively, with a significant wave height of 1 meter for each. These unitary spectrums where used for the unitary spectrum propagation method and the unitary wave parameters propagation method.

In the case of this study, as said before, propagating all the spectrums of the deepwater database is significantly long. For this reason, to test the unitary method, only 6 spectrums were selected from the registry to undergo the full propagation. The selection of these spectrums followed the same selection proposed by the University of Valparaiso (2009), which considered: (a) two of the most probable spectrums during summer, (b) two of the most probable spectrums during winter, (c) a bimodal spectrum, and (d) a trimodal spectrum. The selecting of (a) and (b) was made by identifying the most probable period-direction pair during the mentioned seasons and then picking 2 spectrum with these characteristics from the registry; the selection of (c) and (d) was made visually by analyzing the whole series through a video. These spectrums were used to make the full spectral propagation, with and without activated non-linear processes. They can be seen in the appendices. The wave parameters for these spectrums are shown in Table 5-2.

Finally, for the full wave parameters propagation, synthetic spectrums with the same energy distribution as the unitary spectrums were created using the wave parameters extracted from the complete (not truncated) spectrums in deepwater. These wave parameters were also used for the unitary wave parameters method.

Table 5-2: Wave parameters for incident deepwater spectrums.

	Significant wave height (m)	Peak period (s)	Peak direction (degr)
Trimodal	2.58	15.98	229.7
Bimodal	4.30	14.28	222.1
Summer 1	2.68	12.37	223
Summer 2	2.89	12.12	218.7
Winter 1	2.71	13.17	236.2
Winter 2	2.46	14.19	232.2

5.3 Comparison of propagation methods

As no measured data was available for this test, the results of each method are compared between themselves. It may be assumed though that the full spectral propagation with non-linear processes activated (depth-induced breaking, triads, bottom friction and whitecapping) is the most accurate method.

The first necessary comparison is to measure the importance of non-linear processes in this particular case. For this, two simulations were carried out for the 6 chosen deepwater spectrums, one with, and one without non-linear processes. The results for the 10 meters water depth point are shown in Figure 5-2. The graph shows for each spectrum the relative difference between the wave parameters of the case without non-linear processes and the case that considers these processes. For the mean wave direction, a 180º difference represents 100% error.

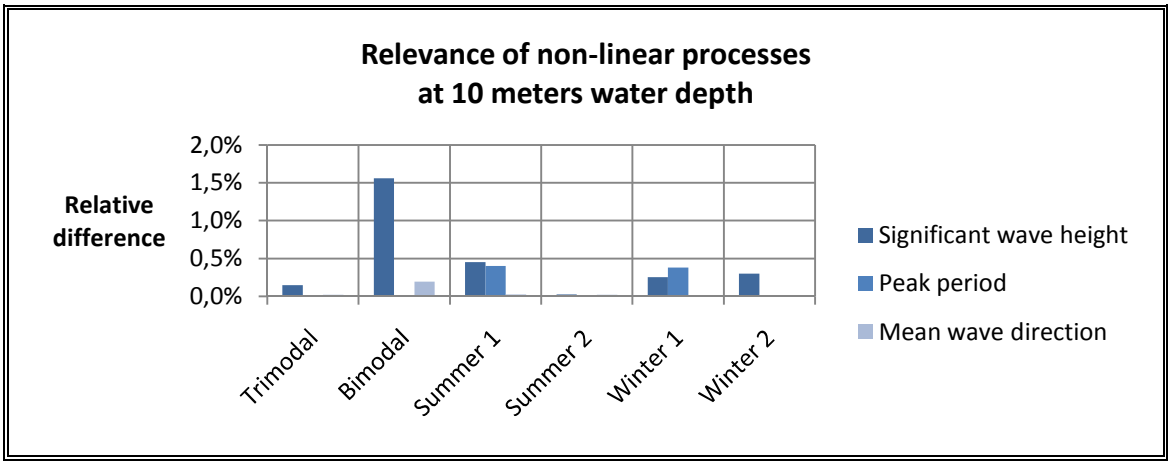

Figure 5-2: Difference in wave parameters between considering or not non-linear processes, at the 10 meters water depth point. All results bellow 1.5%.

As Figure 5-2 shows, the biggest difference occurs in the bimodal case (which is also the most energetic) for the significant wave height, but it doesn't get over 1.6%. In the other cases, the relative differences are below 0.5%. In the 50 and 20

meters points (shown in the appendices), the differences are even smaller. Although only 6 representative cases were used, there is enough evidence to conclude that non-linear processes are not significantly important in this case, and therefore, the unitary propagation method can be used.

The second comparison is done between the spectrums produced with the proposed method (i.e. the unitary spectrum propagation method) and with the full propagation with deactivated non-linear processes, for the 6 chosen deepwater spectrums. This comparison is essential because it tests if the proposed method is giving good results. Furthermore, in this case, it serves to verify the method's validity in a different scenario.

Figure 5-3 shows the relative difference between the unitary method and the full propagation (with non-linear processes not active) at the 10 meters water depth point. This gives an idea of the distortion in wave parameters when applying the proposed method. It is seen that for every case, the differences between these two methods is barely 0.5%.

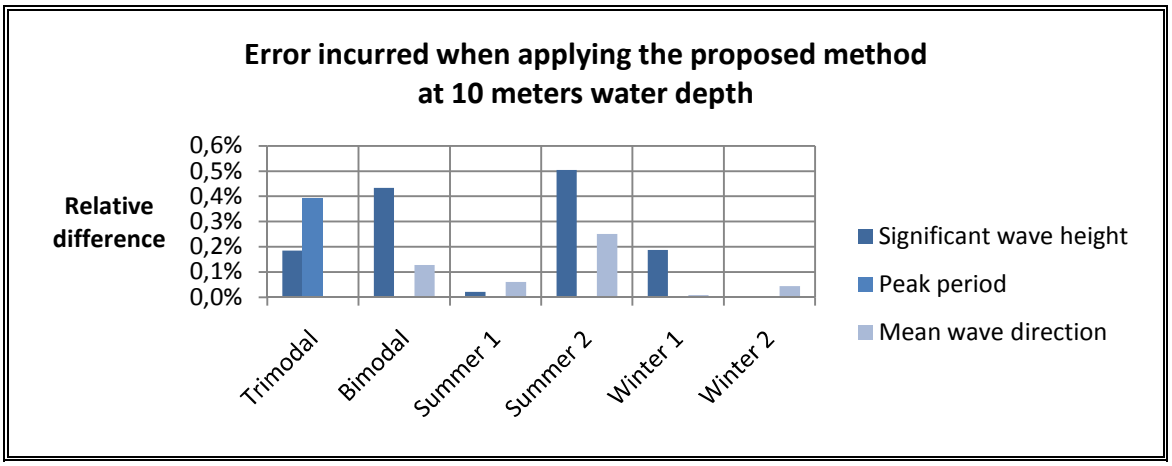

Figure 5-3: Difference in wave parameters when applying the proposed method instead of the full propagation with deactivated non-linear processes. All differences are below 0.5%.

In the case of the spectrums' shape, Figure 5-4 and Figure 5-5 show the output spectrums for the unitary method and for the full propagation, with and without non-linear processes, in the 10 meters water depth point. In this case, only the trimodal and bimodal cases are shown for being the most complex. The bimodal case also represents the most energetic case (Table 5-2). Visually the differences are barely noticeable. Again, at the 50 and 20 meters points, the differences were even smaller.

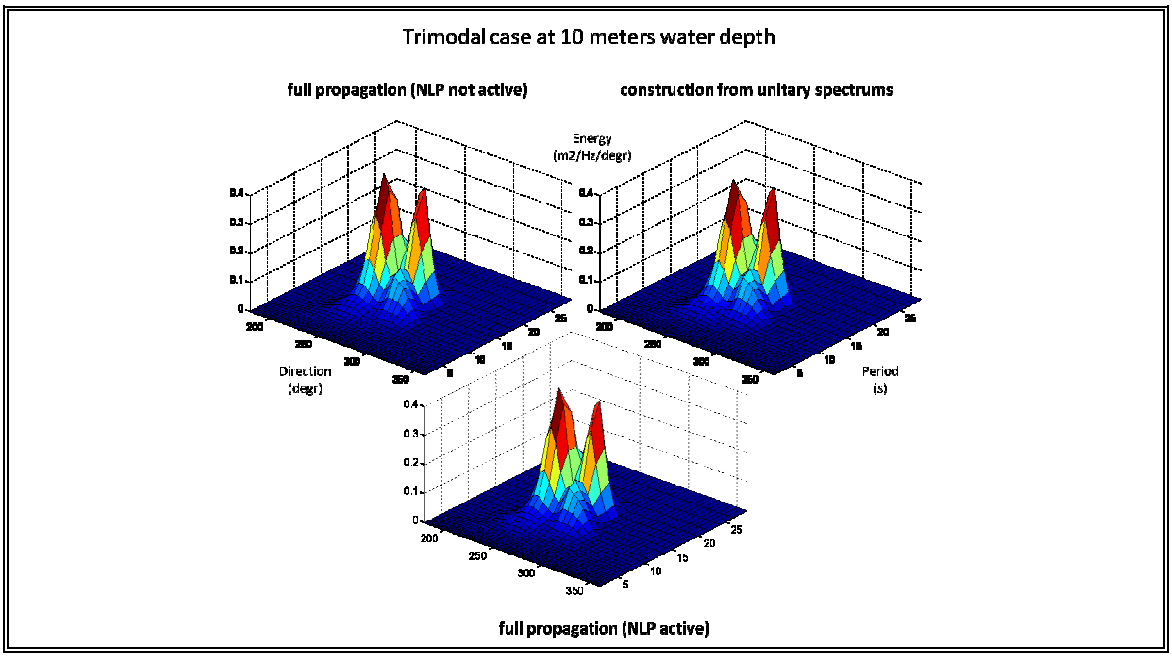

Figure 5-4: Visual comparison of output spectrums for the trimodal case at 10 meters. NLP stands for Non-Linear Processes.

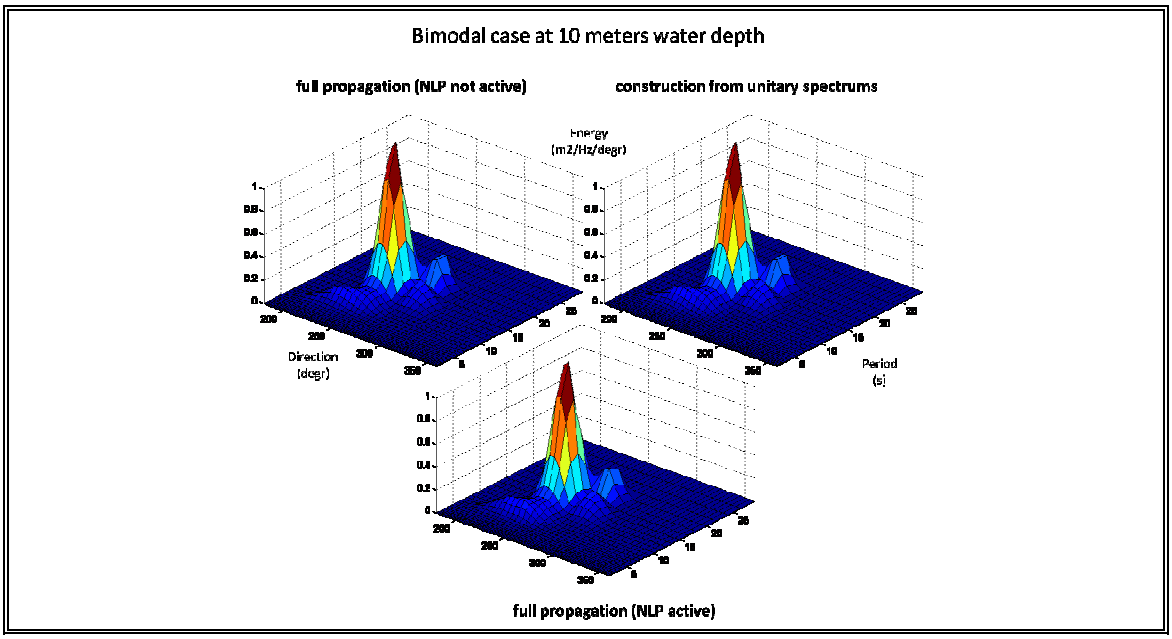

Figure 5-5: Visual comparison of output spectrums for the bimodal (and most energetic) case at 10 meters. NLP stands for Non-Linear Processes.

Finally, a comparison between the 4 propagation methods is made taking into account only the resulting wave parameters. Figure 5-6 shows the output wave parameters at the 10 meters water depth point for the 6 chosen cases. The full spectrum propagation shown here considers non-linear processes. It can be seen that both spectral methods behave similar. The same happens between both wave parameters methods. The main difference between spectral and wave parameters propagation is the tendency from the wave parameters methods to overestimate the wave height and underestimate the peak periods when compared to the spectral propagation. In this example it can also be seen that, in most cases, the full wave parameters method is closer to the spectral propagations' results than the unitary wave parameters method. In the case of the mean wave direction, the 4 methods behave similar, with differences of less than 3 degrees (although not much refraction occurs in this test case). The differences at 20 and 50 meters water depth for the 3 wave parameters were smaller (Appendix C).

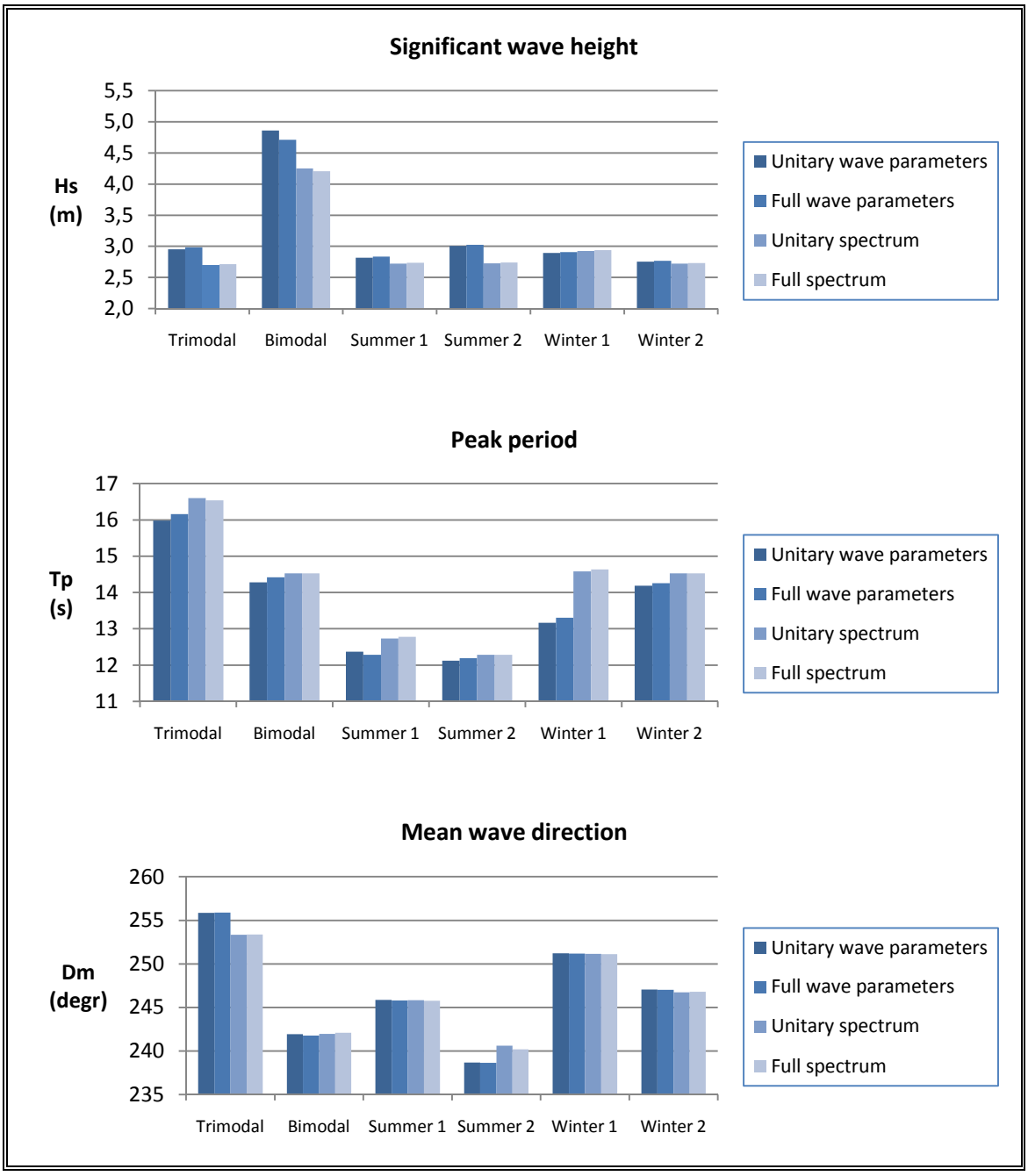

Figure 5-6: Difference in wave parameters from different propagation methods at 10 meters water depth.

5.4 Application

The purpose of this application is to determine the wave energy resource in a specific site in the coast of Chile, following the study prepared by Universidad de Valparaiso in 2009. Once the entire 6 years spectral database is transferred from deep to shallow water (specifically to the points located at 50, 20 and 10 meters of water depth) and the spectrums are reconstructed using the unitary spectral method, the wave power is calculated from the spectrums in the following way (Monárdez et al., 2008):

$$P = \rho g \int_0^{2\pi} \int_0^{\infty} E(f,\theta) C_g(f,h) df d\theta \qquad (5.1)$$

With P being the mean wave power (defined as the mean energy transfer rate per unit width through a vertical plane perpendicular to the direction of waves, in units of W/m), ρ being the water density (kg/m^3), g the gravitational acceleration (m/s^2), $E(f,\theta)$the variance density spectrum (in units of m^2/Hz/degree) and $C_g(f,h)$ the group velocity (in m/s), equal to equation (2.21). For the calculation of k in equation (2.21), the dispersion relation is used (equation (2.17)).

To determine the mean wave power, only the sites located at 50 and 20 meters water depth were used. The site at 10 meters depth was discarded because: (1) it is probable that non-linear processes which are not being considered and that result in a loss of wave energy are acting (e.g. bottom friction, breaking), and (2) several studies have proven that the wave power decreases towards the coast (Monárdez et al., 2008; Folley & Whittaker, 2009) which makes the 10 m point less relevant for an offshore Wave Energy Conversion (WEC) Device (more info in Previsic et al., 2004). Although wave power can decrease towards the coast, other parameters such as directional spreading (which decreases towards the coast due to refraction) and distance to the shore (which can directly affect the costs) can make the 10 m point attractive depending on the WEC device employed. For the purpose of this application though, the gross mean wave power is the only relevant parameter.

The box plots in Figures 5-7, 5-8, 5-9 and 5-12 show the 25th, 50th and 75th percentiles, while the whiskers represent the 2nd and 98th percentiles.

Figure 5-7 shows the mean wave power calculated from the spectrums for the 6 years of information at 50 m and 20 m water depth. It can be noticed that at 50 m the mean wave power is approximately 34 kW/m and it slightly decreases towards the coast, reaching 32 kW/m at 20 m (an approximately 6% reduction).

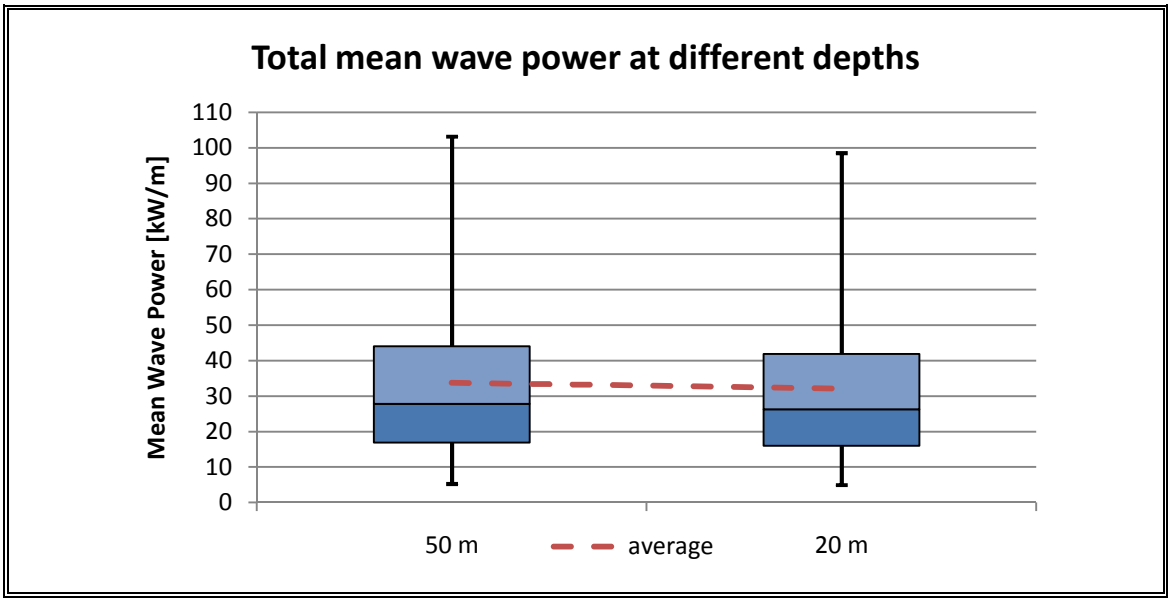

Figure 5-7: Box plot showing the total mean wave power and percentiles calculated from spectrums at different depths. Wave power decreases 6% towards the coast.

The main cause for the power reduction when varying depth according to Folley & Whittaker (2009) is refraction. Bottom friction and wave breaking typically results in a loss of less than 10% of the gross wave energy from 50 m to 10 m depth (Folley & Whittaker, 2009). In this case, bottom friction, wave breaking and other non-linear processes are not represented, so all the energy loss should correspond to the reduction in wave height due to refraction. This effect can be compensated if a site that focalizes the wave energy is chosen (e.g. headlands ans capes) (Monárdez et al., 2008).

With the results at the 50 m water depth point, the annual and montlhy variability of the mean wave power was analysed. Figure 5-8 shows the variation in mean wave power through the year, taking for the calculation the average wave power for each month in the 6 years of information. It can be noticed that the mean wave power has a small seasonal variation, having its maximum during winter (May through August) and its minimum during summer (November through February), with a mean of 33.8 kW/m during the year (dashed line). The difference between the maximum (Jun, 41.6 kW/m) and the minimum (Dec, 27.6 kW/m) is less than 34%, showing that the site has a stable energy condition. Moreover, the 25th percentile never descends the 15.5 kW/m, which indicates that 75% of the time a WEC device could be operating with this available gross power. The 98th percentile shows extreme events, specially occurring during autumn, winter and fall. Notice that this statistics were calculated with only 6 years of information.

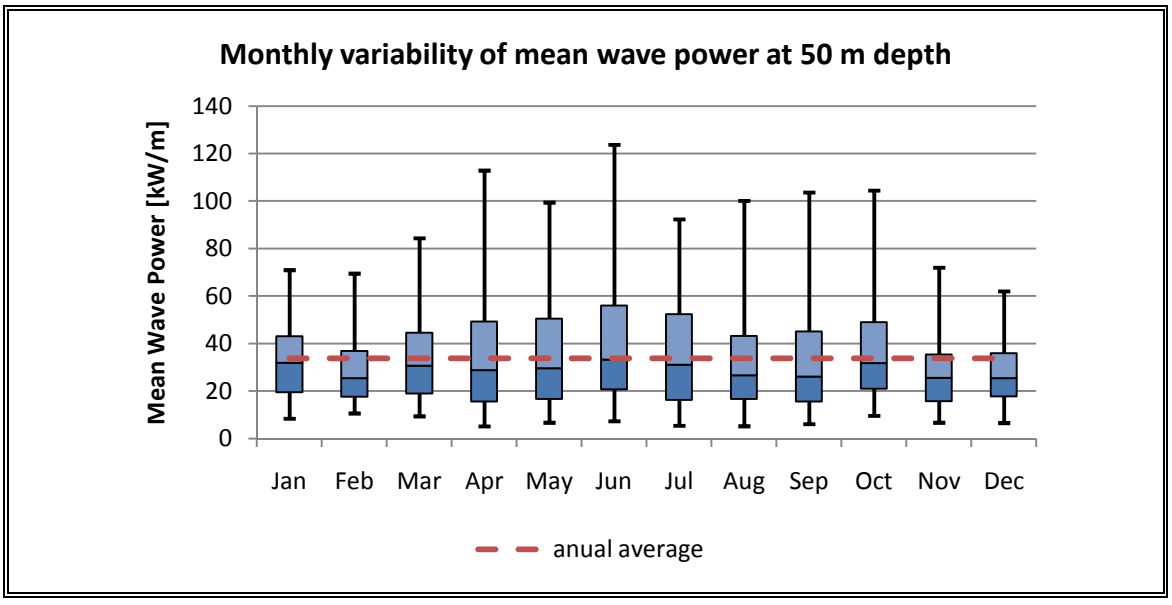

Figure 5-8: Monthly variation of the mean wave power and its percentiles. There is small variation through the year, with max in winter and min in summer.

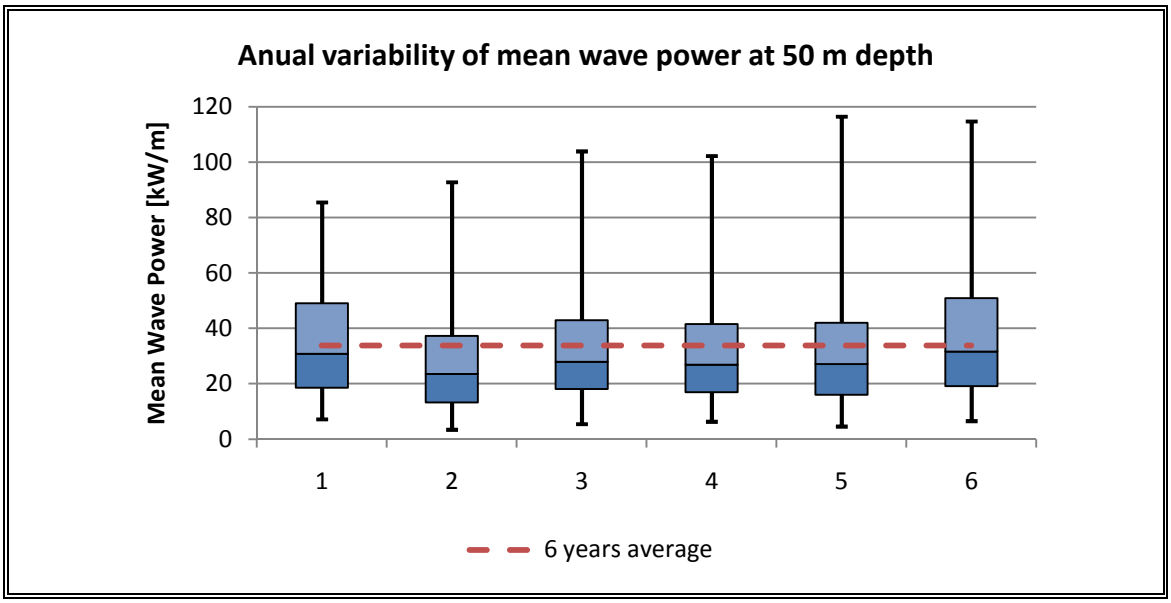

Figure 5-9: Annual variation of the mean wave power and its percentiles. Difference between years is visible.

Regarding the annual variability of mean wave power, Figure 5-9 shows that the variation is significant. The average mean wave power during these 6 years is 33.8 kW/m, while in the less energetic year it descends to 28 kW/m and in the most energetic year it ascends to 39 kW/m. It is therefore important to have more data to make a good estimation of this variation (one of the reasons that SHOA requires a 20 year long database for the approval of studies of oceanographic nature (SHOA, 2005)).

Now, to demonstrate the importance of spectral information in determining the wave power, the wave power was also determined using the summarized statistical wave parameters (in particular, H_s, T_p and mean wave direction). Notice that these wave parameters were calculated from the spectrums obtained in the unitary spectrum propagation, not the unitary wave parameters propagation (which, as seen, tends to overestimate H_s). The mean wave power using wave parameters is (ABP Marine Enviromental Research Ltd, 2008):

$$P = 0.0623 \rho g H_s^2 C_g \qquad (5.2)$$

Where H_s is the significant wave height (in meters). This formula comes from the typical wave power equation (see equation (2.20)) with the difference that H_s is used instead of H, according to the following relation (Goda, 2000):

$$H = H_{rms} = \frac{H_S}{1.416} \tag{5.3}$$

The reason for not using directly H_s in equation (2.20) is that by definition H_s represents the mean wave height of only the highest one third waves, and for the energy power calculation all waves have to be considered. This is properly represented with parameter H_{rms} (ABP Marine Enviromental Research Ltd, 2008).

For the calculation of C_g another transformation has to be made to replace the peak period T_p with the energy period T_e, which is a more accepted statistic for wave power calculation (ABP Marine Enviromental Research Ltd, 2008). The energy period is defined as (Universidad de Valparaiso, 2009):

$$T_e = m_{-1}/m_0 \tag{5.4}$$

With,

$$m_n = \int m^n E(f) df \tag{5.5}$$

Where m_n represents the nth moment of the variance density spectrum $E(f)$.

The reason for using the energy period (instead of the mean period for example), is that it gives more weight to the longer periods and less weight to the shorter periods, which is useful if a WEC device is to be used (which is unable to get energy from short periods) (Universidad de Valparaiso, 2009).

Of course equation (5.4) can be used only if the variance density spectrum is available. If that is not the case, a relation between the peak period T_p and the energy period T_e must be used. ITTC(2002) presented the following relation:

$$T_e = (0.8255 + 0.03852\gamma - 0.005537\gamma^2 + 0.0003154\gamma^3)T_p \tag{5.6}$$

Where γ represents the peakness factor in the JONSWAP spectrum (Hasselman et al., 1973). Because the peakness factor is not known (in the case only wave parameters are available) the relation between the peak period and the peakness factor shown in Table 5-3 can be used (Smith et al., 2001).

Table 5-3: Gamma parameter as a function of peak period (Smith et al., 2001)

T_p(s)	10	11	12	13	14	15	16	17	18	19	20
γ	3.3	4	4	5	5	6	6	7	7	8	8

The methodology will therefore be, for every pair $[H_s, T_p]$: (1) Calculate γ from Table 5-3; (2) Calculate the energy period T_e from equation (5.6); (3) Calculate C_g from equation (2.21) (using the dispersion relation [eq. 2.17] to find k); and (4) Calculate the mean wave energy in equation (5.2). This methodology is similar to the one used by Acuña(2008).

Figure 5-10 shows the difference between spectral an parametrical calculation of the mean wave power in the 6 years of information, for the 50 m and the 20 m water depth sites. The parametrical calculation used by Acuña (2008) overestimates the mean wave power in approximately 12%. This significant difference may be explained by the bimodal characteristic of the spectrums in Chile (Nicolau del Roure, 2004). Statistical wave parameters (H_{sig} and T_p) concentrate all the energy in the peak period, which has a direct impact in the calculation of the group velocity (C_g), and therefore, the mean wave power (equation (5.2)). Besides, the calculation of the energy period (T_e) is based on 2 approximations: the use of equation (5.6) and the use of Table 5-3. Another approximation is made regarding the transformation between H_{sig} and H_{rms}. All these approximations may not be suitable for the wave characteristics in the site of study.

Notice that the difference in mean wave power estimation in this case comes only from the data source (i.e. spectral or parametric calculation of the mean wave

power). This does not include the added error of the propagation type (spectral vs. parametric), which overestimates the significant wave height. The result of a parametric propagation plus a parametric wave power estimation therefore could increase even more the difference in wave power estimation.

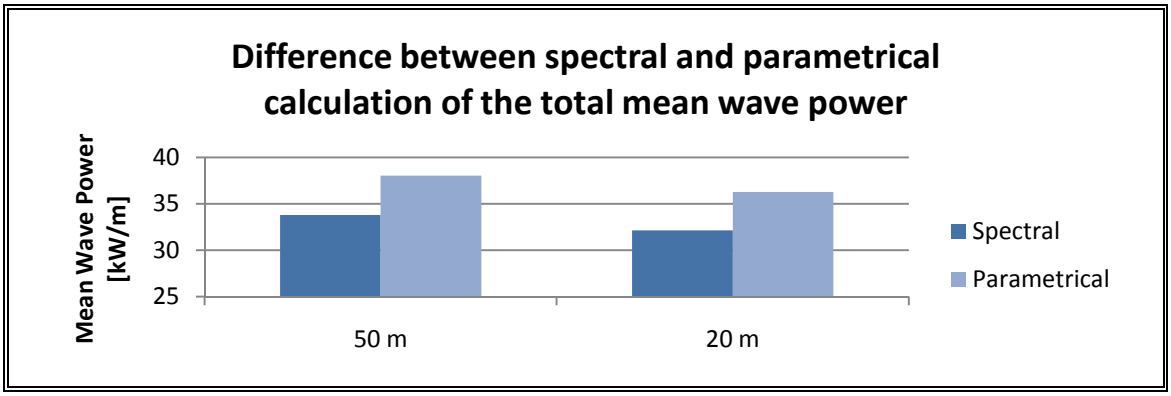

Figure 5-10: Difference between spectral and parametrical calculation of mean wave power. Parametrical calculation has an overestimation of approximately 12%.

With the spectral propagation, additional information regarding the different components of the sea state can be obtained. For instance, Figure 5-11 shows the relative contribution of each frequency component to the total mean wave energy in a month. This was obtained by integrating each spectrum only in its directional dimension (equation (5.1)) and then averaging the components $E(f_i)$ of each spectrum in a month. With this information it is possible to know which component wave is contributing with the larger amount of power.

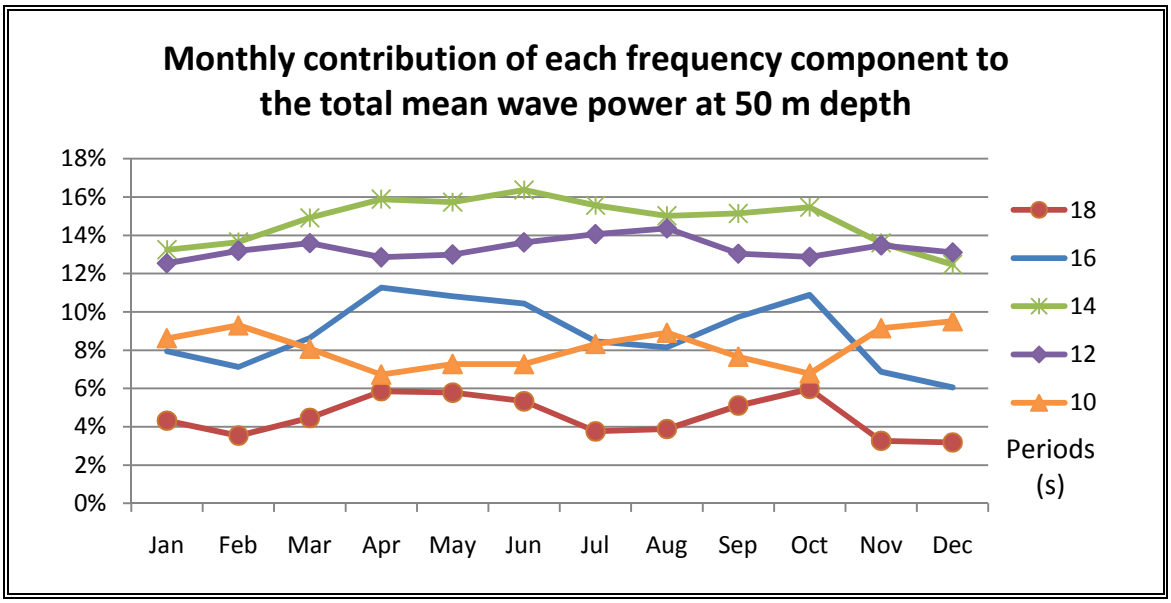

Figure 5-11: Monthly contribution of each component wave to the total mean wave power at 50 m depth. 14 to 12 seconds waves are the predominant.

It can be seen that the wave periods between 12 and 14 seconds are the larger contributors to the mean wave power throughout the year. Smaller period waves (10 s) appear only on summer (probably due to windy conditions) while larger periods (16 s – 18 s) contribute more on winter (due to storms generated in the Pacific).

The previous analysis can only be made with spectral information. With statistical wave parameters though, a distribution of the peak periods through the year can be obtained (Figure 5-12). This information is useful as it gives a good estimation of the range of periods in which a WEC device should operate. Figure 5-12 shows that the mean peak period is almost constant through the year, with an average of 12.6 seconds. The 98^{th} and 2^{nd} percentiles show a deviation from the average peak period of ± 4 seconds.

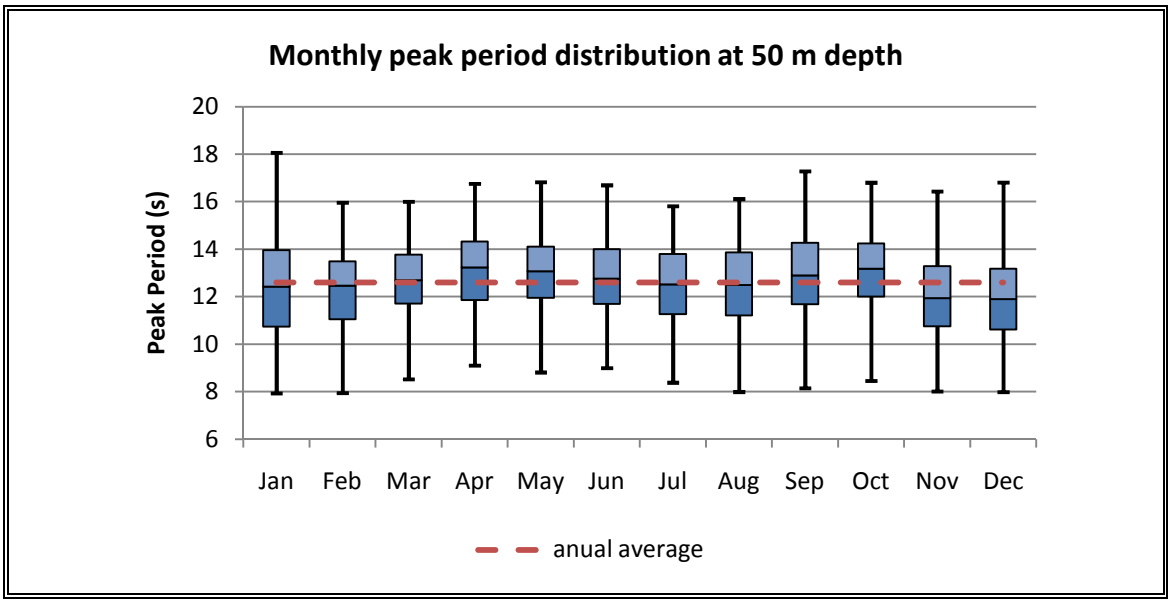

Figure 5-12: Monthly distribution of peak periods. Mean peak period has little variation through the year.

Another use for the spectral information regards wave's directions. If the spectrum is integrated only in the frequencies (see equation (5.1)) the mean wave power directional distribution can be obtained. This is done by calculating the mean wave power for each directional bin an averaging the whole 6 year data. Figure 5-13 show the results. There, it can be seen that most of the gross mean wave power comes from the SW, shifting to the West when approaching the coast. Also, the directional spreading gets narrower with shallower waters. These are 2 indicators of refraction. This behavior in waves direction can make the 20 m site more suitable for a WEC device, although the total mean wave power is smaller.

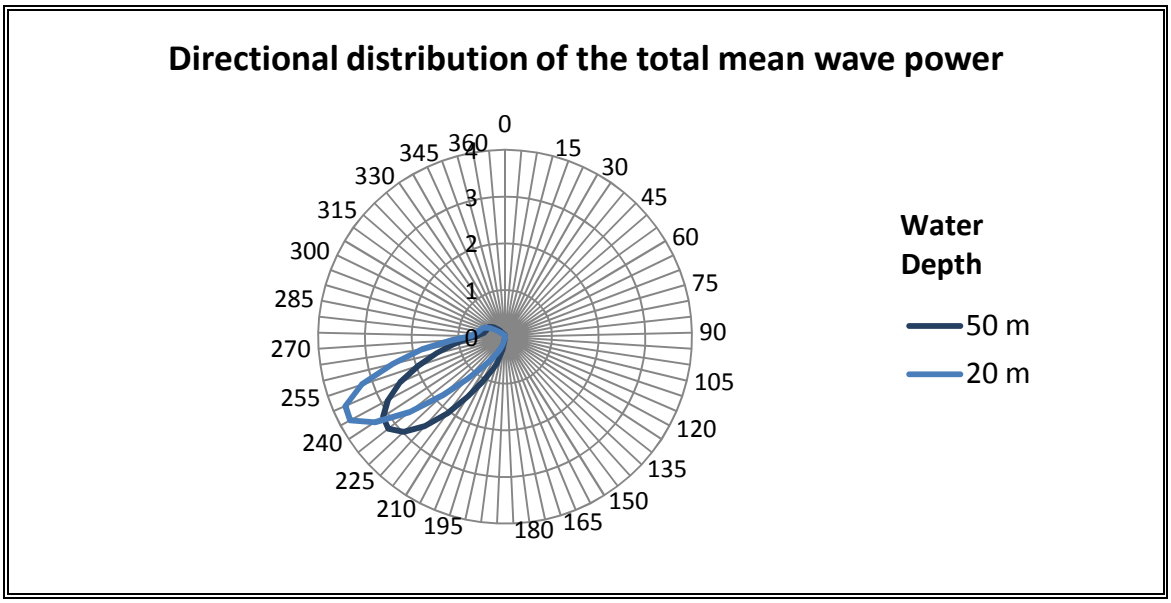

Figure 5-13: Directional distribution of the mean wave power. A change in direction and spreading can be observed when approaching the coast.

With statistical wave parameter information, the occurrence probability of waves from different directions and heights can be calculated. Figure 5-14 shows a histogram using the wave parameters of H_{sig} and mean wave direction during the 6 years of information to construct an occurrence probability rose. Here, it is also possible to observe the effects of refraction that shifts the mean wave direction and narrows the "directional spread" as waves propagates towards the coast (notice that in this case the directional spread is not related to the spectrum but to the tendency of mean wave direction). The difference with Figure 5-13 is that it doesn't consider each directional component of a sea state, it only one direction for each case.

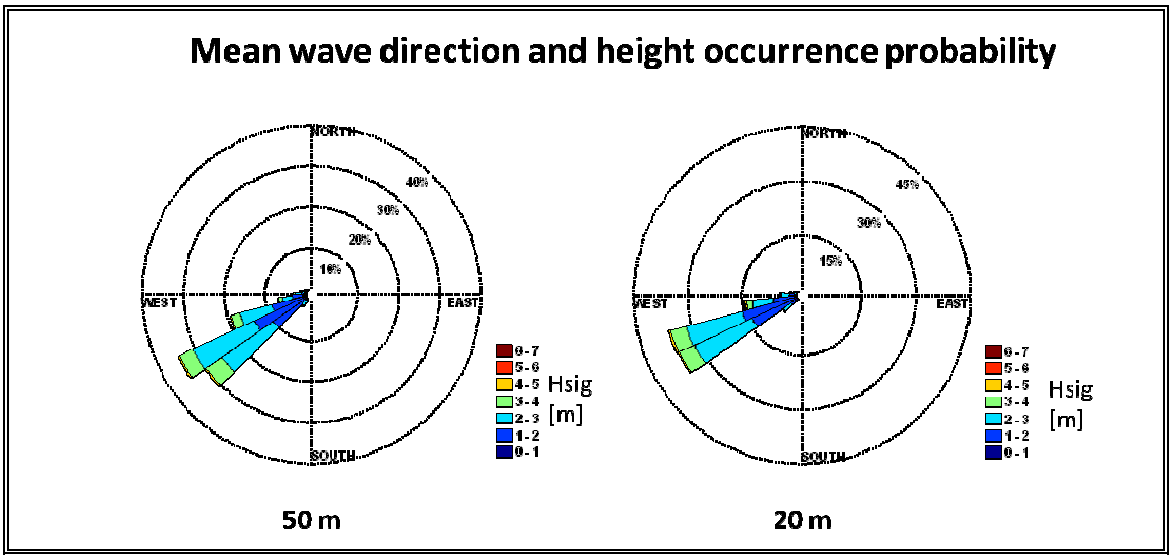

Figure 5-14: Histogram of mean wave direction and height. Refraction can be observed as waves shift when approaching the coast.

Finally, one of the advantages of spectral information in the case of mean wave power estimation is that the mean wave power can be estimated considering only the portion of the spectrum with directions aligned to the WEC device needs. In other words, equation (5.1) can be integrated only in a sector of directions, not in all directions. This allows discarding wave energy coming from directions that are not suitable for the WEC device, thus not overestimating the wave power. A similar treatment can be done with the frequencies, "filtering" all periods that are not useful for the device. In addition, the integration can include the device's power conversion matrix (which gives an effective output power for each H_{sig} - T_p pair; Acuña, 2008). This exercise was not done in this application because the goal was to obtain the total gross wave power, independent of the device.

6. CONCLUSIONS

The most important conclusions found in this study are listed below.

The importance of having spectral information

The importance of having spectral information relies on the fact that wave parameters cannot represent the sea state conditions with every wave component, which is necessary to properly calculate the design parameters of a structure or a wave energy conversion device (WEC; Previsic et al., 2004).

As an example, a harbor opened to the north could be properly designed to operate with waves coming from the south, which are present in the wave parameters because they represent the dominant component. But what the wave parameters can't tell is the existence of a very small component coming from the north, which although small, can bring trouble inside the port if reflections and resonance effects occur.

Another example is the calculation of the wave power, necessary to estimate the exploitable energy resources for a WEC. In this case, spectral information provides better results because it calculates the power contribution of every component instead of approximating this value using wave parameters. Moreover, with a spectrum it is possible to determine the wave power that comes from specific directions and periods, thus not adding power for the directions and periods that are away from the WEC's working range.

Full spectral information thereby will always be preferred over wave parameters, although its importance depends on the situation.

The importance of how wave parameters are extracted

As it became clear in this study, it is very important to know the way wave parameters are extracted from a spectrum if a simulation is to be done relying on this type data. Special consideration is needed in cases where the direction of the waves is almost parallel to the coast. The reason is that, by integrating the spectrum in all directions to get the wave parameters, the energy propagating offshore is also considered, and with the simulation, that energy is finally propagated onshore. The best choice will be, if possible, to extract the wave parameters from the portion of directions of the spectrum heading towards the coast.

The importance of how mean wave power is calculated

As it was seen, the calculation of the mean wave power through statistical wave parameters overestimated the mean wave power calculated with a spectrum (independent of the deep to shallow water propagation used). One of the reasons is that there are too many assumptions when changing the typical wave parameters H_{sig} and T_p to the H_{rms} and T_e needed for the power calculation. Besides, "bunching" all energy in one period leads to a bad estimation (C_g is different for each frequency, which is not considered if wave parameters are used).

Contrary to a structural design, where an overestimation of parameters could increases the "safety"; in a wave power study an overestimation of the energy is not helpful.

The comparison between methods

Regarding the different types of propagation, a conclusion that can be clearly taken from this study is that the spectral propagation is more accurate, in terms of output wave parameters, than a wave parameters propagation. The spectral propagation also delivers results in means of spectrums, which is preferred for being a more complete type of information.

The second conclusion derived from the comparison between methods is that a full wave parameters propagation will not always delivers better results than a unitary wave parameters propagation. In one particular case of this study, better results were obtained with the unitary wave parameters method, underscoring the fact that in a full wave parameter propagation special concern needs to be put in the energy distribution for it to work properly.

The last conclusion regarding methods comparison is that in the case of the proposed method, most of the error added, in comparison to a full spectral propagation, comes from the fact that non-linear processes are not considered. If the method is compared to a full spectral propagation with non-linear processes deactivated, the mean difference in wave parameters are all below 1%.

The tendency of the methods

Unfortunately, the data obtained in this study is not sufficient to conclude the tendency of the methods in terms of bias; i.e., it cannot be stated if the methods tend to generally

overestimate or underestimate the wave parameters when compared to actual measurements. It can be fairly stated though that propagations through wave parameters show a tendency to overestimate the significant wave height and underestimate the peak period when compared to spectral propagations. Nevertheless, Nicolau del Roure (2004) states that the wave parameters propagation's tendency to overestimate or underestimate the wave height depends on the bathymetry and the site where the energy is being transferred.

The advantages and disadvantages of the proposed method

The proposed method allows transforming any number of spectrums from one site to another with a limited number of simulations. This can bring huge savings in computational time. The results are that: (1) the wave parameters differ in less than 1% from a full spectral propagation, and (2) the spectrum's shape is accurately represented in the output site.

The downside of the method is that it works only in cases where non-linear effects are negligible, or close to negligible. To test the importance of non-linear effects in the problem, a preceding comparison between full spectral propagation, with and without non-linear processes, is recommended. If the number of required simulations is relatively low, then the application of this method is not really necessary and a full spectral propagation is recommended to account for such non-linear effects.

The method is also sensible to the number of unitary spectrums considered; therefore it must be ensured that all the direction-frequency space is covered by them. The recommendation is to consider one peak period for each frequency bin and one peak direction every 15º, for a JONSWAP (in frequency) and Goda & Susuki (in direction) energy distribution (with parameters $\gamma = 3.3$ and $s_{\max} = 60$ respectively). In the same line, the election of these distributions is arbitrary, and the method should work independent of this selection (which can be investigated in a future study).

6.1 Future investigations

Some aspects of this thesis than can be improved or further investigated in the future are:

- To determine *a priori* if the proposed method can be applied by means of the Ursell number, which is a dimensionless quantity that relates the wave height, the wave length and the water depth to indicate the nonlinearity of the problem. In this study, the relevance of non-linear effects is done my simulating the propagation with and without non-linear processes activated in the model and then comparing the results.
- To quantitatively measure the difference in spectral shape between the proposed method and the full spectral propagation. In this work the difference is only examined visually.
- To evaluate the impact of propagating unitary spectrums with different energy distributions and the impact of propagating more or less number of spectrums. The method should converge for larger number of unitary spectrums.

REFERENCES

ABP Marine Enviromental Research Ltd. (2008). *Atlas of UK Marine Renewable Energy Resources: Technical Report.* South Hampton: Department for Business, Enterprise & Regulatory Reform.

Acuña, H. (2008). *Evaluación del potencial de la energía en Chile.* Valparaiso: Memoria de título Universidad Técnica Federico Santa María.

Battjes, J. A. (1994). Shallow water wave modelling. *Proc. Int. Symp. Waves — Phys. Numer. Modell.* (págs. 1-23). Vancouver: University of British Columbia.

Battjes, J. A., & Janssen, J. P. (1978). Energy loss and set-up due to breaking of random waves. *in Proceedings of 16th International Conference on Coastal Engineering* (págs. 569-587). New York: Am. Soc. of Civ. Eng.

Berkhoff, J. C. (1972). Computation of combined refraction-diffraction. *Proceedings of 13th International Conference on Coastal Engineering* (págs. 471-490). New York: Am. Soc. of Civ. Eng.

Booij, N., Ris, R. C., & Holthuijsen, L. H. (1999). A third-generation wave model for coastal regions 1: Model description and validation. *Journal of geophysical research* , 104 (c4), 7649-7666.

Collins, J. I. (1972). Prediction of Shallow-Water Spectra. *Journal of Geophysical Research , 77* (15), 2693-2707.

Dean, R. G., & Dalrymple, R. A. (1991). *Water wave mechanics for engineers and scientists.* Singapore: World Scientific.

Dingemans, M. W. (1997). *Water Wave Propagation Over Uneven Bottoms, part 1, Linear Wave Propagation* (Vol. 13). River Edge, N.J.: World Sci.

Fassardi, C. (2008). The transformation of deepwater wave hindcasts to shallow water. *8th international workshop on wave hindcasting and forecasting.* Oahu.

Folley, M., & Whittaker, T. J. (2009). Analysis of the nearshore wave energy resource. *Renewable Energy* , 1709-1715.

Freilich, M. H., & Guza, R. T. (1984). Nonlinear effects on shoaling surface gravity waves. *Philos. Trans. R. Soc. London , A311*, 1-41.

Goda, Y. (1970). A synthesis of breaker indices. *Trans. Japan Soc. Civil Engrs , 2* (2), 227-230.

Goda, Y. (2000). *Random seas and design of maritime structures.* Singapore: World Scientific Publishing.

Goda, Y. (1988). Statistical variability of sea state parameters as a function of a wave spectrum. *Coastal Engineering in Japan , 1* (31), 39-52.

Goda, Y., & Suzuki, Y. (1975). Computation of refraction and diffraction of sea waves with Mitsuyasu's directional spectrum. *Tech. Note of Port and Harbour Res. Inst. (in Japanese)* .

Hasselmann, K., Barnett, T. P., Bouws, E., Carlson, H., & Cartwright, D. E. (1973). Measurements of wind-wave growth and swell decay during the Joint North Sea Wave Project (JONSWAP). *Deutsche Hydr. Zeit Reihe* .

Holthuijsen, L. H. (2007). *Waves in Oceanic and Coastal Waters.* New York: Cambridge University Press.

ITTC. (2002). Proceedings of the 23rd ITTC. Volume II. Final Reports and Recomendations., (pág. 547). Venecia.

Janssen, P. A. (1991a). Quasi-linear theory of wind-wave generation applied to wave forecasting. *Journal of Physical Oceanography , 21*, 1631-1642.

Kirby, J. T. (1986). Higher-order approximation in the parabolic equation method for water waves. *J. Geophys. Res. , 91* (C1), 933-952.

Komen, G. J., Cavaleri, L., Donelan, M., Hasselmann, K., Hasselmann, S., & Janssen, P. (1994). *Dynamics and Modelling of Ocean Waves.* New York: Cambridge University Press.

Komen, G. J., Hasselmann, S., & Hasselmann, K. (1984). On the existence of a fully developed wind-sea spectrum. *Journal of Physical Oceanography , 14*, 1271-1285.

Madsen, O. S., Poon, Y.-K., & Graber, H. C. (1988). Spectral wave attenuation by bottom friction: theory. *in Proceedings 21th International Conference on Coastal Engineering* (págs. 492-504). New York: Am. Soc. of Civ. Eng.

Madsen, P. A., & Sørensen, O. R. (1992). A new form of the Boussinesq equations with improved linear dispersion characteristics, 2, A slowly-varying bathymetry. *Coastal Eng. , 18*, 183-205.

Miles, J. W. (1981). Hamiltonian formulations for surface waves. *Appl. Sci. Res. , 37*, 103-110.

Mitsuyasu, H., Tasai, F., Suhara, T., Mizuno, S., & Ohkusu, M. (1975). Observation of the directional spectrum of ocean waves using a cloverleaf buoy. *Journal of Physical Oceanography* , 750-760.

Monárdez, P., Acuña, H., & Scott, D. (2008). Evaluation of the Potential of wave energy in Chile. *Proc. of the ASME 27th Int. Conf. on Offshore Mechanics and Arctic Eng.* Estoril.

Munk, W. H. (1950). Origin and generation of waves. *Proc. 1st Conf. Coastal Engineering* (págs. 1-4). New York: ASCE.

Nicolau del Roure, F. (2004). *Evaluación de metodologías de transferencia de oleaje desde aguas profundas hacia aguas someras.* Trabajo de título, Universidad de Chile, Santiago.

Nwogu, O. (1994). Nonlinear evolution of directional wave spectra in shallow water. *Proc. 24th Int. Conf. Coastal Engineering* (págs. 467-481). New York: ASCE.

Percival, D. B., & Walden, A. T. (1993). *Spectral Analysis for Physical Applications.* Cambridge: Cambridge University Press.

Peregrine, D. H. (1967). Long waves on a beach. *J. Fluid Mech. , 27*, 815-827.

Previsic, M., Bedard, R., & Hagerman, G. (2004). *Offshore Wave Energy Conversion Devices.* EPRI Assessment.

Radder, A. C. (1992). An explicit Hamiltonian formulation of surface waves in water of finite depth. *J. Fluid Mech. , 237*, 435-455.

Radder, A. C. (1979). On the parabolic equation method for water-wave propagation. *J. Fluid Mech. , 95*, 159-176.

Ris, R. C., Holthuijsen, L. H., & Booij, N. (1999). A third-generation wave model for coastal regions 2: Verification. *Journal of geophysical research* , 104 (c4), 7667-7681.

SHOA. (2005). *Instrucciones oceanográficas N°1.* Valparaiso.

Smith, J. M., Sherlock, A. R., & Resio, D. (2001). *STWAVE: Steady State Spectral Wave Model User's Manual for STWAVE.* US Army Corps of Engineers.

Stewart, R. H. (2002). *Introduction to Physical Oceanography.* Texas: A&M University.

Tolman, H. L. (2002b). *Testing of WAVEWATCH-III version 2.22 in NCEP's NWW3 ocean wave model suite.* Washington: National Center for Enviromental Prediction.

Universidad de Valparaiso. (2009). *Evaluación del potencial de energía del oleaje entre la IV y la X regiones, Chile.* Reñaca.

WAMDI Group. (1988). The WAM model - A third generation ocean wave prediction model. *Journal of Physical Oceanography , 18*, 1775-1810.

Whitham, G. B. (1974). *Linear and Nonlinear Waves.* New York: John Wiley.

APPENDICES

APPENDIX A: RECORDS OF INCIDENT PEAK PERIODS AND DIRECTIONS IN ANCON

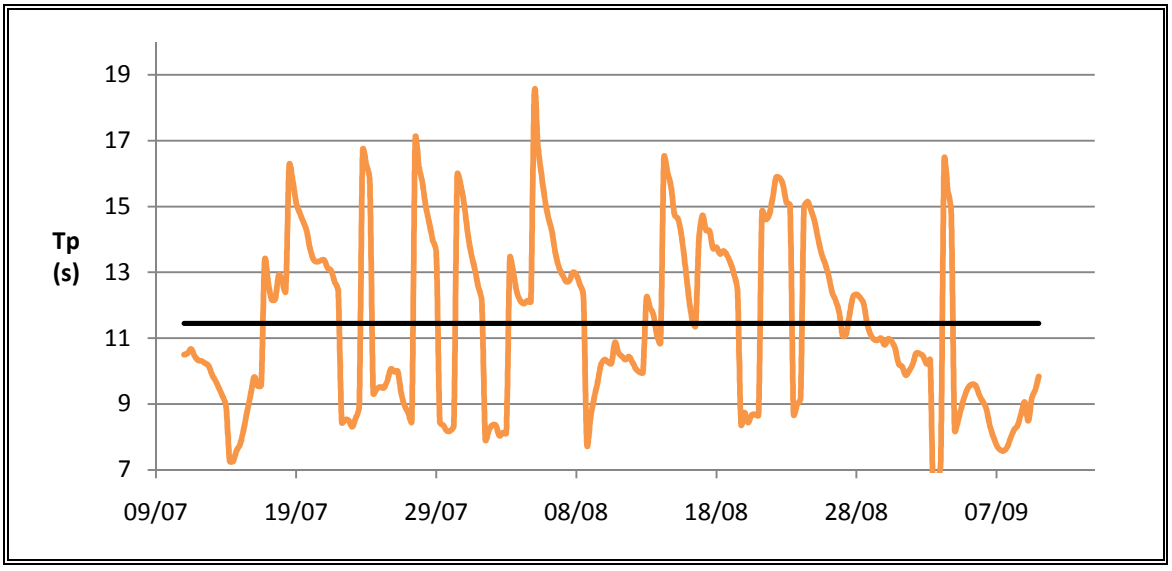

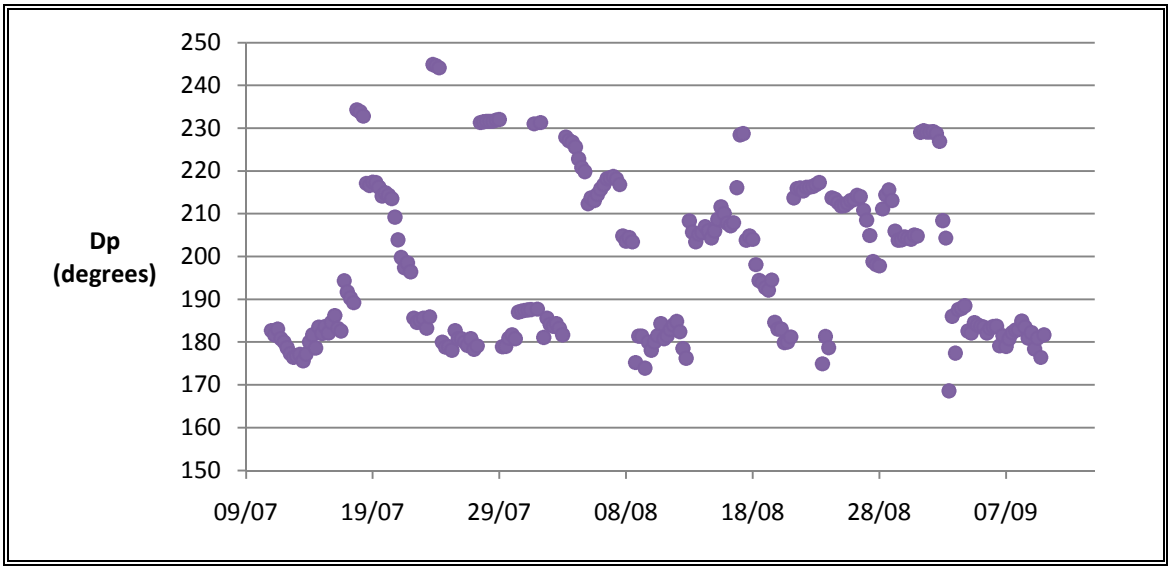

APPENDIX B: THE SIX CHOSEN INPUT SPECTRUMS FOR CURAUMILLA

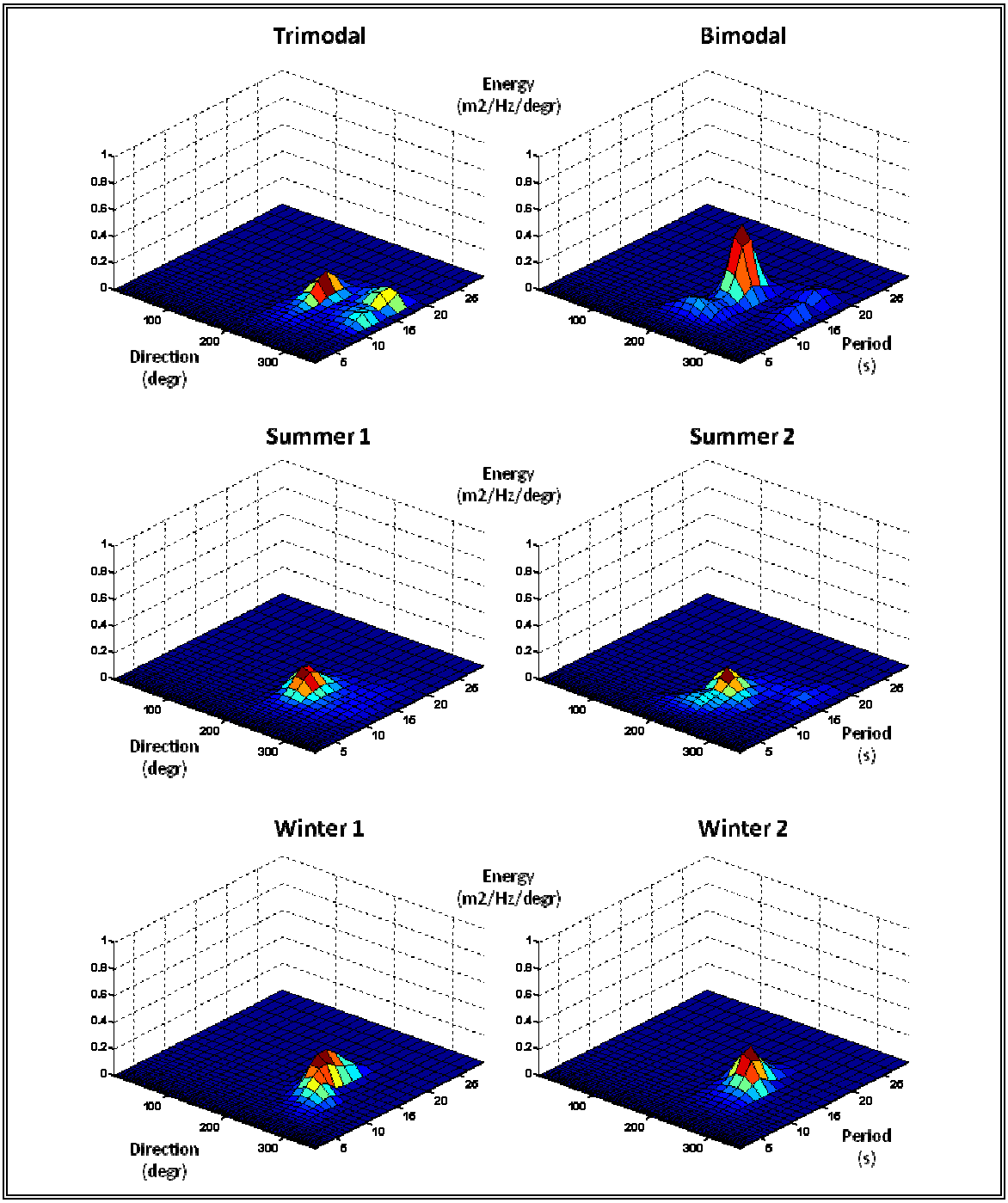

APPENDIX C: RELEVANCE OF NON-LINEAR PROCESSES AT VARIOUS DEPTHS

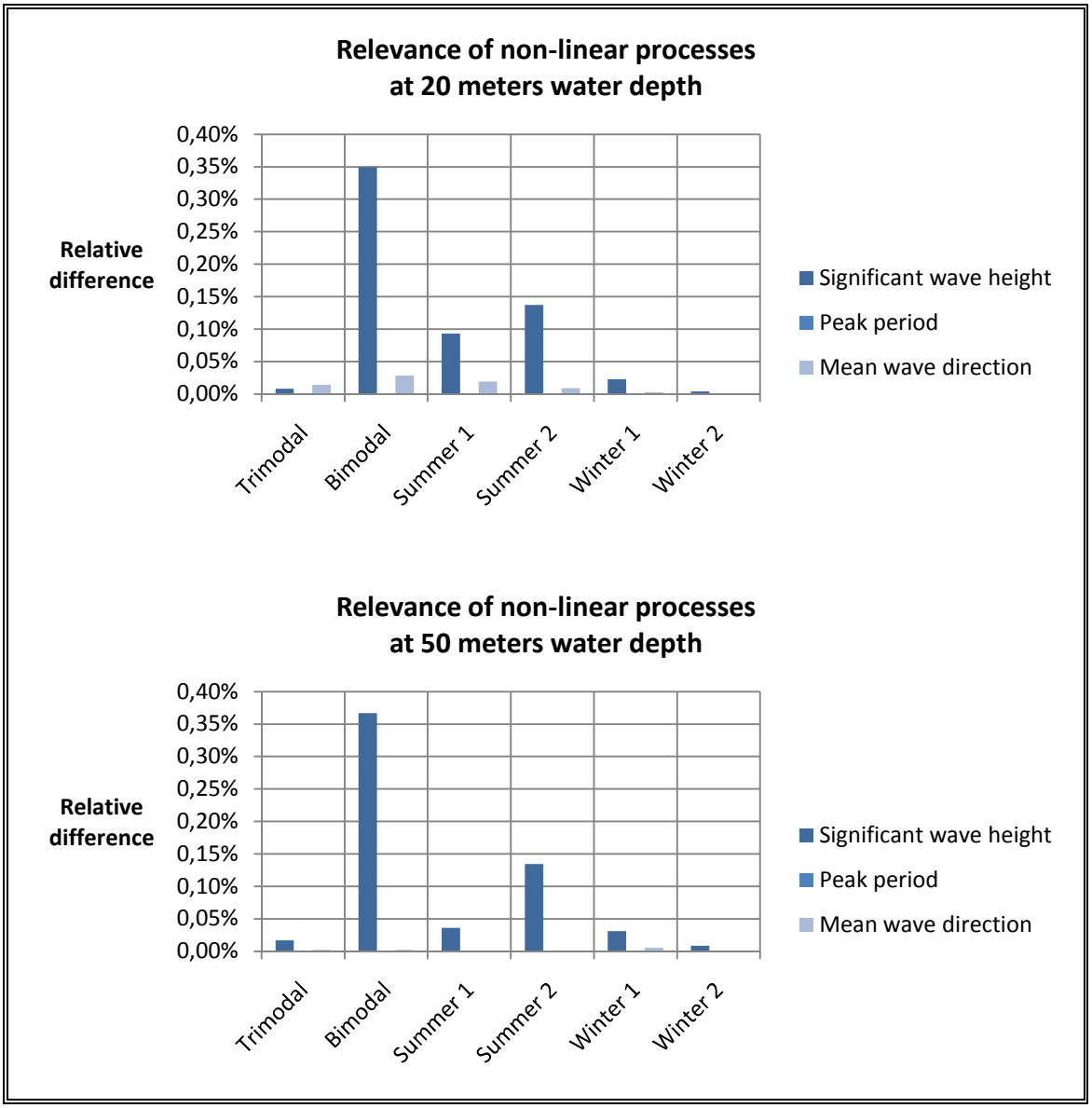

APPENDIX D: WAVE PARAMETERS FOR DIFFERENT PROPAGATION METHODS AT VARIOUS DEPTHS

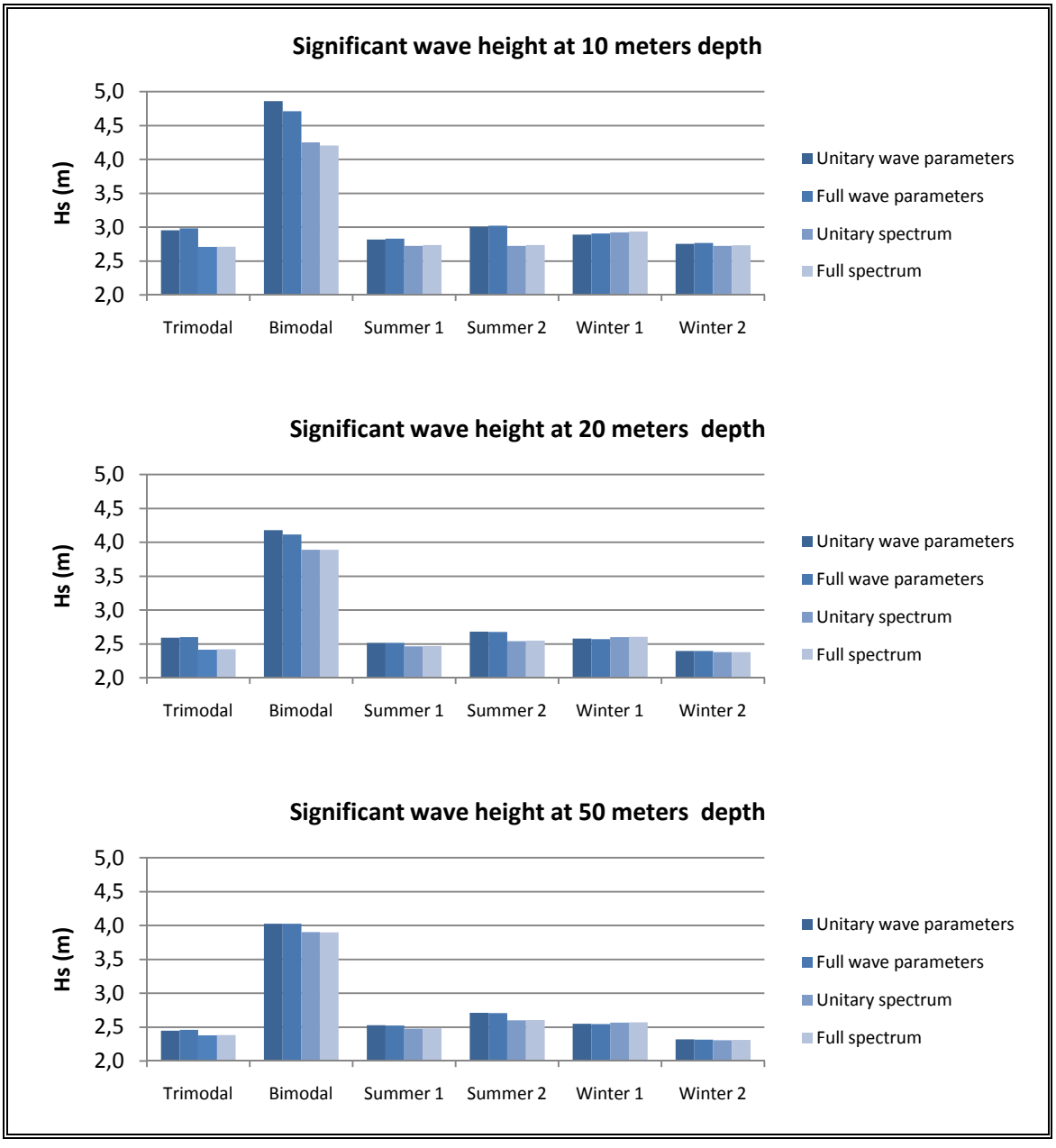

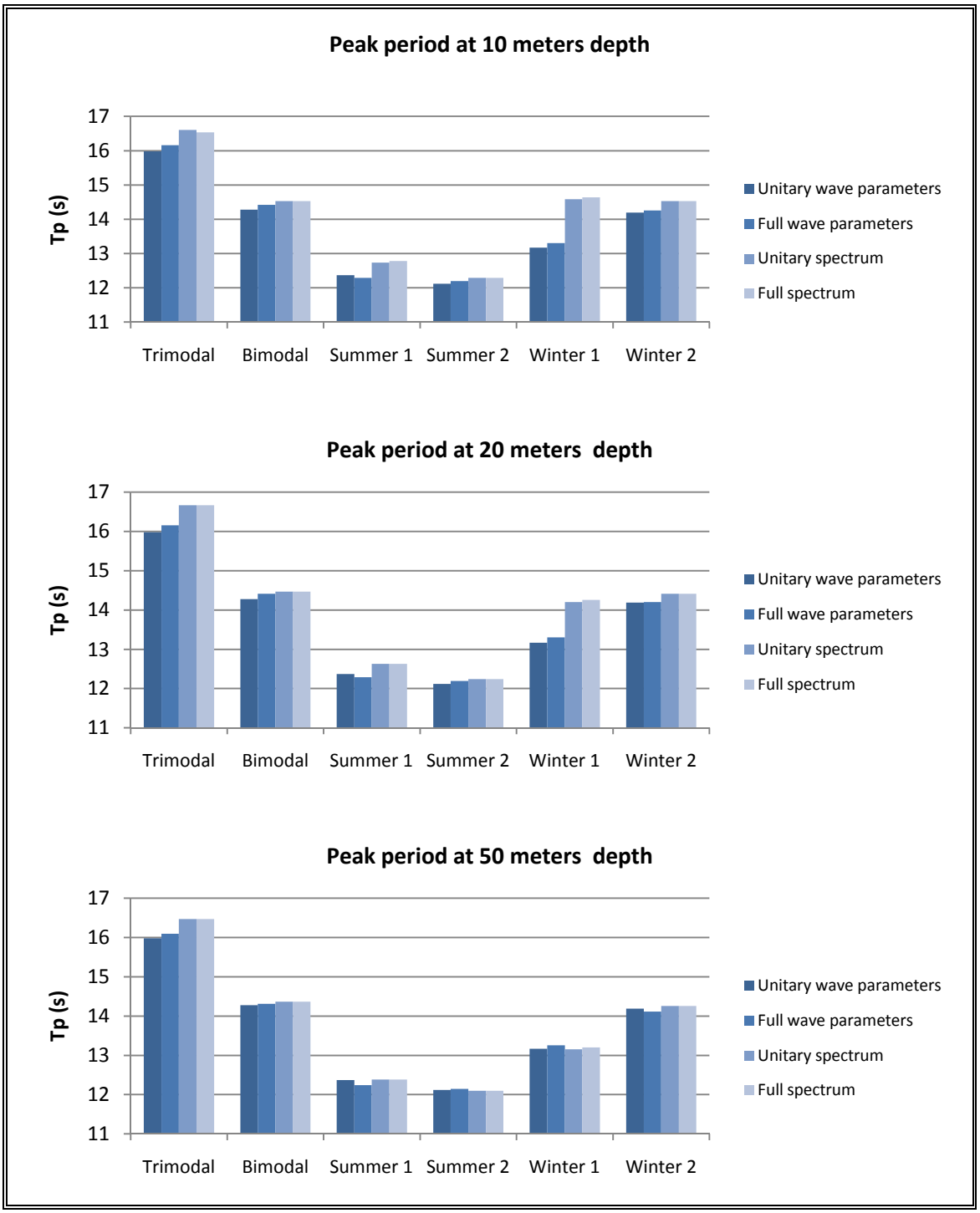
Peak period at 10 meters depth
Tp (s)
17
16
15
14
13
12
11
Trimodal
Bimodal
Summer 1
Summer 2
Winter 1
Winter 2
Unitary wave parameters
Full wave parameters
Unitary spectrum
Full spectrum
Peak period at 20 meters depth
Tp (s)
17
16
15
14
13
12
11
Trimodal
Bimodal
Summer 1
Summer 2
Winter 1
Winter 2
Unitary wave parameters
Full wave parameters
Unitary spectrum
Full spectrum
Peak period at 50 meters depth
Tp (s)
17
16
15
14
13
12
11
Trimodal
Bimodal
Summer 1
Summer 2
Winter 1
Winter 2
Unitary wave parameters
Full wave parameters
Unitary spectrum
Full spectrum

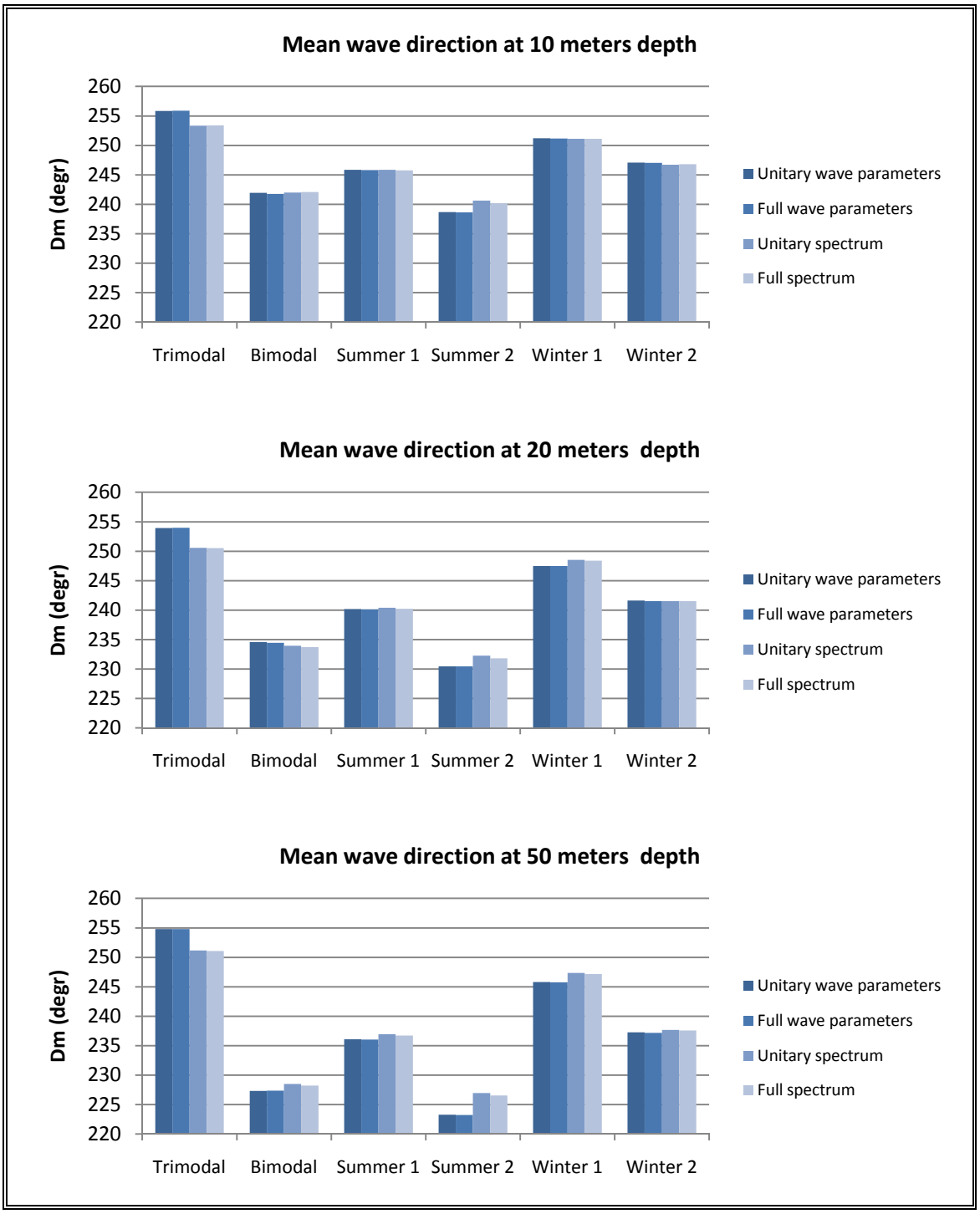
Mean wave direction at 10 meters depth
Dm (degr)
260
255
250
245
240
235
230
225
220
Trimodal
Bimodal
Summer 1
Summer 2
Winter 1
Winter 2
Unitary wave parameters
Full wave parameters
Unitary spectrum
Full spectrum
Mean wave direction at 20 meters depth
Dm (degr)
260
255
250
245
240
235
230
225
220
Trimodal
Bimodal
Summer 1
Summer 2
Winter 1
Winter 2
Unitary wave parameters
Full wave parameters
Unitary spectrum
Full spectrum
Mean wave direction at 50 meters depth
Dm (degr)
260
255
250
245
240
235
230
225
220
Trimodal
Bimodal
Summer 1
Summer 2
Winter 1
Winter 2
Unitary wave parameters
Full wave parameters
Unitary spectrum
Full spectrum